

**SPECTRAL ANALYSIS OF LANTHANIDE
COMPLEXES WITH ESSENTIAL AMINO ACIDS:
KINETIC AND THERMODYNAMIC APPROACH**

by

ZEVIVONÜ THAKRO



Submitted to

NAGALAND UNIVERSITY

In Partial Fulfillment of the Requirements for Award of the Degree

of

DOCTOR OF PHILOSOPHY IN CHEMISTRY

DEPARTEMENT OF CHEMISTRY

NAGALAND UNIVERSITY

LUMAMI-798627

NAGALAND, INDIA

2022



नागालैण्ड विश्वविद्यालय NAGALAND UNIVERSITY

(केंद्रीय विश्वविद्यालय) / (A Central University)

मुख्यालय : लुमामी, जिला : जुन्हेबोटो (नागालैण्ड) – 798 627
Hqrs: Lumami, Dist: Zunheboto, Nagaland – 798 627

Prof. M. Indira Devi

Department of Chemistry.

e-mail: camindira@yahoo.co.in

CERTIFICATE

This is to certify that **Ms. Zevivonü Thakro**, a registered Research Scholar for Ph.D. degree in Chemistry under Nagaland University has carried out her research work under my guidance and supervision. Her thesis entitled “**Spectral analysis of Lanthanide complexes with essential amino acids: Kinetic and Thermodynamic approach**” embodies the original research work and has fulfilled all the requirements according to the accordinf to the rules /regulations of Nagaland University.

Further, to the best of my knowledge, the research work has not been submitted to any other University/Institution for the award of any degree or diploma.

(Prof. M. Indira Devi)

Supervisor



नागालैण्ड विश्वविद्यालय NAGALAND UNIVERSITY

(केंद्रीय विश्वविद्यालय) / (A Central University)

मुख्यालय : लुमामी, जिला : जुन्हेबोटो (नागालैण्ड) – 798 627

Hqrs: Lumami, Dist: Zunheboto, Nagaland – 798 627

Department of Chemistry.

CERTIFICATE

This is to certify that **Miss Zevivonü Thakro**, a registered Research Scholar for Ph.D. degree in Chemistry under Nagaland University, bearing Ph.D. Registration No. **787/2017**, has satisfactorily completed all the courses offered in the Pre-Ph.D Course Work Programme in the Department of Chemistry, Nagaland University, Hqrs. Lumami.

The course includes:

CHEM-601 Research Methodology

CHEM-602 Advance in Chemistry

CHEM-603 Literature Review, Report Writing and Presentation.

Upasana
19/12/22
(Head)

Department of Chemistry
Nagaland University



नागालैण्ड विश्वविद्यालय NAGALAND UNIVERSITY

(केंद्रीय विश्वविद्यालय) / (A Central University)

मुख्यालय : लुमामी, जिला : जुन्हेबोटो (नागालैण्ड) – 798 627
Hqrs: Lumami, Dist: Zunheboto, Nagaland – 798 627

Department of Chemistry.

DECLARATION

I, **Ms. Zevivonu Thakro** bearing Ph.D. Registration No. **787/2017** with effect from **30th August 2016**, hereby declare that my Ph.D. thesis entitled “**Spectral analysis of Lanthanide complexes with essential amino acids: Kinetic and Thermodynamic approach**” is the record of original work done by me and the contents of this thesis did not comprise of the basis for the award of any previous degree/ diploma to me or to anybody else in any other University/Institute to the best of my knowledge.

This Ph. D. thesis is submitted in compliance with the UGC Regulation 2016 dated May 05, 2016 (Minimum Standard and Procedure for Award of M. Phil. /Ph. D. Degree) to Nagaland University for the degree of Doctor of Philosophy in Chemistry.

Zevivonu

(**Zevivonü Thakro**)
Research Scholar

Upasana
19/12/22
(Head)

Department of Chemistry
Nagaland University

Indira Devi
19/12/2022

(**Prof. M. Indira Devi**)
Supervisor

Acknowledgements

I would want to use this opportunity to express my gratitude and appreciation to each person who has assisted me in completing my doctoral programme.

Firstly I thank our Almighty God for blessings me with wisdom, good health, and guidance throughout my research journey.

I extend my heartfelt and profound gratitude to **Prof. M. Indira Devi**, my research supervisor, for allowing me to work under her. I appreciate all of her gentle, consistent advice, inspiration, and support. Her insightful comments have always been a foundation, without which it would not have been possible to finish this work. I am the person I am now as a result of the years I spent learning under her direction.

I acknowledge a deep sense of gratitude to all the teaching faculties of the Chemistry department, Nagaland University: **Prof. Upasana Bora Sinha (Head of Department), Prof. Dipak Sinha, Dr. I. Tavishe Phucho, Dr. M. Prabhakar, Dr. N.A. Choudhury, Dr. Seram Dushila Devi** for their useful suggestions and assistance that helped me to keep my progress on track.

My sincere gratitude to **Nagaland University** for providing the essential resources I needed to carry out my research. I am also grateful to the University Grant Commission **Non-NET** for providing the Financial assistance.

I extend my sincere gratitude to **Dr. Abenthung Ovung**, Technical Assistant in Chemistry, NIT Chümoukedima for his assistance with the UV-vis analysis.

I owe my sincere thanks to **Dr. Moaienla Ao**, Assistant professor, Patkai Christian College, Seithekema for her assistance in the Theoretical analysis.

My gratitude and thanks to the non-teaching staffs **Mr. S. Bendangtemsu, Ms. Sunepjungla, Ms. Temsuienla Amer, Ms. Lovi, Mr. Johnny Yanthan, Mr. Phyobemo Patton** for their immense support throughout my research period.

My greatest indebtedness goes to my labmates, **Miss Juliana Sanchu, Mr. Chubazenba Imsong, Mr. Mhasiriekho Ziekhri, Mr. Punazungba Imsong, Ms. Sentienla Imsong** for their love and support.

Special thanks to my research scholar friends from other laboratories and department for their wonderful friendship and encouragement.

On my personal note, I would like to acknowledge my family members and friends whose love, support, guidance, and prayers have encouraged and pushed me to achieve where I have reached now.

Last but not least, I want to thank everyone who has influenced and contributed to the completion of this study endeavour, whether directly or indirectly.

Zevivonü Thakro



Sl. No. : 16-

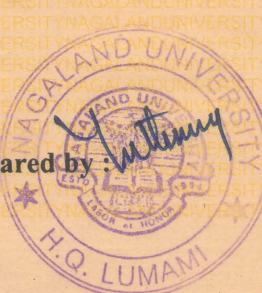
59086

NAGALAND**UNIVERSITY****STATEMENT OF MARKS**
Ph. D COURSE WORK EXAMINATION, 2017**DEPARTMENT OF CHEMISTRY**

The following are the marks secured by **Zevivonu Thakro**
Roll No. **13/16** of Ph.D Course Work Examination held in **2017**

Subject(s)/Paper(s)	Max. Marks	Minimum Qualifying Marks	Marks Secured
Paper No. Chem-601 Research Methodology	100	35	74
Paper No. Chem-602 (D) Advance in Chemistry	100	35	67
Paper No. Chem-603 Literature Review, Report Writing and Presentation	100	35	66
Total Aggregate Marks			207
Average Pass Mark – 55 %			

Result	Division	Percentage
Passed	I Division	69 %

Marks compared by: COE/Dy. Reg./AR (Exams) 

NAGALAND




UNIVERSITY

HEAD QUARTERS : LUMAMI

Ph. D COURSE WORK EXAMINATION

This is to certify that Mr/Ms.....
Zevivonu Thakro.....
13/16..... is qualified in the Ph. D Course Work Examination
of Nagaland University bearing Roll No..... Nagaland University held in the Year 20.....
in the Department of..... Chemistry 17


Head of Department
Department of Chemistry
Nagaland University


Dean
School of Sciences
Nagaland University
Lumami Nagaland
School of Science

Lists of Figures

Figure number	Figure Caption	Page no.
<i>Chapter 1</i>		
Fig. 1.1	Regulatory role of Mg^{2+} in the insulin secretion from pancreatic beta cells.	5
Fig. 1.2	Structure of L-phenylalanine	8
Fig. 1.3	Structure of L-methionine	9
Fig. 1.4	Structure of L-leucine	9
Fig. 1.5	Structure of the three essential amino acids in its zwitterionic form.	13
Fig. 1.6	Bonding nature of the zwitterions L-leucine under different pH.	13
<i>Chapter 2</i>		
Fig. 2.1	Procedure for stock solution preparation.	37
Fig. 2.2	Schematic representation of the experimental process.	38
<i>Chapter 3</i>		
Fig. 3.1	2D and 3D structures of L-phenylalanine.	43
Fig. 3.2	Phenylalanine in (a) neutral and (b) Zwitterion state.	44
Fig. 3.3	Bonding nature of the zwitterionic form of L-Phenylalanine at different pH.	45
Fig. 3.4	UV-vis absorption spectra of the $4f-4f$ electronic transitions of Pr^{3+} , $Pr(III):Phe$ and $Pr(III):Phe:Mg(II)$ complexes in ACN:Water (50% v/v) solvent.	48
Fig. 3.5	UV-vis absorption spectra of the $4f-4f$ electronic transitionsof Pr^{3+} , $Pr(III):Phe$ and $Pr(III):Phe:Mg(II)$ complexes in Dioxane:Water(50% v/v) solvent.	48

Fig. 3.6	Comparative UV-vis absorption spectra of Pr(III):Phe complex in different aquated solvents of C ₃ H ₇ NO, CH ₃ OH, C ₄ H ₈ O ₂ , and CH ₃ CN.	52
Fig. 3.7	UV-vis absorption spectra of <i>4f-4f</i> electronic transitions of Pr ³⁺ , Pr(III):Phe and Pr(III):Phe:Mg(II) complexes in 50% v/v aquated DMF solvent in different pH 4.	53
Fig. 3.8	UV-vis absorption spectra of <i>4f-4f</i> electronic transitions of Pr ³⁺ , Pr(III):Phe and Pr(III):Phe:Mg(II) complexes in 50% v/v aquated DMF solvent in different pH 6.	53
Fig. 3.9	Absorption spectra of Pr(III):Phe:Mg(II) complexation at 303 K and in different time intervals.	56
Fig. 3.10	Absorption spectra of Pr(III):Phe:Mg(II) complexation at 308 K and in different time intervals.	57
Fig. 3.11	Plot of P _{obs} and Time in hours for the ³ H ₄ → ³ P ₂ transition of Pr(III):Phe:Mg(II) at four different temperatures (a) 298 K, (b) 303 K, (c) 308 K, (d) 313 K.	62
Fig. 3.12	Plot of log k versus (1/T) × 10 ³ for the complexation of Pr(III):Phe:Mg(II) in an aqueous medium.	62
Chapter 4		
Fig. 4.1	2D and 3d structures of L-methionine.	76
Fig. 4.2	Bonding nature of the zwitterions L-methionine under different pH mediums.	78
Fig. 4.3	Possible reaction of Pr(III) with L-methionine under different pH medium	78
Fig. 4.4	UV-vis absorption spectra of <i>4f-4f</i> electronic transitions of Pr ³⁺ , Pr(III):Met and Pr(III):Met:Mg(II) complexes in 50% v/v aquated ACN solvent.	82
Fig. 4.5	UV-vis absorption spectra of the <i>4f-4f</i> electronic transitions of Pr ³⁺ , Pr(III):Met and Pr(III):Met:Mg(II) complexes in 50% v/v aquated Dioxane solvent.	82
Fig. 4.6	UV-vis absorption spectra of the <i>4f-4f</i> electronic transitions of Pr ³⁺ , Pr(III):Met & Pr(III):Met:Mg(II) complex in 50% v/v aquated DMF solvent at pH 4.	85

Fig. 4.7	UV-vis absorption spectra of the <i>4f-4f</i> electronic transitions of Pr^{3+} , Pr(III):Met & $\text{Pr(III):Met:Mg(II)}$ complex in 50% v/v aquated DMF solvent at pH 6.	85
Fig. 4.8	Absorption spectra of $\text{Pr(III):Met:Mg(II)}$ complexation at 298 K and in different time intervals.	88
Fig. 4.9	Absorption spectra of $\text{Pr(III):Met:Mg(II)}$ complexation at 313 K and in different time intervals.	89
Fig. 4.10	P_{obs} vs Time in hours at various temperatures: (a) 298 K, (b) 303 K, (c) 308 K, (d) 313 K for the ${}^3\text{H}_4 \rightarrow {}^3\text{P}_2$ transition of $\text{Pr(III):Met:Mg(II)}$.	94
Fig. 4.11	$\log k$ vs $(1/T) \times 10^3$ for $\text{Pr(III):Met:Mg(II)}$ complex in 50% v/v aquated DMF medium.	94
Chapter- 5		
Fig. 5.1	2D and 3D structure of L-leucine	108
Fig. 5.2	Bonding properties of L-leucine at various pH medium.	110
Fig. 5.3	Possible interaction between Pr^{3+} and L-leucine in acidic media.	111
Fig. 5.4	<i>4f-4f</i> electronic transition absorption spectra (UV-vis) of Pr^{3+} , Pr(III):Leu & $\text{Pr(III):Leu:Mg(II)}$ complex in aquated dioxane (50% v/v)	113
Fig. 5.5	<i>4f-4f</i> electronic transition absorption spectra (UV-vis) of Pr^{3+} , Pr(III):Leu & $\text{Pr(III):Leu:Mg(II)}$ complex in aquated DMF (50% v/v)	113
Fig. 5.6	<i>4f-4f</i> electronic transition absorption spectra (UV-vis) of Pr^{3+} , Pr(III):Leu & $\text{Pr(III):Leu:Mg(II)}$ complex at pH 4.	116
Fig. 5.7	<i>4f-4f</i> electronic transition absorption spectra (UV-vis) of Pr^{3+} , Pr(III):Leu & $\text{Pr(III):Leu:Mg(II)}$ complex at pH 6.	116
Fig. 5.8	Absorption spectra of $\text{Pr(III):Leu:Mg(II)}$ complexation at 298 K and in different time intervals.	119
Fig. 5.9	Absorption spectra of $\text{Pr(III):Leu:Mg(II)}$ complexation at 303 K and in different time intervals.	120
Fig. 5.10	P_{obs} vs Time in hours at different temperatures: (a) 298 K, (b) 303 K, (c) 308 K, (d) 313 K for the ${}^3\text{H}_4 \rightarrow {}^3\text{P}_2$ transition of	125

	Pr(III):Leu:Mg(II).	
Fig. 5.11	log k vs $(1/T) \times 10^3$ for Pr(III):Leu:Mg(II) complex.	125
Chapter- 6		
Fig. 6.1	Possible interaction between Nd ³⁺ and L-phenylalanine in different pH media.	139
Fig. 6.2	Possible interaction between Nd ³⁺ and L-methionine in different pH media.	139
Fig. 6.3	Possible interaction between Nd ³⁺ and L-leucine in different pH media.	140
Fig. 6.4	UV-vis absorption spectra of the <i>4f-4f</i> electronic transitions of Nd ³⁺ , Nd(III):Phe and Nd(III):Phe:Mg(II) complexes in DMF:Water (50% v/v) solvent.	142
Fig. 6.5	UV-vis absorption spectra of the <i>4f-4f</i> electronic transitions of Nd ³⁺ , Nd(III):Met and Nd(III):Met:Mg(II) complexes in ACN:Water(50% v/v) solvent.	144
Fig. 6.6	UV-vis absorption spectra of the <i>4f-4f</i> electronic transitions of Nd ³⁺ , Nd(III):Met and Nd(III):Met:Mg(II) complexes in Dioxane:Water(50% v/v) solvent.	144
Fig. 6.7	UV-vis absorption spectra of the <i>4f-4f</i> electronic transitions of Nd ³⁺ , Nd(III):Leu and Nd(III):Leu:Mg(II) complexes in DMF:Water (50% v/v) solvent.	146
Fig. 6.8	UV-vis absorption spectra of the <i>4f-4f</i> electronic transitions of Nd ³⁺ , Nd(III):Leu and Nd(III):Leu:Mg(II) complexes in Methanol:Water (50% v/v) solvent.	146

Lists of Tables

Table number	Table Caption	Page no.
Chapter- 1		
Table 1.1	Discovery of the lanthanides	1
Table 1.2	Properties of amino acids	7
Table 1.3	Comparison of Magnesium with Lanthanide ion characteristics	11
Chapter- 2		
Table 2.1	Selection rules for magnetic dipole and induced electric dipole transitions	28
Table 2.2	Hypersensitive transitions of Lanthanide ions	29
Table 2.3	The Zero-order energies and partial derivatives* with respect to F_K and ξ_{4f} parameters for Pr(III)	32
Table 2.4	Matrix elements* $U^{(\lambda)}$ for Pr(III) aquo	35
Chapter- 3		
Table 3.1	Computed values of the energy interaction parameters; percent covalency (δ), bonding ($b^{1/2}$), Nephelauxetic ratio (β), Racah parameters E_k , Lande Spin-orbit interactions $\xi_{4f} (cm^{-1})$, and Slater-Condon factor $F_k (cm^{-1})$ parameter of Pr^{3+} and its complexes in 50% (v/v) aquated solvents.	49
Table 3.2	Computed and observed values of energy (cm^{-1}) and RMS values for Pr^{3+} and its complexes in (50% v/v) aquated solvents.	50
Table 3.3	Observed and calculated oscillator strengths ($P \times 10^6$) and Judd-Ofelt intensity parameters (T_λ , $\lambda = 2, 4, 6 \times 10^{10} cm^{-1}$) for Pr^{3+} complex with L-phenylalanine and Mg^{2+} in aquated solvents.	51
Table 3.4	Observed and calculated oscillator strengths ($P \times 10^6$) and Judd-Ofelt intensity parameter (T_λ , $\lambda = 2, 4, 6 \times 10^{10} cm^{-1}$) parameters of Pr(III) with L-phenylalanine in presence of Mg^{2+} in aquated DMF solvent at different pH.	54
Table 3.5	Computed value of energy interaction parameters Slater-Condon	

	$F_K(\text{cm}^{-1})$, Spin-Orbit Interaction $\xi_{4f}(\text{cm}^{-1})$, Nephelauxetic ratio (β), bonding ($b^{1/2}$), and covalency (δ) parameters of Pr(III) with L-phenylalanine in presence/absence Mg^{2+} in aquated DMF solvent.	55
Table 3.6	Observed and calculated oscillator strengths ($P \times 10^6$) and Judd-Ofelt intensity parameter (T_λ , $\lambda = 2, 4, 6 \times 10^{10} \text{ cm}^{-1}$) parameters for Pr(III):Phe:Mg(II) complex at 298 K and in different time intervals.	58
Table 3.7	Observed and calculated oscillator strengths ($P \times 10^6$) and Judd-Ofelt intensity parameter (T_λ , $\lambda = 2, 4, 6 \times 10^{10} \text{ cm}^{-1}$) parameters for Pr(III):Phe:Mg(II) complex at 303 K and in different time intervals.	59
Table 3.8	Observed and calculated oscillator strengths ($P \times 10^6$) and Judd-Ofelt intensity parameter (T_λ , $\lambda = 2, 4, 6 \times 10^{10} \text{ cm}^{-1}$) parameters for Pr(III):Phe:Mg(II) complex at 308 K and in different time intervals.	60
Table 3.9	Observed and calculated oscillator strengths ($P \times 10^6$) and Judd-Ofelt intensity parameter (T_λ , $\lambda = 2, 4, 6 \times 10^{10} \text{ cm}^{-1}$) parameters for Pr(III):Phe:Mg(II) complex at 313 K and in different time intervals.	61
Table 3.10	Rate Constants at different temperatures and Activation Energy for Pr(III):Phe:Mg(II) complex.	63
Table 3.11	Rate constants and thermodynamic parameters for Pr(III):Phe:Mg(II) complex at different temperatures.	63
Chapter- 4		
Table 4.1	Observed and calculated values of oscillator strengths ($P \times 10^6$) and Judd-Ofelt intensity parameter [T_λ , ($\lambda = 2, 4, 6$) $\times 10^{10} \text{ cm}^{-1}$] of Pr^{3+} with L-methionine in presence/absence of Mg^{2+} in various aquated organic solvent (50% v/v).	83
Table 4.2	Computed value of energy interaction parameters Slater-Condon $F_K(\text{cm}^{-1})$, Spin-Orbit Interaction $\xi_{4f}(\text{cm}^{-1})$, Nephelauxetic ratio (β), bonding ($b^{1/2}$), and covalency (δ) parameters of Pr^{3+} free ion, Pr(III) with Methionine in presence and absence of Mg^{2+} in various aquated organic solvents.	84
Table 4.3	Observed and calculated oscillator strengths ($P \times 10^6$) and Judd-Ofelt intensity parameters [T_λ , ($\lambda = 2, 4, 6$) $\times 10^{10} \text{ cm}^{-1}$] of Pr^{3+} with L-methionine in presence/absence of Mg^{2+} in different pH in aquated DMF solvent.	86

Table 4.4	Computed value of energy interaction parameters Slater-Condon $F_K(\text{cm}^{-1})$, Spin-Orbit Interaction $\xi_{4f}(\text{cm}^{-1})$, Nephelauxetic ratio (β), bonding ($b^{1/2}$), and covalency (δ) parameters of Pr^{3+} with Methionine in presence/absence Mg^{2+} in different pH in aquated DMF solvent.	87
Table 4.5	Observed and calculated oscillator strengths ($P \times 10^6$) and Judd-Ofelt intensity parameters [T_λ ($\lambda = 2, 4, 6$) $\times 10^{10} \text{ cm}^{-1}$]: At 298 K and in various time intervals for Pr(III):Met:Mg(II) complex.	90
Table 4.6	Observed and calculated oscillator strengths ($P \times 10^6$) and Judd-Ofelt intensity parameter [T_λ ($\lambda = 2, 4, 6$) $\times 10^{10} \text{ cm}^{-1}$] parameters: At 303 K and in various time intervals for Pr(III):Met:Mg(II) complex.	91
Table 4.7	Observed and calculated oscillator strengths ($P \times 10^6$) and Judd-Ofelt intensity parameter [T_λ ($\lambda = 2, 4, 6$) $\times 10^{10} \text{ cm}^{-1}$]: At 308 K and in various time intervals for Pr(III):Met:Mg(II) complex.	92
Table 4.8	Observed and calculated oscillator strengths ($P \times 10^6$) and Judd-Ofelt intensity parameter [T_λ ($\lambda = 2, 4, 6$) $\times 10^{10} \text{ cm}^{-1}$]: At 313 K and in various time intervals for Pr(III):Met:Mg(II) complex.	93
Table 4.9	Rate Constants and Activation Energy for Pr(III):Met:Mg(II) complex at various temperatures.	95
Table 4.10	Rate constants and thermodynamic parameters for Pr(III):Met:Mg(II) complex at various temperatures.	95
Chapter- 5		
Table 5.1	Observed and calculated P and T_λ ($T_\lambda, \lambda = 2, 4, 6 \times 10^{10} \text{ cm}^{-1}$) intensity parameters of Pr(III) with L-leucine in presence and absence of Mg^{+} in different aquated organic solvents.	114
Table 5.2	Computed value of $F_K(\text{cm}^{-1})$, $\xi_{4f}(\text{cm}^{-1})$, β , $b^{1/2}$, and δ parameters of Pr(III) free ion, Pr(III) with L-leucine in the presence and absence of Mg^{2+} .	115
Table 5.3	Computed value of $F_K(\text{cm}^{-1})$, $\xi_{4f}(\text{cm}^{-1})$, β , $b^{1/2}$, and δ parameters of Pr(III) free ion, Pr(III) with L-leucine in the presence and absence of Mg^{2+} at various pH.	117
Table 5.4	Observed and calculated P and T_λ ($\lambda = 2, 4, 6 \times 10^{10} \text{ cm}^{-1}$) intensity parameter of Pr(III) with L-leucine in the presence and absence of Mg^{2+} in different pH mediums.	118

Table 5.5	Observed and calculated P and T_{λ} , ($\lambda = 2, 4, 6$) at 298 K and in various time intervals for the complex Pr(III):Leu:Mg(II).	121
Table 5.6	Observed and calculated P and T_{λ} , ($\lambda = 2, 4, 6$) at 303 K and in various time intervals for the complex Pr(III):Leu:Mg(II).	122
Table 5.7	Observed and calculated P and T_{λ} , ($\lambda = 2, 4, 6$) at 308 K and in various time intervals for the complex Pr(III):Leu:Mg(II).	123
Table 5.8	Observed and calculated P and T_{λ} , ($\lambda = 2, 4, 6$) at 313 K and in various time intervals for the complex Pr(III):Leu:Mg(II).	124
Table 5.9	Rate Constants and Activation Energy for Pr(III):Leu:Mg(II) complex at various temperatures.	126
Table 5. 10	Rate constants and thermodynamic parameters for Pr(III):Leu:Mg(II) complex at various temperatures.	126
Chapter- 6		
Table 6.1	Computed value of energy interaction parameters Slater-Condon F_K (cm^{-1}), Spin-Orbit Interaction ζ_{4f} (cm^{-1}), Nephelauxetic ratio (β), bonding ($b^{1/2}$), and covalency (δ) parameters of Nd(III) free ion, Nd(III) with L-phenylalanine in the presence and absent of Mg^{2+} .	143
Table 6.2	Computed value of energy interaction parameters Slater-Condon F_K (cm^{-1}), Spin-Orbit Interaction ζ_{4f} (cm^{-1}), Nephelauxetic ratio (β), bonding ($b^{1/2}$), and covalency (δ) parameters of Nd(III) free ion, Nd(III) with L-methionine in the presence and absent of Mg^{2+} .	145
Table 6.3	Computed value of energy interaction parameters Slater-Condon F_K (cm^{-1}), Spin Orbit Interaction ζ_{4f} (cm^{-1}), Nephelauxetic ratio (β), bonding ($b_{1/2}$), and covalency (δ) parameters of Nd(III) free ion, Nd(III) with L-leucine in presence and absent of Mg^{2+} .	147

CONTENTS

<i>Lists of Figures</i>	v-viii
<i>Lists of Tables</i>	ix-xii
Chapter- 1: Introduction	1-25
1.1 lanthanide	1-2
1.1.1 General features of Lanthanides	2-3
1.1.2 Importance of lanthanides	3-4
1.2 Magnesium	4
1.2.1 Role of Mg^{2+} in biological system	4-6
1.3 Amino Acids	6-7
1.3.1 Essential amino acids and Non-essential amino acids	8
1.3.2 L-phenylalanine	8
1.3.3 L-methionine	9
1.3.4 L-leucine	9-10
1.4 Role of lanthanide in biochemistry	10-11
1.5 Metal Complexes of Amino acids with Lanthanide ions	11-14
1.6 Literature Survey	14-18
1.7 Aims and Objectives	18-19
References	20-25
Chapter- 2: Methodology	26-42
2.1 Introduction	26
2.1.1 Magnetic Dipole Transition	26
2.1.2 Induced Electric Dipole Transition	26-27
2.1.3 Electric Quadrupole Transition	27
2.1.4 Selection Rules	27-28
2.1.5 Hypersensitive and Non-hypersensitive transitions	28-29

	2.1.6 Pseudohypersensitive transitions	30
2.2 Theoretical		30-31
	2.2.1 Energy parameters	31-33
	2.2.2 Intensity parameters	33
	2.2.2.1 Oscillator strength (P)	33-34
	2.2.2.2 Judd-Ofelt parameters (T_{λ})	34-35
	2.2.3 Reaction dynamics/Thermodynamics theory	36
2.3 Experimental		36
	2.3.1 Materials used	36-37
	2.3.2 Methods	37
	2.3.2.1 Stock solution preparation	37
	2.3.2.2 Experimental procedure	38
References		39-42
CHAPTER- 3: Absorption spectral and thermodynamic analysis for the complexation of Pr^{3+} with L-phenylalanine in the presence/ absence of Mg^{2+} using 4f-4f transitions spectra as probe		43-75
3.1 Introduction		43
	3.1.1 Phenylalanine	43-44
	3.1.2 Bonding nature of L-phenylalanine with Praseodymium	44-46
3.2 Experimental Section		46
	3.2.1 Materials and Methods	46
3.3 Calculations		46
	3.3.1 Energy parameters	47
	3.3.2 Intensity parameters	47
	3.3.3 Reaction dynamics/Thermodynamics theory	47
3.4 Results and Discussions		48-70

3.5 Conclusion	70-71
References	72-75
CHAPTER- 4: Complexation of Pr^{3+} with L-methionine in the presence/absence of Mg^{2+}: their reaction dynamics and thermodynamic properties	76-106
4.1 Introduction	76
4.1.1 Methionine	76-77
4.1.2 Bonding nature of L-methionine with Praseodymium	77-78
4.2 Experimental Section	79
4.2.1 Materials and Methods	79
4.3 Calculations	80
4.3.1 Energy parameters	80
4.3.2 Intensity parameters	81
4.3.3 Reaction dynamics/thermodynamics theory	81
4.4 Results and Discussions	82-101
4.5 Conclusion	101-102
References	103-107
CHAPTER- 5: Absorption spectral analysis for the complexation of Pr^{3+} with L-leucine in the presence/absence of Mg^{2+}: 4f-4f transition as a probe	108-136
5.1 Introduction	108
5.1.1 Leucine	108-109
5.2 Materials And Methods	109-110
5.3 Metal complexes of Lanthanide with Amino acids	110-111
5.4 Calculations	111
5.4.1 Energy parameters	111

	5.4.2 Intensity parameters	112
	5.4.3 Reaction dynamics/Thermodynamics theory	112
5.5 Results and Discussions		113-132
5.6 Conclusion		132-133
References		134-136
CHAPTER 6: Absorption spectral study of Nd(III) with L-phenylalanine, L-methionine, L-leucine in presence/absence of Mg(II)		137-153
6.1 Introduction		137-138
6.2 Metal complexes of Lanthanide with Amino acids		139-140
6.3 Experimental Section		140
	6.3.1 Materials and Methods	140-141
6.4 Calculations		141-142
6.5 results and Discussions		142-150
6.6 Conclusion		150
References		151-153
APPENDIX-I PLAGIARISM REPORT		
APPENDIX-II Workshop and Seminars attended		
APPENDIX-III Lists of Publications		

CHAPTER 1

INTRODUCTION

This chapter provides information on the discovery, characteristics, significance, and applications of lanthanide. We discussed at great length the roles that magnesium (Mg^{2+}) plays in our biological systems. The properties, roles, and significance of the three selected ligands (L-phenylalanine, L-methionine, and L-leucine) were fully elucidated. Furthermore, the functions of lanthanides in biochemistry and their interactions with amino acids are included. The Aims and objectives of the study are also highlighted in this chapter.

1.1 Lanthanide

The Lanthanides are the f-block series the *f*-block series where the differentiating electron reaches the antepenultimate shell's 4f orbital. This series starts from Lanthanum ($_{57}\text{La}$) and proceeds through the subsequent 14 elements i.e., Lutetium ($_{71}\text{Lu}$). They are collectively called rare earth with the generic symbol “Ln”. Since the outermost and penultimate shells each contain the same amount of electrons, they are quite similar to one another.



The lanthanide correlates to the 4f electron shell's steady filling, wherein the outer $5s^2$ and $5p^6$ shells are there to shield them. With n ranging from 0 (La) to 14 (Lu), lanthanides have the typical electronic configuration $[\text{Xe}]4f^n5d^16s^2$, and their most stable oxidation state particularly in water is +3 with a $[\text{Xe}]4f^n$ arrangement. However, a rich chemistry of their divalent state is already emerging in nonaqueous solvents [1,2].

Table 1.1: Lanthanides and their discovery [3].

Lanthanide	Etymology of Name	Year	Discoverer
Lanthanum	Lanthanum: Greek for “to lie hidden”	1839	Mosander
Cerium	Ceres, an asteroid discovered in 1801	1803	1. Berzelius and Hisinger 2. Klaproth
Praseodymium	From Greek: prasios = green; dymium = twin	1885	Von Welsbach
Neodymium	From Greek: Neo = new; dymium = twin	1885	Von Welsbach
Promethium	Prometheus, the greek God who stole fire from Heaven	1947	1. Marinsky 2. Glenn

	for men's use.		3. Coryel
Samarium	From its ore, Samarskite, named after the Russian engineer Samarski	1879	De Boisbaudran
Europium	Europe	1889	Crookes
Gadolinium	After the Finnish chemist Gadolin	1880	Marignac
Terbium	After the town of Ytterby in Sweden	1843	Mosander
Dysprosium	From Greek: Dysprositors = hard to get at	1886	De Boisbaudran
Holmium	Holmia, Latinized version of Stockholm	1879	1. Cleve 2. Soret
Erbium	After the town of Ytterby in Sweden	1843	Mosander
Thulium	After Thule, the Roman name for the northernmost region of the inhabitable world.	1878	Cleve
Ytterbium	After the town of Ytterby in Sweden	1878	Marignac
Utecium	Lutetia, Latin for Paris	1908 1907	1. Von Welsbach 2. Urbain

1.1.1 General features of lanthanides

Lanthanide ions exhibit 3 types of electronic transitions. The banned and weak intra configuration $f-f$ transitions, whose absorption coefficients are often M^{-1} and less than $10 M^{-1} cm^{-1}$. The associated transitions are relatively narrow, and the barycenter of the split bands caused by the ligandfield is not greatly affected by the ion's chemical environment. Because of this, lanthanide ions are excellent candidates for optical probes. For instance, the symmetry of the metal-ion environment is precisely described by a rigorous investigation of the splitting utilizing group-theory concepts [4]. Additionally, the majority of the ions are luminescent, either fluorescently [e.g., Yb(III), Er(III), Ho(III), Nd(III), and Pr(III)] or phosphorescently [e.g., red Gd(III), Eu(III), which emits in the UV, orange Sm(III), yellow Dy(III), blue Tm(III) and

green Tb(III)]. Their emission colors cover the full electromagnetic spectrum, from ultraviolet (UV) to visible and near-infrared (NIR) ranges (0.3-2.2 μm). They can be utilized in trichromatic phosphors for illumination since they are often quite pure. The presence of "lanthanide contraction," a constant reduction in ionic and atomic size with ascending atomic number, is a crucial characteristic of lanthanide elements. The increased nuclear charge caused by inner sphere 4f-electrons is the primary factor for lanthanide shrinkage [5,6].

The overall lanthanide contraction is of comparable size as the expansion observed while transitioning from the first to the second set of transitions, and as a result, the contraction may have been predicted to happen when transitioning from second to third. With the consequence that the 2nd and 3rd members of each set of transition elements have almost identical sizes and characteristics, the interaction of lanthanides in reality essentially cancels out the projected rise [7,8].

1.1.2 Importance of Lanthanide

The potential of trivalent lanthanide to be used as structural probes has caught the interest to study the ions of trivalent lanthanide with ligands such as peptides or amino acids and their bonding character in the field of biological chemistry [9–11]. Although only traces of lanthanides have been found in whole-body analyses, it has been noted that they have no known biological role. The lanthanide coordination compounds in solution have innovative approaches in the development of laser materials, the study of transuranic elements, and as spectral models for analyzing the structures, functions, and reactivity of bio-systems involving lanthanides as spectral probes, despite their minor role in our biological systems [12]. Lanthanide complexes have been

investigated for their intriguing and crucial trial such as their ability to bind oxygen reversibly, structural probes in biological systems, and catalytic activity in the hydrogenation of olefins [13–15]. Lanthanide salts were first investigated in a clinical trial for antimicrobial, anticoagulant, and other pharmacological properties in the early part of the century. Lanthanide ions possess the properties of antitumor, antibacterial, and antiviral agents when coordinate with organic ligands and participate effectively in many important biochemical activities [16–18].

Lanthanides, rare earth elements (RE), are essential components of numerous modern technologies such as;



1.2 Magnesium

Magnesium is a vital component that is found in the human body as Mg^{2+} ion and it is the 4th highest amount of cation present in the human body is magnesium. After potassium, magnesium is the cation that is found in cells in the greatest concentration [18]. It serves a variety of purposes in the human body, notably as a cofactor [19]. The average adult has a body composition magnesium content of roughly 1000 mmol, or 24 g, or 20 mmol/kg of lean body mass [4]. Muscles as well as other soft tissue retain roughly 40–50% of the overall magnesium content, whereas bones retain approximately 50–60% of it.

1.2.1 Role of Mg^{2+} in biological system

It has been well documented that Magnesium (Mg^{2+}) supplies energy by promoting the synthesis of adenosine triphosphate (ATP), which runs the billions of cells in our

body. The energy provided by this mineral is essential for the functioning of both plants' and animals' enzymes [20]. Numerous essential processes, including muscle contraction, neuromuscular transmission, glycemic regulation, myocardial contraction, and blood pressure, are regulated by Mg^{2+} [21,22].

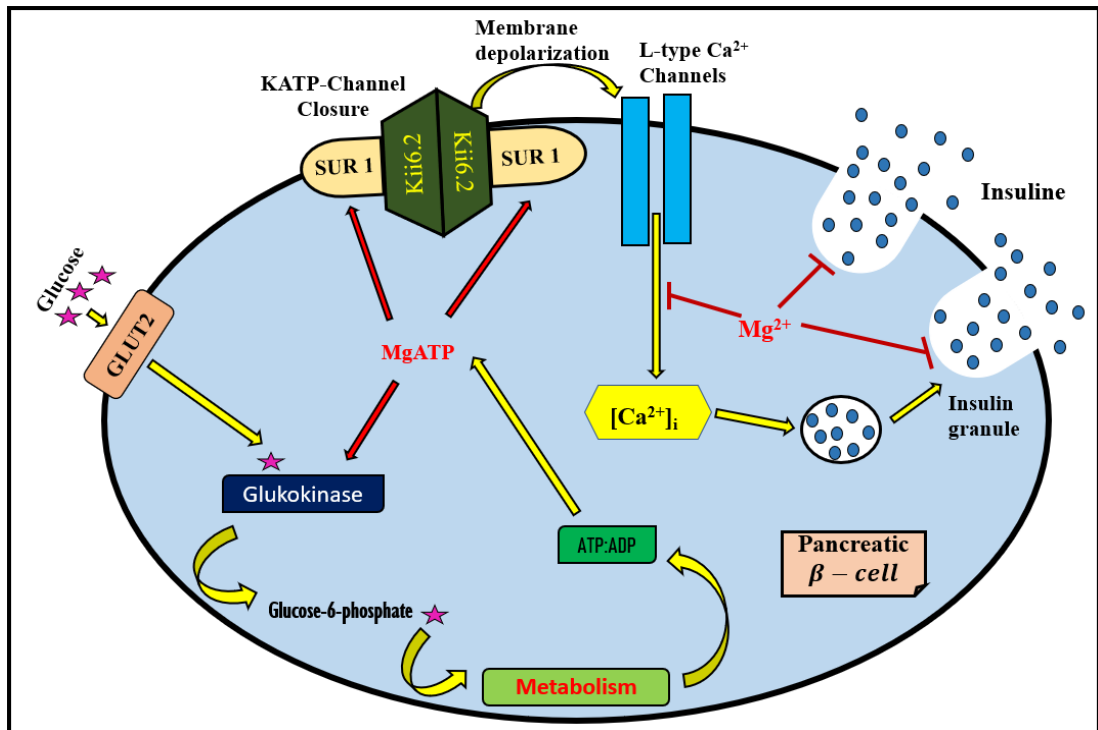


Figure 1.1: Regulatory role of Mg^{2+} in the insulin secretion from pancreatic beta cells.

In addition to being a necessary element for maintaining good health, Mg^{2+} is also crucial for the control of insulin and glucose homeostasis. Mg^{2+} deficiency (MgD) and type 2 diabetes mellitus (T_2D) are clinically linked, however, the molecular mechanisms by which Mg^{2+} contributes to insulin resistance (IR) still remain obscure [23–25].

This macronutrient contributes to the production of RNA and DNA, protein, lipid, and carbohydrate metabolism, cell membrane integrity, bone and calcium (Ca)

metabolism, and neurological and immune system development by acting as a cofactor or stimulator in more than 300 enzymatic processes [22,26,27].

Although magnesium plays an important role in our biological system, due to its diamagnetic character, they are spectroscopically inactive. The lanthanide is spectroscopically active due to its paramagnetic nature, therefore the replacement of Mg(II) by lanthanide(III) can give pertinent information about its interaction with the amino acids. Pr(III) possesses ionic radii comparable to Mg^{2+} and they exhibit an isomorphic character with the bonding behavior of Mg(II) with biomolecules, its complexation can provide useful information in the study of biological systems.

1.3 Amino Acids

Amino acids are molecules that combine with other molecules to form proteins and are considered as the building blocks of life [28]. Despite the existence of hundreds of amino acids in nature, proteins that are made up of alpha-amino acids are among the most common. However, the genetic coding contains just 22 alpha amino acids [29].

Depending on where the main structural functional groups are located, amino acids can be categorized as alpha (α), beta (β), gamma (γ), or delta (δ) amino acids. In addition, there are classifications for side chain group type, polarity, and ionization (aliphatic, acyclic, aromatic, containing hydroxyl or sulfur, etc.) [30].

Table 1.2: Properties of amino acids

Sl. No	Amino Acids and symbol	Class	Polarity	Abundance in Protein	Essential/ Non-essential
1	<u>Alanine</u> (Ala)	Aliphatic	Nonpolar	8.76	Non-essential
2	<u>Arginine</u> (Arg)	Fixed cation	Basic polar	5.78	Non-essential
3	Asparagine (Asn)	Amide	Polar	3.93	Non-essential
4	Aspartate (Asp)	Anion	Brønsted base	5.49	Non-essential
5	Cysteine (Cys)	Thiol	Brønsted acid	3.87	Non-essential
6	Glutamine(Gln)	Amide	Polar	5.02	Non-essential
7	Glutamate (Glu)	Anion	Brønsted base	7.14	Non-essential
8	Glycine (Gly)	Aliphatic	Nonpolar	5.53	Non-essential
9	Histidine (His)	Aromatic cation	Brønsted acid and base	1.25	Essential
10	Isoleucine (Ile)	Aliphatic	Nonpolar	2.91	Essential
11	Leucine (Leu)	Aliphatic	Nonpolar	6.73	Essential
12	Lysine (Lys)	Cation	Brønsted acid	2.32	Essential
13	Methionine (Met)	Thioether	Nonpolar	5.19	Essential
14	Phenylalanine (Phe)	Aromatic	Nonpolar	9.68	Essential
15	Proline (Pro)	Cyclic	Nonpolar	5.49	Non-essential
16	Serine (Ser)	Hydrocyclic	Polar	2.26	Non-essential
17	Threonine (Thr)	Hydrocyclic	Polar	6.32	Essential
18	Tryptophan (Trp)	Aromatic	Nonpolar	7.03	Essential
19	Tyrosine (Tyr)	Aromatic	Brønsted acid	1.38	Non-essential
20	Valine (Val)	Aliphatic	Nonpolar	3.9	Essential
21	Selenocystein (Sec)	-	-	-	Essential
22	Pyrrolysine (Pyl)	-	-	-	Non-essential

1.3.1 Essential amino acids and Non-essential amino acids

Amino acids are categorized as essential or non-essential depending on several factors. Amino acids which cannot be produced or synthesized by our body and are taken up as food supplements are called essential amino acids.

On the contrary, 'alpha'-amino acids that are required for individual health and growth, which are produced by the person's body are referred to as non-essential amino acids. There are 9 essential and 11 non-essential amino acids.

However, for the current study, we have chosen only three essential amino acids (l-phenylalanine, L-methionine & L-leucine).

1.3.2 L-phenylalanine

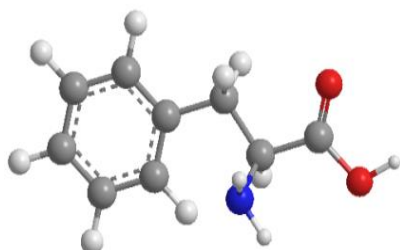


Figure 1.2: Structure of L-phenylalanine

L-phenylalanine is an aromatic essential amino acid required for the production of dopamine and norepinephrine neurotransmitters. They play a crucial role in the structure and operation of several proteins and enzymes [31,32]. L-phenylalanine deprivation may result in mental illnesses such as decreased libido, sadness, anxiety, and chronic tiredness [33]. Likewise, an excessive buildup of L-phenylalanine may result in pathological disorders such as chronic obstructive lung disease, heart failure, coronary artery disease, pulmonary hypertension, and systemic hypertension [34].

1.3.3 L-methionine

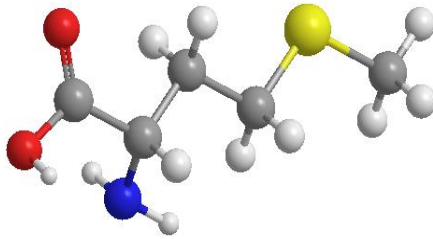


Figure 1.3: Structure of L-methionine

Methionine, also known as 2-amino-4-(methylthio)butanoic acid, is a sulfur-containing aliphatic essential amino acid that is indispensable for many physiological and biochemical metabolism. Supplementing or restricting methionine can affect an organism's natural antioxidant capacity by causing the synthesis of endogenous enzymes that reduce oxidative stress and, as a result it will lead to DNA damage, neuropsychiatric disorders, cardiovascular disease, cancer, and neurodegenerative illnesses [35].

1.3.4 L-leucine

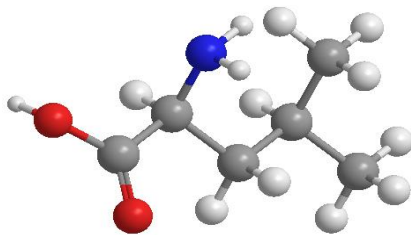


Figure 1.4: Structure of L-leucine

Leucine, or 2-Amino-4-methylpentanoic acid, is a branch-chained amino acid that functions as a substrate for protein synthesis and thus becomes crucial for modulating protein metabolism [36]. Leucine's carbon skeleton can also be used to produce ATP, just like that of other amino acids. The effects of leucine supplementation have been studied in a variety of conditions, including aging, muscle injury, obesity,

protein/energy deficiency, and diabetes mellitus [37,38]. The prevalence of metabolic illnesses has increased to alarming levels around the world, and since Leucine modulates signaling pathways involved in metabolism regulation, researching nutritional supplements containing leucine may be useful in the treatment and prevention of obesity and diabetes as a critical role [39,40].

1.4 Role of lanthanide in biochemistry

Despite the fact that f-block elements, which are part of the lanthanide and actinide transition series, are not known to play a crucial part in the processes of life, they are nonetheless important. Of all the inorganic elements in the periodic table, the lanthanides without a doubt present some of the most intriguing, difficult, and significant chemical and biological challenges [10]. This is mainly due to the characteristics that their outer electron configuration and related energy levels impart, in addition to their negligible chemical and radio toxicities. The paramagnetic nature of lanthanides is responsible for the higher magnetic moment due to the number of unpaired electrons in 4f orbitals [11,15]. They play a crucial role in practical applications such as Nuclear Magnetic Resonance Spectroscopy (NMR) and Nuclear Magnetic Resonance Imaging (MRI). Because of their strong magnetic moments and high relaxation efficiencies, Gd(III) complexes, particularly those containing polyamino-polycarboxylic acids, are effective contrast enhancers. Following the compartmentalization of sodium during the assault of *lschaemia*, dysprosium and thulium chelates have proven to be good shift reagents. For research using electron microscopy or x-ray diffraction, lanthanides can be employed as heavy atom "stains" [3,4].

Thermodynamic properties of metal ion binding site, e.g. for Mg(II) can be elucidated through competition or exchange reactions with lanthanide ions. This is important because Magnesium an essential and ubiquitous element has very few properties, which can be used to probe its Biochemistry *in situ*. The lanthanide(III) ions, make almost a biomimetic agent for Mg(II) (Table 1.3) [41].

Table 1.3: Variations in the properties of magnesium and lanthanide ions.

Property	Ln(III)	Mg(II)
Coordination number	6-12 reported 8 or 9 favoured	6-12 reported 6-7 favoured
Coordination Geometry	Highly flexible	Highly flexible
Preference for donor sites	O>N>S	O>N>S
Ionic radii (\AA)	0.86-1.22 (CN 6-9)	1.00-1.18 (CN 6-9)
Type of bonding	Electrostatic	Electrostatic
Hydration number	8 or 9	6
Water exchange rate constant (s^{-1})	$\sim 5 \times 10^7$	$\sim 5 \times 10^8$
Crystal field stabilization	Negligible	None
Spectroscopic behaviour	Spectroscopic in nature (both optical and magnetic)	Spectroscopically inactive
Complex stability	Strong complexes	Weak complexes

1.5 Metal Complexes of Amino acids with Lanthanide ions

Since amino acids are the most essential building blocks of biological systems, our knowledge of how lanthanide ions interact with these systems can be enhanced. This can be done by researching the lanthanide-amino acid complexes in solution chemistry and discovering different species that might be in dynamic equilibria in

solution in physiological settings. The flexibility with which a large number of coordinating O-atoms can be accommodated structurally is possibly attributable to the ionic nature of lanthanide bonding. The entire structure, which is characterized by such a great deal of Ln-O bonding, is stabilized by the lanthanide ions' strong Lewis acidity and hence high oxophilicity [9].

Through the extensive coordination chemistry of the lanthanide ions with amino acids under both low- and high-pH conditions, a great variety of coordination modes have been identified for these biologically significant ligands [45]. Extensive bridging interactions by the carboxylate groups, be it in the skeleton or in the side chain, are key to the formation of these complexes; the amino group remains protonated at low pH and affects a complex's solid-state structure by participating in hydrogen-bonding interactions between different complex units. At higher pH, however, lanthanide coordination by the neutral amino group has been found, in addition to the expected coordination by the carboxylate group(s). It is probably the synergetic coordination of the carboxylate and amino groups that leads to the assembly of these highly sophisticated and aesthetically pleasing cluster complexes [43].

Amino acids generally possess functional groups ($-\text{NH}_2$ & $-\text{COOH}$) with the capability to tune the size and dimensions of optimistic materials, while their side chains (-R group) remain intact [42]. When Amino acids are in the gaseous phase they exist in the neutral form. The amino acids exist in the neutral form when they are in the gas phase [43]. However, they exist in zwitterions form when they are in the aqueous solution [44,45]

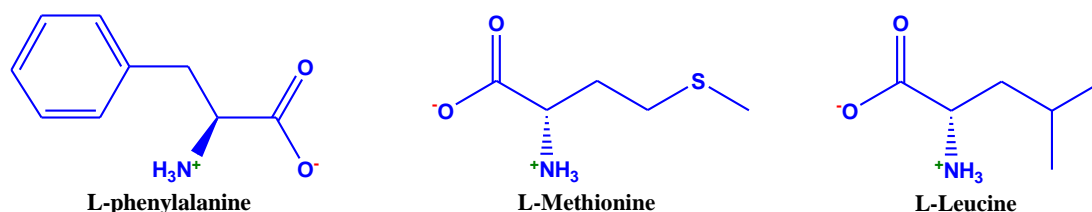


Fig 1.5: Structure of the three essential amino acids in the zwitterionic form.

Bonding of the ligand with the metal relies on the pH values, that is when the pH value is low, the oxygen atom binds with the metal while if the pH value is high then both Oxygen and nitrogen bond with the metal [46].

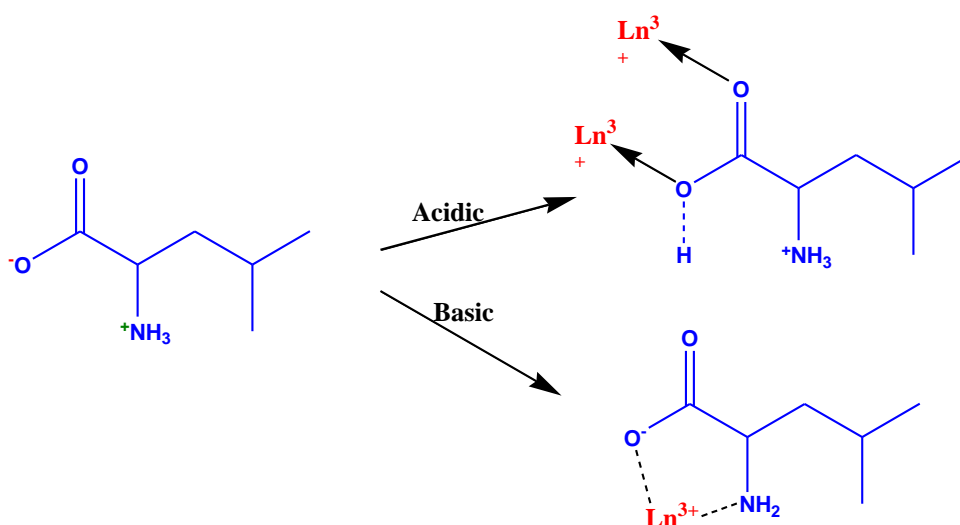


Fig 1.6: Bonding nature of the zwitterions L-leucine under different pH.

On the matter of complex formation, lanthanides are classified as “class A” or “hard” acceptors, and therefore prefer “class A” or “hard” donor ligands (in the order $\text{O} > \text{N} > \text{S}$ and $\text{F} > \text{Cl}$). Coordination numbers vary from 6 to 12 in general; biologically relevant coordination numbers are 8 or 9. Consequently, the complexes can have a variety of geometrical conformations [9]. In the presence of water, complexes with nitrogen, sulphur and halogen (except fluorine) are not suitable, but if these donor

sites are a part of multi-donor ligands these donor sites are involved in strong complexation with lanthanides.

1.6 Literature Survey

In the early part of the 20th century, human clinical trials were conducted to determine the potential of lanthanide salts to have antimicrobial, anticoagulant, and other pharmacological effects [47,48].

Misra et al suggested an altered procedure for evaluating spectral parameters (i.e., bonding, nephelauxetic, spin-orbital interaction, energy interaction, Judd-Ofelt parameters, and oscillator strength) of 4f - 4f transitions in Pr(III) and Nd(III) complexes [49].

K. Binnemans investigated the Judd-Ofelt intensity parameter's sensitivity and dependability by contrasting simulated and experimental absorption spectra [50].

Misra and Somerer studied the $^3\text{H}_4 \rightarrow ^3\text{P}_2$, $^3\text{H}_4 \rightarrow ^3\text{P}_1$, $^3\text{H}_4 \rightarrow ^3\text{P}_0$, and $^3\text{H}_4 \rightarrow ^1\text{D}_2$ transitions of Pr(III) complexes in solution media. These transitions exhibit notable intensification, as revealed by the quantitative study of 4f-4f spectra and comparing absorption spectrophotometry absorbance difference. Furthermore, when Pr(III) combines with ligands that have various structural properties and binding capacities, it exhibits a wide range of oscillator strength. Given that they do not adhere to the selection criteria, these transitions cannot be regarded as hypersensitive. They reported that though these transitions do not follow the selection rule yet high sensitivity can be observed in Pr(III) transitions. They denoted such transitions as "Ligand Mediated Pseudohypersensitivity" after taking into account the solution spectra of 173 species [51].

Henrie et al have demonstrated that high values suggest inner sphere complexation whereas outer sphere complexation is indicated by low oscillator strength levels. The present complexes have low values for the T_2 , T_4 , and T_6 variables, suggesting that outer-sphere complexation is more prevalent [52].

Jerico et al investigated how the phenomenological 4f-4f intensity behaves in compounds containing the Nd^{3+} ion with L-histidine, L-glutamic acid, L-aspartic acid, glycine, Aspartame, and DL-malic acid in aqueous solution, based on the pK values and partial charges of these molecules' carboxylate groups on the oxygen. According to their findings, the strength of the hypersensitive transitions increases as the pH rises to a level of about 5.4. The Nd^{3+} ion hydrolyzes at pH levels higher than 5.5. T_2 is generally the T_λ parameter that is most responsive to the ligand properties and coordination geometry. When the monocarboxylic and dicarboxylic species were taken into account independently, they discovered that T_2 had changed linearly with Pk_1 [53].

Hussain et al studied trivalent lanthanide compounds with 2,2'-bipyridine and reported on their optical absorbance and NMR results. The ratio of the intra-molecular and paramagnetic shifts has been reported. Additionally, they investigated complexes of Pr, Nd, Ho, Er, and Dy in a variety of solvents (viz, MeOH, pyridine, DMSO, and DMF). Their findings suggested that the chemical conditions of the lanthanide ion have a significant impact on the spectrum content. Research has shown that the ligand polarisation effect may explain why pyridine exhibits the greatest increase in oscillator strength and DMSO exhibits the least rise in oscillator strength [54].

Khan and Iftikhar have investigated lanthanide compounds with mixed ligands. Pr^{3+} , Nd^{3+} , Ho^{3+} , and Er^{3+} compounds in non-aqueous solvents exhibit hypersensitivity and

absorbance spectra (pyridine, DMSO, DMF, and methanol). The oscillator strengths for the hypersensitive and non-hypersensitive transitions were developed, and the ligand (solvent) structures and ligand coordination properties are used to describe changes in oscillator strengths and band shapes concerning the type of solvent [55].

Zhang and Wang examined, measured, and researched the polymer-doped with Neodymium(III) (Nd^{3+}) absorption spectrum (methyl methacrylate). They discovered that the nephelauxetic effect in the spectrum has been compared to the extra Nd^{3+} doped spectrum from different matrices. By employing Taylor series expansion, they calculated the F_2 , F_4 , and F_6 Slater- Condon parameters as well as the Lande parameter. It is based on the supposition that F_2 , F_4 , F_6 , and $4f$ influence how much energy there is between the J levels of the $4f^n$ arrangement. They claimed that there was a link between the covalency factor and the nephelauxetic parameter. Increases in the degree of covalency, mixing of the $4f$ -ligands, and nephelauxetic action all occur together [56].

Sumitra et al investigated the Pr(III) and glutathione reduced (GSH) complex $4f$ - $4f$ transitions in the presence/absence of Zn(II), comparing their absorption and spectral analyses. The studies were conducted in a variety of agitating organic solvents, including CH_3OH , CH_3CN , DMF, and dioxane, as well as their equimolar mixes, at various pH levels (3.0, 4.0, 5.0, and 6.0). According to their findings, DMF is the best solvent, while pH 6 is the most favorable one for complexation [57].

Bendangsenla et al have carried out extensive research on how Pr(III) interacts with nucleosides and nucleotides in various chemical solvents. By varying these assessed factors, it was possible to deduce how Pr(III) binds to various ligands, such as

adenosine and ATP, both with and without the presence of Ca^{2+} . They came to the conclusion that DMF is the most recommended solvent while methanol is the least. This is caused by the N-donor ligand, which is more electronegative than methanol's O-donor ligand. Additionally, it has been noted that adenosine is more sensitive to ATP when they are bound together [58].

As a way to predict in vivo intracellular complexation of uracil with Ca(II) in vitro, Ch. Victory Devi reports the interaction of Pr(III) and Nd(III) with uracil in the presence of Ca(II) in various aqueous organic solvents. According to their findings in this work, Ln(III) ions prefer greater coordination numbers when bound to calcium-selective ligands. This impact should be taken into consideration while using Ln(III) ions to investigate the structure of calcium binding sites in and around biomolecules [59].

Noarem et al investigated the use of several aqueous organic solvents to analyze the absorption spectra caused by the interaction between Pr(III) and the L-tryptophan system displaying 4f-4f transitions in the presence and absence of Zn(II) (methanol, dioxane, acetonitrile and N,N-dimethylformamide). They evaluated energy parameters as well as the intensity parameters to observe the variation in these parameters to study the nature of the bond formed between Pr(III) and L-tryptophan. They reported that DMF was the best solvent for increasing 4f-4f electric dipole intensity out of the four studied [60].

Utilizing UV-Vis absorption spectroscopy, Tiwari et al. investigated the 4f-4f transition spectra of the neodymium ion (Nd^{3+}) in several solvents (water, DMSO, and

DMA). They have computed the energy as well as the intensity parameters using Nd^{3+} absorption spectra ($^4\text{I}_{9/2} \rightarrow ^2\text{P}_{1/2}$, $^4\text{I}_{9/2} \rightarrow ^4\text{G}_{9/2}$, $^4\text{I}_{9/2} \rightarrow ^4\text{G}_{7/2}$, $^4\text{I}_{9/2} \rightarrow ^4\text{G}_{5/2}$, $^4\text{I}_{9/2} \rightarrow ^4\text{F}_{9/2}$, $^4\text{I}_{9/2} \rightarrow ^4\text{F}_{7/2}$) as a probe. They claimed that upon interaction, a covalent bond was formed between the ligand and the Nd^{3+} . Furthermore, it has been claimed that the DMSO has the most impact on Nd^{3+} as compared to water and DMA when it comes to the redshift in energy bands seen for organic solvents [61].

The literature survey revealed that mixed ligand complexes of some transition metals with amino acids have been studied for their synthesis, characterization, and biological importance. Additionally, comparative investigations conducted *in vivo* and *in vitro* have demonstrated how lanthanides bind. Two lanthanide or actinide metal atoms are attached to each transferrin molecule, just like iron, as per research done *in vitro* using the trivalent lanthanides Pu(IV) , Th(IV) , and a variety of others. This was clearly shown by UV difference spectroscopy and other methods [62-64].

1.7 Aims and Objectives

Ln^{3+} can replace Mg^{2+} in many macromolecular processes, including the majority of biosystems, since their radii are comparable, and their biological activities are unaffected. Employing metal and lanthanide complexes as probes in diagnosing medical imaging equipment has been of great importance to the success of these techniques. Kinetic investigations including thermodynamic parameters of the simultaneous complexation of $\text{Pr}^{3+}/\text{Nd}^{3+}$ ion involving biologically important biological ligands in the presence and absence of Mg^{2+} in aqueous and different aquated organic solvents *in vivo* using $4f-4f$ transitions as a probe has not been reported so far, therefore we shall attempt to introduce that observation in this current dissertation.

The scheme will be as follows:

1. To use absorption difference and comparative absorption spectrophotometry involving $4f-4f$ transition as a probe in understanding the binding characteristics of lanthanide with biological ligands.

a) Assessment of Energy interaction parameters

To calculate the various spectral parameters like Slater- Condon (F_k), Lande factor ($\xi 4f$), Nephelauxetic ratio (β), bonding parameter ($b^{1/2}$) and percentage covalency (δ).

b) Assessment of Intensity parameters

To conduct a thorough analysis of the variations in the intensity parameters such as oscillator strength (P) and Judd-Ofelt electric dipole intensity (T_λ , $\lambda=2,4,6$) parameters of complexes in presence and absence of Mg^{2+} in different aquated organic solvents.

2. Kinetic studies of the complexation of lanthanides by determining the rate of reactions using oscillator strengths of $^3H_4 \longrightarrow ^3P_2$ transition against time.

3. Evaluation of thermodynamic parameters.

To attempt to do some preliminary kinetic studies of the complexation of Pr^{3+} with the ligands chosen in the presence and absence of Mg^{2+} metal ion, by evaluating the activation energy (E_a) and thermodynamic parameters like ΔH^0 , ΔS^0 and ΔG^0 .

REFERENCES

- [1] J.G. Bu, Ä.P. Fe, Benefiting from the Unique Properties of Lanthanide Ions, 39 (2006) 53–61. <https://doi.org/10.1021/ar0400894>.
- [2] E. Echenique-Errandonea, R.F. Mendes, F. Figueira, D. Choquesillo-Lazarte, G. Beobide, J. Cepeda, D. Ananias, A. Rodríguez-Diéguez, F.A. Almeida Paz, J.M. Seco, Multifunctional Lanthanide-Based Metal-Organic Frameworks Derived from 3-Amino-4-hydroxybenzoate: Single-Molecule Magnet Behavior, Luminescent Properties for Thermometry, and CO₂ Adsorptive Capacity, *Inorg. Chem.* 61 (2022) 12977–12990. <https://doi.org/10.1021/acs.inorgchem.2c00544>.
- [3] C.H. Evans, *Biochemistry of the Lanthanides*, 1990. <https://doi.org/10.1007/978-1-4684-8748-0>.
- [4] L. Eyring, K.A. Gschneidner, *Handbook on the physics and chemistry for rare earths*. Vol. 24, 1999. <http://www.sciencedirect.com/science/handbooks/0168123/26>.
- [5] J. Bünzli, S. V. Eliseeva, Basics of Lanthanides Photophysics. In *Lanthanide Luminescence*, Hänninen P., Härmä H. *Lanthan. Lumin. Springer Ser. Fluoresc.* (Methods Appl. 7 (2010) 1–45. <https://doi.org/10.1007/4243>.
- [6] S.N. Misra, S.O. Somerer, Absorption Spectra of Lanthanide Complexes in Solution, *Appl. Spectrosc. Rev.* 26 (1991) 151–202. <https://doi.org/10.1080/05704929108050880>.
- [7] M. Seitz, A.G. Oliver, K.N. Raymond, The lanthanide contraction revisited, *J. Am. Chem. Soc.* 129 (2007) 11153–11160. <https://doi.org/10.1021/ja072750f>.
- [8] S.G. Wang, W.H.F. Schwarz, Lanthanide diatomics and lanthanide contractions, *J. Phys. Chem.* 99 (1995) 11687–11695. <https://doi.org/10.1021/j100030a011>.
- [9] A.M. Măciucă, A.C. Munteanu, V. Uivarosi, Quinolone complexes with lanthanide ions: An insight into their analytical applications and biological activity, *Molecules*. (2020). <https://doi.org/10.3390/molecules25061347>.
- [10] J.A. Cotruvo, *The Chemistry of Lanthanides in Biology: Recent Discoveries, Emerging Principles, and Technological Applications*, ACS Cent. Sci. (2019). <https://doi.org/10.1021/acscentsci.9b00642>.
- [11] R.B. Martin, F.S. Richardson, Lanthanides as probes for calcium in biological systems, *Q.Rev.Biophys.* (1979). <https://doi.org/10.1017/S0033583500002754>.
- [12] W. Wernsdorfer, Chemistry brings qubits together, *Nat. Nanotechnol.* 4 (2009) 145–146. <https://doi.org/10.1038/nnano.2009.21>.
- [13] S.N. Misra, M.I. Devi, The synthesis and determination of the octacoordinated

- structure of Pr(III) and Nd(III) complexes with β -diketones and diols in non aqueous solutions: Evidence of some participation of π -electron density of diols with Pr(III) and Nd(III) in complexation, *Spectrochim. Acta - Part A Mol. Biomol. Spectrosc.* (1997). [https://doi.org/10.1016/S1386-1425\(97\)00064-4](https://doi.org/10.1016/S1386-1425(97)00064-4).
- [14] X.M. Qiao, C.X. Zhang, Y.K. Kong, Y.Y. Zhang, A Mononuclear Lanthanide Metal Compounds Based on the Nitronyl Nitroxide Radicals: Synthesis, Crystal Structure, and Magnetic Properties, *Synth. React. Inorganic, Met. Nano-Metal Chem.* 46 (2016) 841–846. <https://doi.org/10.1080/15533174.2014.989594>.
- [15] E.M. Stephens, S. Davis, M.F. Reid, F.S. Richardson, Empirical Intensity Parameters for the $4f \rightarrow 4f$ Absorption Spectra of Nine-Coordinate Neodymium(III) and Holmium(III) Complexes in Aqueous Solution, *Inorg. Chem.* (1984). <https://doi.org/10.1021/ic00194a040>.
- [16] K.B. Gudasi, V.C. Havanur, S.A. Patil, B.R. Patil, Antimicrobial study of newly synthesized lanthanide(III) complexes of 2-[2-hydroxy-3-methoxyphenyl]-3-[2-hydroxy-3-methoxybenzylamino]-1,2-dihydroquinazolin-4(3H)-one, *Met. Based. Drugs*.2007(2007). <https://doi.org/10.1155/2007/37348>.
- [17] S. Alghool, M.S. Zoromba, H.F.A. El-Halim, Lanthanide amino acid Schiff base complexes: Synthesis, spectroscopic characterization, physical properties and in vitro antimicrobial studies, *J. Rare Earths.* 31 (2013) 715–721. [https://doi.org/10.1016/S1002-0721\(12\)60347-0](https://doi.org/10.1016/S1002-0721(12)60347-0).
- [18] M.P. Cabral Campello, E. Palma, I. Correia, P.M.R. Paulo, A. Matos, J. Rino, J. Coimbra, J.C. Pessoa, D. Gambino, A. Paulo, F. Marques, Lanthanide complexes with phenanthroline-based ligands: insights into cell death mechanisms obtained by microscopy techniques, *Dalt. Trans.* 48 (2019) 4611–4624. <https://doi.org/10.1039/c9dt00640k>.
- [19] A.M. Al Alawi, S.W. Majoni, H. Falhammar, Magnesium and Human Health: Perspectives and Research Directions, *Int. J. Endocrinol.* (2018). <https://doi.org/10.1155/2018/9041694>.
- [20] S.M. El-Megharbel, M.S. Refat, F.A. Al-Salmi, R.Z. Hamza, In situ neutral system synthesis, spectroscopic, and biological interpretations of magnesium(Ii), calcium(ii), chromium(iii), zinc(ii), copper(ii) and selenium(iv) sitagliptin complexes, *Int. J. Environ. Res. Public Health.* (2021). <https://doi.org/10.3390/ijerph18158030>.
- [21] J. Bertinato, C.W. Xiao, W.M.N. Ratnayake, L. Fernandez, C. Lavergne, C. Wood, E. Swist, Lower serum magnesium concentration is associated with diabetes, insulin resistance, and obesity in South Asian and white Canadian women but not men, *Food Nutr. Res.* (2015). <https://doi.org/10.3402/fnr.v59.25974>.
- [22] U. Gröber, J. Schmidt, K. Kisters, Magnesium in prevention and therapy, *Nutrients.* (2015). <https://doi.org/10.3390/nu7095388>.

- [23] K. Kostov, Effects of magnesium deficiency on mechanisms of insulin resistance in type 2 diabetes: Focusing on the processes of insulin secretion and signaling, *Int. J. Mol. Sci.* (2019). <https://doi.org/10.3390/ijms20061351>.
- [24] H. Xu, X. Li, H. Adams, K. Kubena, S. Guo, Etiology of metabolic syndrome and dietary intervention, *Int. J. Mol. Sci.* (2019). <https://doi.org/10.3390/ijms20010128>.
- [25] V.A. Salunkhe, R. Veluthakal, S.E. Kahn, D.C. Thurmond, Novel approaches to restore beta cell function in prediabetes and type 2 diabetes, *Diabetologia*. (2018). <https://doi.org/10.1007/s00125-018-4658-3>.
- [26] M. Pelczy, The Role of Magnesium in the Pathogenesis of Metabolic Disorders, (2022).
- [27] G.K. Schwalfenberg, S.J. Genies, The Importance of Magnesium in Clinical Healthcare, *Scientifica (Cairo)*. 2017 (2017). <https://doi.org/10.1155/2017/4179326>.
- [28] G. Zhu, X. Zhu, Q. Fan, X. Wan, Raman spectra of amino acids and their aqueous solutions, *Spectrochim. Acta - Part A Mol. Biomol. Spectrosc.* 78 (2011) 1187–1195. <https://doi.org/10.1016/j.saa.2010.12.079>.
- [29] J.D. Stephenson, S.J. Freeland, Unearthing the root of amino acid similarity, *J. Mol. Evol.* 77 (2013) 159–169. <https://doi.org/10.1007/s00239-013-9565-0>.
- [30] W.R. Taylor, The classification of amino acid conservation, *J. Theor. Biol.* 119 (1986) 205–218. [https://doi.org/10.1016/S0022-5193\(86\)80075-3](https://doi.org/10.1016/S0022-5193(86)80075-3).
- [31] J.D. Fernstrom, M.H. Fernstrom, Tyrosine, phenylalanine, and catecholamine synthesis and function in the brain, in: *J. Nutr.*, 2007. <https://doi.org/10.1093/jn/137.6.1539s>.
- [32] D.E. Matthews, An overview of phenylalanine and tyrosine kinetics in humans, in: *J. Nutr.*, 2007. <https://doi.org/10.1093/jn/137.6.1549s>.
- [33] M. Remko, D. Fitz, R. Broer, B.M. Rode, Effect of metal Ions (Ni²⁺, Cu²⁺ and Zn²⁺) and water coordination on the structure of L-phenylalanine, L-tyrosine, L-tryptophan and their zwitterionic forms, *J. Mol. Model.* (2011). <https://doi.org/10.1007/s00894-011-1000-0>.
- [34] R. Tan, J. Li, F. Liu, P. Liao, M. Ruiz, J. Dupuis, L. Zhu, Q. Hu, Phenylalanine induces pulmonary hypertension through calcium-sensing receptor activation, *Am. J. Physiol. - Lung Cell. Mol. Physiol.* (2020). <https://doi.org/10.1152/AJPLUNG.00215.2020>.
- [35] Y. Martínez, X. Li, G. Liu, P. Bin, W. Yan, D. Más, M. Valdivié, C.A.A. Hu, W. Ren, Y. Yin, The role of methionine on metabolism, oxidative stress, and diseases, *Amino Acids*. (2017). <https://doi.org/10.1007/s00726-017-2494-2>.

- [36] J.M. Han, S.J. Jeong, M.C. Park, G. Kim, N.H. Kwon, H.K. Kim, S.H. Ha, S.H. Ryu, S. Kim, Leucyl-tRNA synthetase is an intracellular leucine sensor for the mTORC1-signaling pathway, *Cell*. 149 (2012) 410–424. <https://doi.org/10.1016/j.cell.2012.02.044>.
- [37] J.A.B. Pedroso, T.T. Zampieri, J. Donato, Reviewing the effects of l-leucine supplementation in the regulation of food intake, energy balance, and glucose homeostasis, *Nutrients*. 7 (2015) 3914–3937. <https://doi.org/10.3390/nu7053914>.
- [38] L. Fu, A. Bruckbauer, F. Li, Q. Cao, X. Cui, R. Wu, H. Shi, M.B. Zemel, B. Xue, Leucine amplifies the effects of metformin on insulin sensitivity and glycemic control in diet-induced obese mice, *Metabolism*. 64 (2015) 845–856. <https://doi.org/10.1016/j.metabol.2015.03.007>.
- [39] C.J. Lynch, S.H. Adams, Branched-chain amino acids in metabolic signalling and insulin resistance, *Nat. Rev. Endocrinol*. 10 (2014) 723–736. <https://doi.org/10.1038/nrendo.2014.171>.
- [40] N.E. Cummings, E.M. Williams, I. Kasza, E.N. Konon, M.D. Schaid, B.A. Schmidt, C. Poudel, D.S. Sherman, D. Yu, S.I. Arriola Apelo, S.E. Cottrell, G. Geiger, M.E. Barnes, J.A. Wisinski, R.J. Fenske, K.A. Matkowskyj, M.E. Kimple, C.M. Alexander, M.J. Merrins, D.W. Lamming, Restoration of metabolic health by decreased consumption of branched-chain amino acids, *J. Physiol*. 596 (2018) 623–645. <https://doi.org/10.1113/JP275075>.
- [41] S.A. Cotton, Lanthanides: Comparison to 3d Metals, *Encycl. Inorg. Bioinorg. Chem.* (2012) 1–5. <https://doi.org/10.1002/9781119951438.eibc2013>.
- [42] K.K. Gangu, S. Maddila, S.N. Maddila, S.B. Jonnalagadda, Nanostructured samarium doped fluorapatites and their catalytic activity towards synthesis of 1,2,4-triazoles, *Molecules*. (2016). <https://doi.org/10.3390/molecules21101281>.
- [43] M.F. Bush, J. Oomens, R.J. Saykally, E.R. Williams, Effects of alkaline earth metal ion complexation on amino acid zwitterion stability: Results from infrared action spectroscopy, *J. Am. Chem. Soc.* (2008). <https://doi.org/10.1021/ja711343q>.
- [44] A.A. Khan, H.A. Hussain, K. Iftikhar, 4f-4f absorption spectra of nine-coordinate Pr (III) and Nd (III) complexes in different environments, *Spectrochim. Acta - Part A Mol. Biomol. Spectrosc.* 59 (2003) 1051–1059. [https://doi.org/10.1016/S1386-1425\(02\)00277-9](https://doi.org/10.1016/S1386-1425(02)00277-9).
- [45] F. Costanzo, R.G. Della Valle, V. Barone, MD simulation of the Na⁺-phenylalanine complex in water: Competition between cation- π interaction and aqueous solvation, *J. Phys. Chem. B*. (2005). <https://doi.org/10.1021/jp055271g>.

- [46] J.C.G. Bünzli, C. Piguet, Lanthanide-containing molecular and supramolecular polymetallic functional assemblies, *Chem. Rev.* (2002). <https://doi.org/10.1021/cr010299j>.
- [47] U.S.E. Of, C. Oxalate, F.O.R. The, widely prevalent therapeutic, (2015).
- [48] B.Y.E.M.V. Williams, Williams, 1954, 1958)., (1959) 325–332.
- [49] S.N. Misra, K. John, Difference and Comparative Absorption Spectra and Ligand Mediated Pseudohypersensitivity for 4f-4f Transitions of Pr (III) and Nd (III) Difference and Comparative Absorption Spectra and Ligand Mediated Pseudo hypersensi tivi ty for 4f-4f Transitions o, 4928 (2016). <https://doi.org/10.1080/05704929308018115>.
- [50] K.B. C. Gorller-Walrand, Spectral intensities of f-f transitions in Handbook on the Physics and Chemistry of Rare Earths edited by K.A. Gscheneidner Jr. and L. Eyring (North Holland, Amsterdam, 1998), *Handb. Phys. Chem. Rare Earths.* 25 (1998) 101–264.
- [51] Misra, S. N., & Sommerer, S. O. (1992). The Ligand Mediated Pseudohypersensitivity of the $^4I_{9/2} \rightarrow ^4G_{7/2}$, $^4I_{9/2} \rightarrow ^4F_{7/2}$, $^4I_{9/2} \rightarrow ^4F_{5/2}$ and $^4I_{9/2} \rightarrow ^4F_{3/2}$ Transitions of Neodymium(III) Complexes in Solution Media. *Reviews in Inorganic Chemistry*, 12(3-4), 157-182. <https://doi.org/10.1080/15533179208020242>.
- [52] Henrie, D. E., & Choppin, G. R. (1968). Environmental effects on f–f transitions.II.“hypersensitivity” in some complexes of trivalent neodymium. *The Journal of Chemical Physics*, 49(2), 477-481. <https://doi.org/10.1063/1.1670099>.
- [53] S. Jericó, , C. R.Carubelli, , A. M. Massabni, E. B. Stucchi, S. R. D. A. Leite, Malta, Spectroscopic study of the interaction of Nd³⁺ with amino Acids: Phenomenological 4f-4f intensity parameters. *Journal of the Brazilian Chemical Society*, 9 (1998)487-493. <https://doi.org/10.1590/S0103-50531998000500014>.
- [54] H.A. Hussain, A.A. Ansari, K. Iftikhar, Optical absorption and NMR spectroscopic studies on paramagnetic trivalent lanthanide complexes with 2,2'-bipyridine.: The solvent effect on 4f-4f hypersensitive transitions, *Spectrochim. Acta - Part A Mol. Biomol. Spectrosc.* 60 (2004) 873–884. [https://doi.org/10.1016/S1386-1425\(03\)00312-3](https://doi.org/10.1016/S1386-1425(03)00312-3).
- [55] Khan, A.A., & Iftikhar, K. Mixed-ligand lanthanide complexes XI. Absorption spectra and hypersensitivity in the complexes of Pr (III), Nd (III), Ho (III) and Er (III) in nonaqueous solutions. *Polyhedron*, 16(23) (1997) 4153-4161. [https://doi.org/10.1016/S0277-5387\(97\)00138-1](https://doi.org/10.1016/S0277-5387(97)00138-1).
- [56] Zhang, Q., & Wang, P. (1998). Analysis on absorption spectra of Nd³⁺ in poly (methyl methacrylate). *Journal of molecular structure*, 440(1-3), 35-42.

- [57] C. Sumitra, T. D. Singh, M. I. Devi, & Singh, N. R. Calculation of electric Dipole intensity parameters of 4f–4f transitions of Pr (III) and glutathione reduced (GSH) complex in presence and absence of Zn (II). *Spectrochimica Acta Part A: Molecular and Biomolecular Spectroscopy*, 66(4-5) (2007) 1333–1339. <https://doi.org/10.1016/j.saa.2006.06.023>.
- [58] N. Bendangsenla, T. Moaienla, T. David Singh, C. Sumitra, N. Rajmuhon Singh, M. Indira Devi, Evaluation of intensity and energy interaction parameters for the complexation of Pr (III) with selected nucleoside and nucleotide through absorption spectral studies, *Spectrochim. Acta -PartA Mol. Biomol. Spectrosc.* 103 (2013) 160–166. <https://doi.org/10.1016/j.saa.2012.11.011>.
- [59] C.V. Devi, Nd (III) with uracil in presence and absence of Ca (II): A Model on the use of Ln (III) as probes at Ca (II) binding sites in biological systems., 7 (2015) 68–78.
- [60] R. S. Naorem, N.P. Singh, N. M. Singh, 4f – 4f Spectral Analysis and Solvent Effect for the Interaction of Pr(III) with l-Tryptophan Using Different Aqueated Solvents in the Presence and Absence of Zn(II), *Chem. Africa*. 3 (2020) 171–180. <https://doi.org/10.1007/s42250-019-00111-9>.
- [61] Tiwari, H., Dhondiyal, C.C., Bhatt, T. *et al.* 4f–4f Spectral Study and Calculation of Energy Interaction Parameters for Interaction of Nd³⁺ with Different Solvents. *Chemistry Africa* (2022). <https://doi.org/10.1007/s42250-022-00518-x>
- [62] B. I. Alabdaly, Synthesis, Characterization and Antibacterial Activity of New Complexes of Some Lanthanide Ions with Benzo 18- Crown -6 and 221- Cryptand, *J. Appl. Chem.* 6 (2013) 32–39. <https://doi.org/10.9790/5736-0643239>.
- [63] B.D. Aghav, S.K. Patil, R.S. Lokhande, Synthesis, characterization and antibacterial properties of the ternary complexes of cerium with Schiff base derived from 4-aminoantipyrine and some amino acids, *Adv. Appl. Sci. Res.* 6 (2015) 37–43.
- [64] Z. Ahmed, K. Iftikhar, Synthesis and visible light luminescence of mononuclear nine-coordinate lanthanide complexes with 2,4,6-tris(2-pyridyl)-1,3,5-triazine, *Inorg. Chem. Commun.* 13(2010)1253–1258. <https://doi.org/10.1016/j.inoche.2010.07.009>.

CHAPTER- 2

METHODOLOGY

The process of theoretical computations of various parameters has been thoroughly covered in this chapter. The history and backdrop of how the intensity parameters and energy interaction parameters were derived have been described in depth. Furthermore, the techniques along with the materials utilized to conduct the experiments are explained in detail.

2.1 INTRODUCTION

In order to determine the lanthanide system's characteristic frequencies, absorption is a vital technique to use [1]. In solution, the spectral absorption of lanthanide-doped single crystals lanthanide compound has a series of thin lines that ultimately converge into a single absorption band [2,3]. These bands must be attributed to an electronic-to-electronic transition inside the $4f$ shell between $^{2S+1}L_J$ free ion levels (or J-manifolds). They are known as intra-configurational transitions since there is no change in a configuration associated with them [4,5]. For the understanding of the observed transitions, three mechanisms must be taken into account.

- (i) Magnetic-Dipole Transitions.
- (ii) Induced Electric Dipole Transitions.
- (iii) Electric Quadrupole Transition.

2.1.1 Magnetic Dipole Transition

The magnetic dipole transition is caused by the interaction of a spectroscopic active ion with the magnetic field component of light traveling through a magnetic dipole. Magnetic dipole radiations can alternatively be regarded as rotational displacement of charge. Because the sense of rotation is not reversed under inversion through a point (or inversion center) a magnetic dipole transition has even parity. As a result, a magnetic dipole operator has even transformational qualities between phases with equal parity (intra- configurational transition) [6–8].

2.1.2 Induced Electric Dipole Transition

Electric-dipole (ED) transitions with electronic states of the same parity are prohibited by the Laporte selection rule, including f - f transitions. However,

lanthanide ions produce non-centrosymmetrical couplings when a ligand field is present, allowing electronic transitions of the opposite parity ($4f^{n-1}5d^1$ configuration) to mix with the $4f^n$ configuration. This eases the restrictions on selection and permits the transitions. These odd-parity transitions are known as induced ED transitions. The majority of lanthanides' optical transitions are Induced Electric Dipole Transitions, which are the result of an electric dipole's interaction with spectroscopically active lanthanide ion and the electric field vector [1,9–12].

2.1.3 Electric Quadrupole Transition

The displacement with a quadrupole nature leads to the electric quadrupole transition. A quadrupole of electricity is made up of four-point charges with no overall charge and no dipole moment. It may be viewed as two dipoles arranged so that their respective dipole moments cancel one another out. The parity of an electric quadrupole is even. Electric quadrupole transitions are much weaker than a magnetic dipole, which in turn are weaker than induced electric dipole transitions. Due to the shielding effect, the environment has little impact on lanthanide $4f-4f$ transitions, while some induced ED transitions are incredibly sensitive to even minute changes in the surroundings of the Ln(III) ion. They are referred to as "hypersensitive" transitions and they obey the selection rules ($\Delta S = 0$, $|\Delta J| \leq 2$ and $|\Delta L| \leq 2$). Contrary to quadrupole transitions, it is discovered that the magnitude of hypersensitive transitions exhibit significant variability with alterations in the ligand median. Hence, they are called "pseudo-quadrupolar" transitions [13,14].

2.1.4 Selection Rules

Selection rules are only valid in strict conditions and can be relaxed under

circumstances. Only the Russell Saunders Coupling Scheme is applicable to the selection criteria for ΔL and ΔS . As L and S are poor stats in the intermediate coupling scheme, these selection requirements are eased. The selection criteria on ΔJ are tougher to break down since J still functions as a strong quantum number in the intermediate coupling scheme; J-mixing is the one weak effect that can loosen these restrictions. The selection rules on ΔM depend on the point group symmetry of the rare earth site [15,16]. Table 2.1 provides the selection criteria for magnetic dipole and induced electric dipole transitions.

Table 2.1: Selection rules for magnetic dipole and induced electric dipole transitions:

Magnetic Dipole Transition (MD)	Induced Electric Dipole Transition (ED)
$\Delta\tau = \Delta S = \Delta L = 0$	$\Delta L = \pm 1, \Delta\tau = 0, \Delta S = 0, \Delta L \leq 6$
$\Delta J = 0, \pm 1$ but $0 \leftrightarrow 0$ is forbidden	$ \Delta J \leq 6; \Delta L = 2, 4, 6$ if $J = 0$ and $J' = 0$
$M' - M = -P$, where $P = \pm$	$M' - M = -(q+p)$

2.1.5 Hypersensitive and Non-hypersensitive transitions

The $4f$ - $4f$ transition band intensities are less affected by the coordination ambience since the filled $5s$ and $5p$ sub-shells firmly shield the $4f$ -subshell of Ln^{3+} and are regarded as non-hypersensitive transitions. On the other hand, some transitions show significantly high sensitivity with little changes in their coordination environment, and their band intensities become more intensified when a lanthanide ion gets complexed with ligands, and as such, they follow the selection rules, $\Delta S = 0$, $\Delta L \leq 2$ and $\Delta J \leq 2$, known as hypersensitive transitions [17–19]. The hypersensitive transitions of some lanthanides are given in table 2.2.

Table 2.2: Hypersensitive transitions of Lanthanide ions.

Lanthanide	Transition	\approx wavenumber ($\times 10^3 \text{cm}^{-1}$)
$\text{Pr}^{3+} (4f^2)$	$^3\text{H}_4 \rightarrow ^3\text{F}_2$	5.2
$\text{Nd}^{3+} (4f^3)$	$^4\text{I}_{9/2} \rightarrow ^4\text{G}_{5/2}$	17.3
$\text{Pm}^{3+} (4f^4)$	$^5\text{I}_4 \rightarrow ^5\text{G}_2, ^5\text{G}_3$	18.0
$\text{Sm}^{3+} (4f^5)$	$^6\text{H}_{5/2} \rightarrow ^4\text{F}_{3/2}, ^4\text{F}_{1/2}$	6.4
$\text{Eu}^{3+} (4f^6)$	$^7\text{F}_1 \rightarrow ^5\text{D}_1$	18.7
	$^7\text{F}_0 \rightarrow ^5\text{D}_2$	21.5
	$^7\text{F}_2 \rightarrow ^5\text{D}_0$	16.3
$\text{Gd}^{3+} (4f^7)$	$^8\text{S}_{7/2} \rightarrow ^6\text{P}_{7/2}, ^6\text{P}_{5/2}$	32.5
$\text{Dy}^{3+} (4f^9)$	$^6\text{H}_{15/2} \rightarrow ^6\text{F}_{11/2}$	7.7
	$^6\text{H}_{15/2} \rightarrow ^4\text{I}_{5/2}, ^4\text{G}_{11/2}$	23.4
$\text{Ho}^{3+} (4f^{10})$	$^5\text{I}_8 \rightarrow ^5\text{G}_6$	22.1
	$^5\text{I}_8 \rightarrow ^3\text{H}_6$	27.7
$\text{Er}^{3+} (4f^{11})$	$^4\text{I}_{15/2} \rightarrow ^2\text{H}_{11/2}$	19.2
	$^4\text{I}_{15/2} \rightarrow ^4\text{G}_{15/2}$	26.4
$\text{Tm}^{3+} (4f^{12})$	$^3\text{H}_6 \rightarrow ^3\text{F}_4$	5.9
	$^3\text{H}_6 \rightarrow ^3\text{H}_4$	12.7
	$^3\text{H}_6 \rightarrow ^1\text{G}_4$	21.3

2.1.6 Pseudohypersensitive transitions

The solution spectral analysis of Pr^{3+} and Nd^{3+} complexes reveals that some of the transition intensities of Pr^{3+} ions ($^3\text{H}_4 \rightarrow ^3\text{P}_2$, $^3\text{H}_4 \rightarrow ^3\text{P}_1$, $^3\text{H}_4 \rightarrow ^3\text{P}_0$, and $^3\text{H}_4 \rightarrow ^1\text{D}_2$) and Nd^{3+} ($^4\text{I}_{9/2} \rightarrow ^4\text{G}_{7/2}$, $^4\text{I}_{9/2} \rightarrow ^4\text{F}_{7/2}$, $^4\text{I}_{9/2} \rightarrow ^4\text{F}_{5/2}$, and $^4\text{I}_{9/2} \rightarrow ^4\text{F}_{3/2}$) exhibit an exceptionally sensitive character towards minor changes in their coordination ambience even though they could not follow the selection rule. Such transitions are pseudoquadrupole in character and are known as *Ligand Mediated Pseudohypersensitive* transitions since their sensitivity is the inducing result of their coordination environment [20,21]. These Pseudohypersensitive transitions have been used extensively for the absorption spectral study to understand the nature of bonding and structural conformations of Pr(III) with ligands in solution study.

2.2 THEORETICAL

In the present investigation, theoretically computed absorption spectral parameters were employed as a tool to investigate the complexation of Pr^{3+} and Nd^{3+} with Schiff-base ligands (L-phenylalanine, L-methionine, and L-leucine) in the presence/absence of Mg^{2+} ion. For this, the energy interaction parameters: Lande spin-orbit interaction (ζ_{4f}), Racah (E^k), Slater-Condon factor (F_k), nephelauxetic ratio (β), per-cent covalency (δ), and bonding parameter ($b^{1/2}$) as well as the intensity parameters: Oscillator strength (P) and Judd-Ofelt intensity parameters T_λ ($\lambda = 2, 4, 6$) were analyzed in various aqueous solutions: CH_3CN , DMF , $\text{C}_4\text{H}_8\text{O}_2$, and CH_3OH .

Pre-exponential factor (A), activation energy (E_a), rate constant (k), and thermodynamic parameters: ΔS° , ΔG° , and ΔH° have been computed to analyze the

reaction strategies as well as the thermodynamic properties of the complexation process of the metal with ligands.

2.2.1 Energy parameters

As the electrostatic interaction and the spin-orbit interactions between $4f$ -electrons make up the energy (E_{so}) of the $4f$ - $4f$ electronic transition [2,22–24], it can be described as,

$$E_{so} = A_{so} \zeta_{4f} \quad (1)$$

Where radial integral is represented by Lande's parameter ' ζ_{4f} ' and an angular interaction is indicated by ' A_{so} '.

To calculate the energy level of the $4f^n$ arrangement, radial integrals such as ζ_{4f} and F_2 , F_4 , and F_6 , are needed. The Slater-Condon (F_k , $K = 2, 4, 6$) and Lande parameter (ζ_{4f}) of the praseodymium complex may be evaluated by expressing energy as Taylor series expansion. In the first order, energy E_j of the j^{th} level is given by Wong [25]

$$E_j(F_k, \zeta_{4f}) = E_{0j}(F_k^0, \zeta_{4f}^0) + \frac{\partial E_j}{\partial F_k} \Delta F_k + \frac{\partial E_j}{\partial \zeta_{4f}} \Delta \zeta_{4f} \quad (2)$$

Here, the initial energy ' E_{0j} ' is the zero-order energy of the j^{th} level. Equations (3) and (4) represent equated values of F_K and ζ_{4f} .

$$F_k = F_k^0 + \Delta F_k \quad (3)$$

$$\zeta_{4f} = \zeta_{4f}^0 + \Delta \zeta_{4f} \quad (4)$$

The value of ΔE_j is calculated as the difference between E_j and E_{0j} values given as,

$$\Delta E_j = \sum_{k=2,4,6} \frac{\partial E_j}{\partial F_k} \Delta F_k + \frac{\partial E_j}{\partial \zeta_{4f}} \Delta \zeta_{4f} \quad (5)$$

By using the zero-order energy and partial derivatives of Pr(III) ion given by Wong (Table 2.3), equation (5) can be solved by the least square fit technique and the values of ΔF_2 and $\Delta \xi_{4f}$ can be found out by using equation (3). The values of F_4 and F_6 are calculated by the relations,

$$\frac{F_4}{F_2} = 0.1380 \text{ and } \frac{F_6}{F_2} = 0.0150 \quad (6)$$

Table 2.3: The Zero-order energies and partial derivatives* with respect to F_K and ξ_{4f} parameters for Pr(III) [25].

Level	$E_{oj}^{(a)}$	$\frac{\partial E_j}{\partial F_2}$	$\frac{\partial E_j}{\partial F_4}$	$\frac{\partial E_j}{\partial F_6}$	$\frac{\partial E_j}{\partial \xi_{4f}}$
1D_2	16972	45.97	-37.63	510	2.906
3P_0	20412	70.17	81.17	-1253	1.905
3P_1	20990	70.07	80.66	-1278	3.974
3P_2	22220	67.56	68.42	-1077	5.029

$$(a) = \left\{ \begin{array}{ll} F_2^0 = 305.000 \text{ cm}^{-1} & F_4^0 = 51.880 \text{ cm}^{-1} \\ F_6^0 = 5.321 \text{ cm}^{-1} & \xi_{4f}^0 = 730.50 \text{ cm}^{-1} \end{array} \right\}$$

The result of complexation on the spectra is the redshift of all the electronic transitions, the redshift is due to the expansion of the metal orbital radius resulting in the decrease of the inter-electronic repulsion parameters (Slater-Condon, F_k 's or Racah, E_k) between the central metal ion and the ligand orbitals. This phenomenon is known as the Nephelauxetic effect, which measures the change in F_k with respect to free ions and is expressed by a Nephelauxetic ratio ' β ' [24]. In order to explain the

Nephelauxetic effect, the Slater–Condon and Racah parameters have been interpreted as follows.

$$\beta = \frac{F_K^C}{F_K^f} \text{ or } \frac{E_C^K}{E_f^K} \quad (7)$$

Where, Racah parameters are given as E^K for complex and free ions while Slater-Condon parameters as F_K ($K=2, 4, 6$).

The β -effect is associated with the bonding parameter ($b^{1/2}$) and is measured as the amount of $4f$ -orbital mixing. The covalent percentage (δ) and bonding parameter can be calculated with the following equations;

$$b^{1/2} = \left[\frac{1-\beta}{2} \right]^{1/2} \quad (8)$$

$$\delta = \left[\frac{1-\beta}{\beta} \right] \times 100 \quad (9)$$

2.2.2 Intensity parameters

2.2.2.1 Oscillator strength (P)

The intensity of the absorption band is measured by the oscillator strength (P), which is directly related to the absorption curve area. The relationship between the energy of transitional wavenumber (ν), the molar extinction coefficient (ϵ_{max}) and the refractive index (η) of the medium can be used to obtain the oscillator strength (P) as

$$P = 4.6 \times 10^{-9} \left[\frac{9\eta}{(\eta^2 + 1)^2} \right] \int \epsilon_{max} \bar{\nu} d\bar{\nu} \quad (10)$$

Molar extinction, wave number, and Refractive index coefficient are each represented by the symbols, ϵ_{max} , $\bar{\nu}$, and η respectively.

From the absorption band, we can determine the experimental oscillator strength (P_{obs}) values by employing the Gaussian curve analysis as,

$$P_{\text{obs}} = 4.6 \times 10^{-9} \times \epsilon_{\text{max}} \bar{\nu}_{1/2} \quad (11)$$

$\bar{\nu}_{1/2}$ = Half bandwidth [26–29]

2.2.2.2 Judd-Ofelt parameters (T_λ)

An article on $4f-4f$ transition intensities of the Lanthanides by Van Vleck was published in 1937 [30]. Nevertheless, the Judd-Ofelt theory was developed from the work of Judd and Ofelt. Later, the aquo ions of lanthanides were subsequently incorporated into the computation of the oscillator strengths [29]. Using a combination of least square fit methods and other statistical techniques, the matrix element was developed by Carnal *et al*, which is most commonly employed in the solution spectral research as given below:

$$P = \chi \left[\frac{8\pi^2 mc}{3h} \right] \sigma \sum T_\lambda || U^{(\lambda\lambda)} || (2J + 1) \quad (12)$$

Through the matrix of the unit tensor operator ($U^{(\lambda)}$) of rank λ , the T_λ phenomenological parameters keep both the ground and final state ($\langle f^n \Psi J |$ & $| f^n \Psi' J' \rangle$ respectively) connected [31]. These quantities exhibit a sensitive nature toward the type of transition used in their computations and the degree of precision of oscillator strength [32].

Based on Judd and Ofelt's theory of band intensities, an empirical approach was used in the theoretical calculation [29,33]. The transition character is considered to be essentially that of an electric dipole, while the oscillator strength corresponds with the

induced electric dipole transition $\psi J \rightarrow \psi' J'$ that is shown below by the equation (13) given as [34,35],

$$P = \sum_{\lambda=2,4,6} T_{\lambda} \sigma(f^N \psi J \| U^{(\lambda)} \| f^N \psi' J')^2 \quad (13)$$

In this case, ' $U^{(\lambda)}$ ' stands for the matrix element. T_2 , T_4 , and T_6 are the three quantities associated with the radial parts of the $4f^N$ wave functions.

With respect to the absorption of the radiant energy, equation (14) and (15) represent the correlation between the observed intensity of the absorption band and the probability (P).

$$P = \frac{2.303 mc^2}{N\pi e^2} \int \epsilon_i(\sigma) d\sigma$$

$$\text{Or, } P = 4.314 \times 10^{-9} \int \epsilon_i(\sigma) d\sigma \quad (14)$$

Using the observed oscillator strength (P_{obs}) of the lanthanide, Judd and Ofelt calculated the lanthanide intensity as follows,

$$\frac{P_{obs}}{\nu} = [(U^2)^2] \cdot T_2 + [(U^4)^2] \cdot T_4 + [(U^6)^2] \cdot T_6 \quad (15)$$

Where, ν = Wavenumber and U = matrix element

Table 2.4: Matrix elements* $U^{(\lambda)}$ for Pr(III) aquo [36]

Levels	$[(U^2)^2]$	$[(U^4)^2]$	$[(U^6)^2]$
1D_2	0.0026	0.0170	0.0520
3P_0	0	0.1728	0
3P_1	0	0.1707	0
3P_2	0	0.0362	0.1355

2.2.3 Reaction dynamics/Thermodynamics theory

The activation energy of the complex was calculated using the Arrhenius reaction rate equation by plotting $\log k$ (k = rate constant) versus $1/T$.

$$\log k = \log A - \frac{E_a}{2.303R} \frac{1}{T} \quad (16)$$

Pre-exponential factor "A" in this context refers to the orientation or frequency likelihood of collisions.

The slope is used to calculate the activation energy, which is then provided by,

$$E_a = -\text{slope} \times 2.303 \times R \quad (17)$$

By determining the Activation energy (E_a), we can determine the reaction rate (k).

The thermodynamic parameters for the complexation were determined by Van't Hoff plot of $\log k$ against $1/T \times 10^3$ given as

$$\log k = -\frac{\Delta H^\circ}{R} \left[\frac{1}{T} \right] + \frac{\Delta S^\circ}{R} \quad (18)$$

In comparison to the pre-exponential value "A," the specific rate constant "k" increases in a noticeable and significant way as the temperature "T" rises. As a result, under such conditions "A" is neglected.

2.3 EXPERIMENTAL

2.3.1 Materials used

The lanthanides used in this research are Pr(III) nitrate hexahydrate and Nd(III) nitrate hexahydrate of 99.9% purity (Sigma Aldrich). The amino acids extensively used for the study are L-phenylalanine, L-methionine, and L-leucine (HiMedia). The complex

of Lanthanide ion with amino acids is studied extensively in the presence and absence of amino acids. The solvents used; were Dimethylformamide (DMF), Acetonitrile (ACN), Dioxan, and Methanol purchased from Merck, with 99.5% purity.

2.3.2 Methods

2.3.2.1 Stock solution preparation

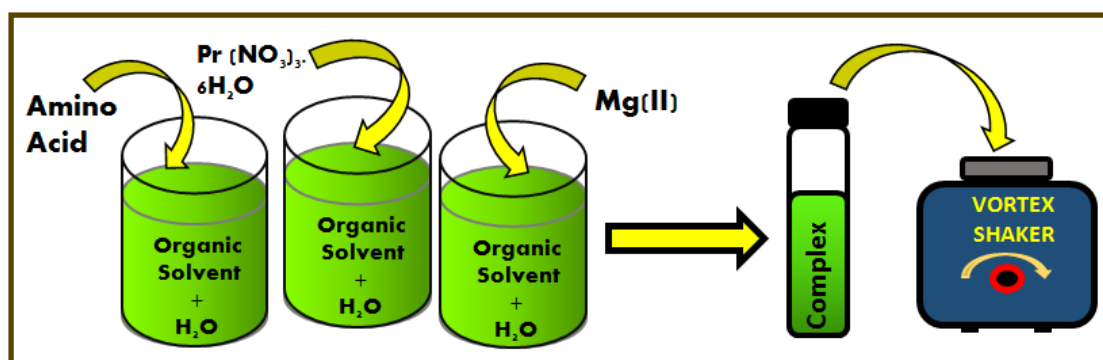


Figure 2.1: Procedure for stock solution preparation.

- Firstly the stock solution of lanthanide was prepared in a beaker. Similarly, the stock solution for the amino acids as well as the Magnesium was prepared.
- The desired amount of the prepared solution was extracted and mixed in a test tube after which it is thoroughly mixed using a vortex shaker.
- The solution concentration was kept at 5×10^{-3} M and the aquated solvents used were maintained at a ratio of 50% v/v.
- Eutech pH 700 digital pH meter was used for the pH measurements.

2.3.2.2 Experimental procedure

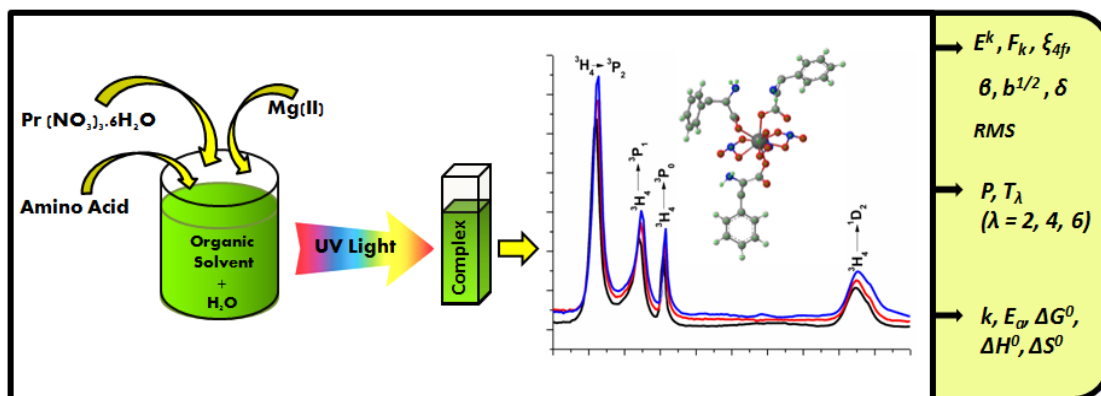


Figure 2.2: Schematic representation of the experimental process

- The thoroughly mixed solutions were poured into the dried and cleaned cuvette and kept in the UV spectrophotometer and allow the UV light to pass through it.
- UV/Vis spectrophotometer (Perkin Elmer Lambda 365) was used for recording the absorption spectra.
- The recorded spectra were thoroughly analyzed to study the interaction of Ln(III) with amino acids in the presence and absence of Mg(II).
- Under different experimental conditions; Different aquated organic solvents (DMF, CAN, Dioxane, Methanol) systems, and at different pH (2, 4, 6) medium the interaction of Metal with the ligand was studied.
- For the Kinetic and thermodynamic study, the experiments were carried out at various temperatures (298K, 303K, 308K & 313K) and at different time intervals of two hours.

REFERENCES

- [1] J.D. Rinehart, M. Fang, W.J. Evans, J.R. Long, A N23- radical-bridged terbium complex exhibiting magnetic hysteresis at 14 K, *J. Am. Chem. Soc.* 133 (2011) 14236–14239. <https://doi.org/10.1021/ja206286h>.
- [2] M.S. N., S.S. O, Absorption Spectra of Lanthanide Complexes in Solution, *Appl. Spectrosc. Rev.* 26 (1991) 151–202. <https://doi.org/10.1080/05704929108050880>.
- [3] Y. Okayasu, J. Yuasa, Structure Determination of Europium Complexes in Solution Using Crystal-Field Splitting of the Narrow f-f Emission Lines, *J. Phys. Chem. Lett.* 12 (2021) 6867–6874. <https://doi.org/10.1021/acs.jpcllett.1c01885>.
- [4] E. Echenique-Errandonea, R.F. Mendes, F. Figueira, D. Choquesillo-Lazarte, G. Beobide, J. Cepeda, D. Ananias, A. Rodríguez-Diéguez, F.A. Almeida Paz, J.M. Seco, Multifunctional Lanthanide-Based Metal-Organic Frameworks Derived from 3-Amino-4-hydroxybenzoate: Single-Molecule Magnet Behavior, Luminescent Properties for Thermometry, and CO₂ Adsorptive Capacity, *Inorg. Chem.* 61(2022) 12977–12990. <https://doi.org/10.1021/acs.inorgchem.2c00544>.
- [5] H. Lueken, Course of lectures on magnetism of lanthanide ions under varying ligand and magnetic fields, *Review.* (2008) 1–91.
- [6] C.M. Dodson, R. Zia, Magnetic dipole and electric quadrupole transitions in the trivalent lanthanide series: Calculated emission rates and oscillator strengths, *Phys. Rev. B - Condens. Matter Mater. Phys.* 86 (2012) 1–10. <https://doi.org/10.1103/PhysRevB.86.125102>.
- [7] P. Taylor, F.S. Richardson, M.T. Berry, M.F. Reid, *Molecular Physics: An International Journal at the Interface Between Chemistry and Physics* Ligand polarization contributions to lanthanide 4f → 4f magnetic dipole transition moments and rotatory strengths, (n.d.) 37–41. [10.1080/00268978600101681](https://doi.org/10.1080/00268978600101681).
- [8] J. Sucher, Magnetic dipole transitions in atomic and particle physics: Ions and psions, *Reports Prog. Phys.* 41 (1978) 1781–1838. <https://doi.org/10.1088/0034-4885/41/11/002>.
- [9] M.F. Reid, F.S. Richardson, *Lanthanide 4f -, Society.* 750 (1984) 3579–3586.
- [10] K.M.S. Saxena, S. Fraga, Electric dipole polarizabilities of lanthanides and actinides, *J. Chem. Phys.* 57 (1972) 1800–1801. <https://doi.org/10.1063/1.1678481>.

- [11] L. Smentek, A. Kędzioriski, Hyperfine-induced $f \leftrightarrow f$ transitions: Effective operator formulation, *Spectrosc. Lett.* 40 (2007) 293–315. <https://doi.org/10.1080/00387010701247548>.
- [12] M.F. Reid, F.S. Richardson, Electric dipole intensity parameters for lanthanide $4f \rightarrow 4f$ transitions, *J. Chem. Phys.* 79 (1983) 5735–5742. <https://doi.org/10.1063/1.445760>.
- [13] L. Eyring, K.A. Gschneidner, Handbook on the physics and chemistry for rare earths. Vol. 24, 1999. <http://www.sciencedirect.com/science/handbooks/01681273/26>.
- [14] G. Hovhannesian, V. Boudon, M. Lepers, Transition intensities of trivalent lanthanide ions in solids: Extending the Judd-Ofelt theory, *J. Lumin.* 241 (2022) 118456. <https://doi.org/10.1016/j.jlumin.2021.118456>.
- [15] P. Taylor, J.C. Barthelat, P. Durand, A. Serafini, Molecular Physics: An International Journal at the Interface Between Chemistry and Physics Non-empirical pseudopotentials for molecular calculations, *Mol. Phys.* 33 (1977) 159–180. <https://doi.org/10.1080/00268977800102401>.
- [16] M. Hatanaka, S. Yabushita, Mechanisms of $f-f$ hypersensitive transition intensities of lanthanide trihalide molecules: a spin-orbit configuration interaction study, *Theor. Chem. Acc.* 133 (2014) 1–15. <https://doi.org/10.1007/s00214-014-1517-2>.
- [17] V.K. Tikhomirov, M. Naftaly, A. Jha, Effects of the site symmetry and host polarizability on the hypersensitive transition $3P_0 \rightarrow 3F_2$ of Pr^{3+} in fluoride glasses, *J. Appl. Phys.* 86 (1999) 351–354. <https://doi.org/10.1063/1.370737>.
- [18] D.G. Karraker, Hypersensitive Transitions of Six-, Seven-, and Eight-Coordinate Neodymium, Holmium, and Erbium Chelates, *Inorg. Chem.* 6 (1967) 1863–1868. <https://doi.org/10.1021/ic50056a022>.
- [19] M.D. Faucher, P.A. Tanner, Energy levels and hypersensitivity of samarium(III) in the elpasolite $\text{Cs}_2\text{NaSmCl}_6$, *J. Phys. Condens. Matter.* 18 (2006) 8503–8522. <https://doi.org/10.1088/0953-8984/18/37/009>.
- [20] S.N. Misra, S.B. Mehta, B.M. Balar, K. John, Absorption difference and comparative absorption spectrophotometry of neodymium(iii) haloacetates in non-aqueous media and in crystalline state, 1992. <https://doi.org/10.1080/15533179208020242>.
- [21] S.N. Misra, K. John, Difference and Comparative Absorption Spectra and

- Ligand Mediated Pseudohypersensitivity for 4f-4f Transitions of Pr (III) and Nd (III) Difference and Comparative Absorption Spectra and Ligand Mediated Pseudo hypersensi tivi ty for 4f-4f Transitions o, 4928 (2016). <https://doi.org/10.1080/05704929308018115>.
- [22] Z. Thakro, M.T. Ao, C. Imsong, J. Sanchu, M. Ziekhri, M.I. Devi, Absorption spectral and thermodynamic analysis for the complexation of Pr 3 + with L-phenylalanine in the presence / absence of Mg 2 + using 4f – 4f transitions spectra as probe, Eur. Phys. J. Plus. 123 (2022) 1–10. <https://doi.org/10.1140/epjp/s13360-022-02765-w>.
- [23] Z. Thakro, J. Sanchu, C. Imsong, M.I. Devi, Complexation of Pr³⁺ with L-methionine in the presence/absence of Mg²⁺: Their reaction dynamics and thermodynamic properties, Chem. Phys. Impact. 4 (2022) 100078. <https://doi.org/10.1016/j.chphi.2022.100078>.
- [24] M. Ziekhri, Z. Thakro, C. Imsong, J. Sanchu, M.I. Devi, Computation of energy interaction and intensity parameters for the complexation of Pr (III) with glutathione at different pH in the presence / absence of Mg 2 + : 4f-4f transition spectra as a probe, 200 (2021). <https://doi.org/10.1016/j.poly.2021.115099>.
- [25] E.Y. Wong, Configuration interaction of the Pr³⁺ ion, J. Chem. Phys. 38 (1963) 976–978. <https://doi.org/10.1063/1.1733794>.
- [26] T.D. Singh, C. Sumitra, N. Rajmuhon Singh, M. Indira Devi, Comparison of electric-dipole intensity parameter for a series of structurally related Pr(III) complexes with ureas and thioureas in non-aqueous media, Asian J. Chem. (2005).
- [27] C. Sumitra, T.D. Singh, M.I. Devi, N.R. Singh, Absorption spectral studies of 4f-4f transitions for the complexation of Pr(III) and Nd(III) with glutathione reduced (GSH) in presence of Zn(II) in different aquated organic solvents and kinetics for the complexation of Pr(III):GSH with Zn(II), J. Alloys Compd. (2008). <https://doi.org/10.1016/j.jallcom.2007.04.153>.
- [28] G.S. Ofelt, Intensities of crystal spectra of rare-earth ions, J. Chem. Phys. (1962). <https://doi.org/10.1063/1.1701366>.
- [29] B.R. Judd, Optical absorption intensities of rare-earth ions, Phys. Rev. (1962). <https://doi.org/10.1103/PhysRev.127.750>.
- [30] J.H. Van Vleck, The puzzle of rare-earth spectra in solids, J. Phys. Chem.

- (1937). <https://doi.org/10.1021/j150379a006>.
- [31] Y. Cao, J. Sun, Y. Zhang, X. Wang, Y. Zhang, D. Gao, L. Wang, calculation for trivalent rare earth ions and its application for Er³⁺-doped NaYF₄ phosphor, (2020). <https://doi.org/10.1039/d0cp04379f>.
- [32] K. Binnemans, C. Görller-Walrand, Lanthanide-containing liquid crystals and surfactants, Chem. Rev. (2002). <https://doi.org/10.1021/cr010287y>.
- [33] A.A. Kornienko, Dependence of the Line Strength of f-f Transitions on the Manifold Energy, 267 (1990) 267–273. <https://doi.org/10.1002/pssb.2221570127>.
- [34] A. Manuscript, rsc.li/pccp, (2018). <https://doi.org/10.1039/C8CP02317D>.
- [35] Y. Tian, B. Chen, R. Hua, J. Sun, L. Cheng, H. Zhong, X. Li, J. Zhang, Y. Zheng, T. Yu, L. Huang, H. Yu, Optical transition , electron-phonon coupling and fluorescent quenching, 2 (2014) 1–7. <https://doi.org/10.1063/1.3551584>.
- [36] W.T. Carnall, P.R. Fields, B.G. Wybourne, Spectral Intensities of the Trivalent Lanthanides and Actinides in Solution. I. Pr³⁺, Nd³⁺, Er³⁺, Tm³⁺, and Yb³⁺, J. Chem. Phys. 42 (1965) 3797–3806. <https://doi.org/10.1063/1.1695840>.

CHAPTER- 3

Absorption spectral and thermodynamic analysis for the complexation of Pr^{3+} with L-phenylalanine in the presence/absence of Mg^{2+} using 4f-4f transitions spectra as probe

In this chapter, theoretically computed absorption spectral parameters were employed as a tool to investigate the complexation of Pr^{3+} with a Schiff-base ligand (L-Phenylalanine) in the presence/absence of Mg^{2+} ion. For the complexation study, the energy interaction parameters, as well as the intensity parameters were analyzed in various aqueous solutions as well as in different pH (2, 4, 5) mediums, done in 50%v/v aquated solvent. The nature of the chemical reaction pathways as well as the thermodynamic behavior were analyzed by computing the parameters like specific rate constant/rate constant (k), pre-exponential factor (A), ΔH^0 , ΔS^0 , and ΔG^0 .

The text of this chapter has been published as:

Z. Thakro, M.T. Ao, C. Imsong, J. Sanchu, M. Ziekhri, M.I. Devi, **Absorption spectral and thermodynamic analysis for the complexation of Pr^{3+} with L-phenylalanine in the presence/absence of Mg^{2+} using 4f-4f transitions spectra as probe**, Eur. Phys. J. Plus. 123 (2022) 1–10. <https://doi.org/10.1140/epjp/s13360-022-02765-w>.

3.1 INTRODUCTION

Due to its unique properties, the applications of lanthanide probes or lanthanide labels are reported to have been increasing extensively in a wide variety [1]. The potential of lanthanide, used as structural probes has played a significant role in the field of biological chemistry imparting an immense interest in studying the ions of trivalent lanthanide with biological ligands such as peptides or amino acids and consequently exploring their bonding characters [2–4]. The increase in the use of lanthanide as a probe is due to the similarities and the ability of the lanthanide to replace Ca^{2+} ions in a distinct and isomorphous form [5–7].

3.1.1 Phenylalanine

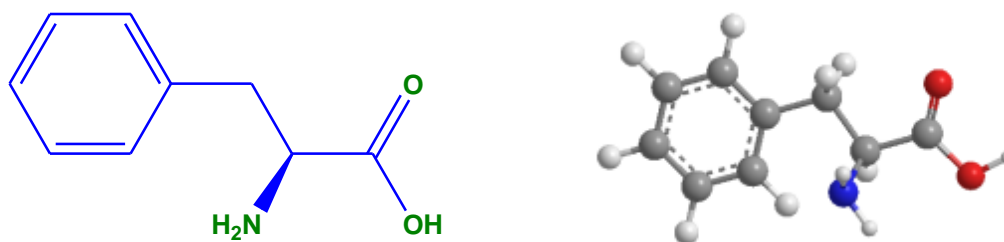


Fig. 3.1: 2D and 3D structures of L-phenylalanine.

In the present study, we chose 2-Amino-3-phenyl-propanoic acid namely L-Phenylalanine (figure 3.1) as the ligand. L-Phenylalanine is an aromatic essential amino acid and is responsible for the biosynthesis of norepinephrine neurotransmitters and dopamine. They are important in the structure and function of many proteins and enzymes. Major dietary sources of L-phenylalanine include meat, fish, eggs, cheese, and milk [8,9]. Phenylalanine plays a key role in the biosynthesis of other amino acids and is important in the structure and function of many proteins and enzymes. Phenylalanine is most commonly used for a skin disorder that causes white patches to develop on

the skin (vitiligo). Deficiency of L-phenylalanine could lead to mental disorders, including low libido, depression, anxiety, and chronic fatigue [10]. On the other hand, excessive accumulation of L-phenylalanine could lead to pathological conditions such as chronic obstructive pulmonary disease, cardiac failure, coronary artery disease, pulmonary hypertension, and systemic hypertension [11]. Therefore, it is worthwhile to investigate the interactions, mode of binding, and molecular structure of this biological ligand (L-phenylalanine) with metal (Pr^{3+}) by employing $4f-4f$ transition spectra as a probe.

3.1.2 Bonding nature of L-phenylalanine with Praseodymium

Amino acids exist in neutral form when they are in the gaseous phase [figure 3.2 (a)] [12]. However, they exist in zwitterionic form when they are in the aqueous solution [figure 3.2 (b)] [10,13,14].

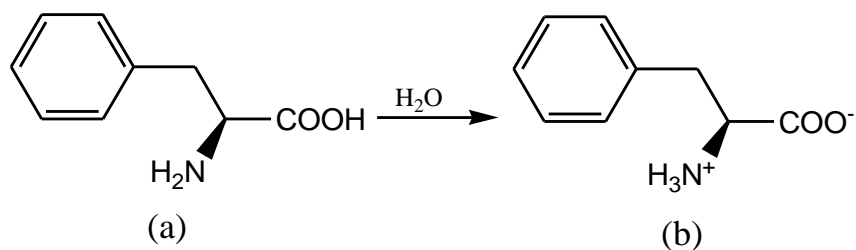


Fig. 3.2: Phenylalanine in (a) neutral and (b) Zwitterion state.

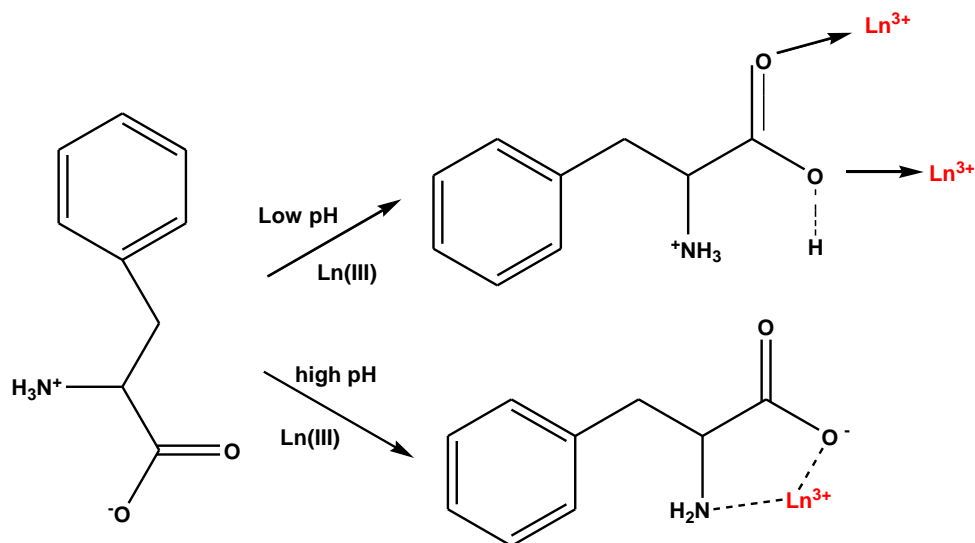


Fig 3.3: Bonding nature of the zwitterionic form of L-phenylalanine at different pH.

Bonding of the ligand with the metal relies on the pH values, that is when the pH value is low, the oxygen atom binds with the metal while if the pH value is high then both oxygen and nitrogen are bonded with the metal (figure 3.3) [15].

In the present investigation, theoretically computed absorption spectral parameters were employed as a tool to investigate the complexation of Pr^{3+} with a Schiff-base ligand (L-phenylalanine) in the presence/absence of Mg^{2+} ion. For this complexation, the energy interaction parameters: Lande spin-orbit interaction (ζ_{4f}), Racah (E^k), Slater-Condon factor (F_k), bonding parameter ($b^{1/2}$), per-cent covalency (δ), and nephelauxetic ratio (β), as well as the intensity parameters: Oscillator strength (P) and Judd-Ofelt intensity parameters $T_\lambda(\lambda = 2,4,6)$ were analyzed in various aqueous solutions: CH_3CN , DMF, $\text{C}_4\text{H}_8\text{O}_2$, and CH_3OH . The complexation of Pr^{3+} with L-phenylalanine in the presence/absence of Mg(II) at different pH (2,4,6) mediums was done in 50% v/v aquated DMF solvent. The nature of the chemical reaction pathways as well as the thermodynamic behavior were analyzed by computing the parameters

like specific rate constant/rate constant (k), pre-exponential factor (A), ΔH^0 , ΔS^0 , and ΔG^0 .

3.2 EXPERIMENTAL SECTION

3.2.1 Materials and Methods

A 99.9% purity of Praseodymium(III)nitrate hexahydrate [$\text{Pr}(\text{NO}_3)_3 \cdot 6\text{H}_2\text{O}$] was purchased from Sigma-Aldrich; the ligand, L-phenylalanine ($\text{C}_9\text{H}_{11}\text{NO}_2$) and Magnesium nitrate hexahydrate [$\text{Mg}(\text{NO}_3)_2 \cdot 6\text{H}_2\text{O}$ of 97.0% purity] from HiMedia. The solvents: Dimethylformamide ($\text{C}_3\text{H}_7\text{NO}$), Methanol (CH_3OH), Dioxane ($\text{C}_4\text{H}_8\text{O}_2$), and Acetonitrile (CH_3CN) used were purchased from HiMedia with 99.5% purity.

For the absorption analysis, the concentration of the solution used for the Pr^{3+} and its complexes Pr(III):Phe (L-Phenylalanine) and Pr(III):Phe:Mg(II) is $5 \times 10^{-3}\text{M}$. The binary mixtures of water with the organic solvents were maintained at 50%v/v. The complexation of Praseodymium (Pr^{3+}) with L-phenylalanine in presence and absence of Mg^{2+} at various pH (2, 4, 6) was studied particularly in a 50%v/v aquated DMF medium. The UV-visible spectra were recorded using Perkin Elmer Lambda 365 UV/Vis spectrometer. For the thermodynamic and kinetic study of the Pr(III):Phe:Mg(II) complex, the spectra were recorded at different temperatures of 298K, 303K, 308K, and 313K by keeping a time interval of two hours gap.

3.3 CALCULATIONS

The following equations are used for the calculations of different parameters. The details of the calculations have been discussed in chapter 2.

3.3.1 Energy parameters

Nephelauxetic ratio ' β '

$$\beta = \frac{F_K^C}{F_K^f} \text{ or } \frac{E_C^K}{E_f^K} \quad (1)$$

Slater–Condon ' F_k ' and Lande spin-orbit parameters ' ξ_{4f} '

$$F_k = F_k^0 + \Delta F_k \quad (2)$$

$$\xi_{4f} = \xi_{4f}^0 + \Delta \xi_{4f} \quad (3)$$

Racah parameter

$$E^1 = \frac{70F_2 + 231F_4 + 20.02F_6}{9} \quad (4)$$

$$E^2 = \frac{F_2 - 3F_4 + 7F_6}{9} \quad (5)$$

$$E^3 = \frac{5F_2 + 6F_4 - 9F_6}{9} \quad (6)$$

Bonding parameter ($b^{1/2}$) and covalent percentage (δ)

$$b^{1/2} = \left[\frac{1-\beta}{2} \right]^{1/2} \quad (7)$$

$$\delta = \left[\frac{1-\beta}{\beta} \right] \times 100 \quad (8)$$

3.3.2 Intensity parameters

Oscillator strength

$$P_{\text{obs}} = 4.6 \times 10^{-9} \times \epsilon_{\text{max}} \bar{\nu}^{1/2} \quad (9)$$

Judd-Ofelt parameters (T_λ)

$$\frac{P_{\text{obs}}}{\nu} = [(U)^2]^2 \cdot T_2 + [(U)^4]^2 \cdot T_4 + [(U)^6]^2 \cdot T_6 \quad (10)$$

3.3.3 Reaction dynamics/thermodynamics theory

$$\log k = \log A - \frac{E_a}{2.303R T} \quad (11)$$

$$E_a = -\text{slope} \times 2.303 \times R \quad (12)$$

$$\log k = -\frac{\Delta H^\circ}{R} \left[\frac{1}{T} \right] + \frac{\Delta S^\circ}{R} \quad (13)$$

3.4 RESULTS AND DISCUSSIONS

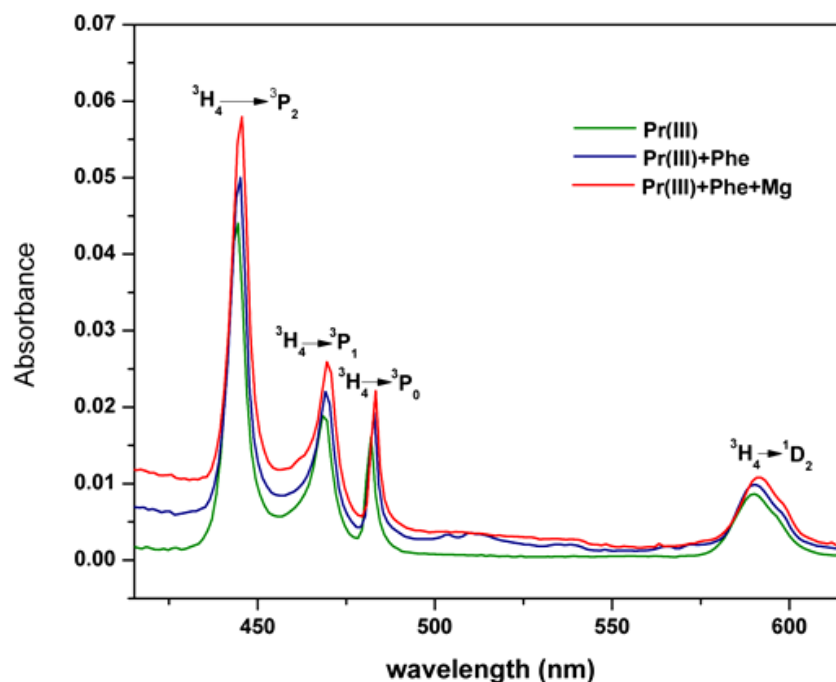


Fig. 3.4: UV-vis absorption spectra of the $4f-4f$ electronic transitions of Pr^{3+} , Pr(III):Phe and $\text{Pr(III):Phe:Mg(II)}$ complexes in ACN:Water (50% v/v) solvent.

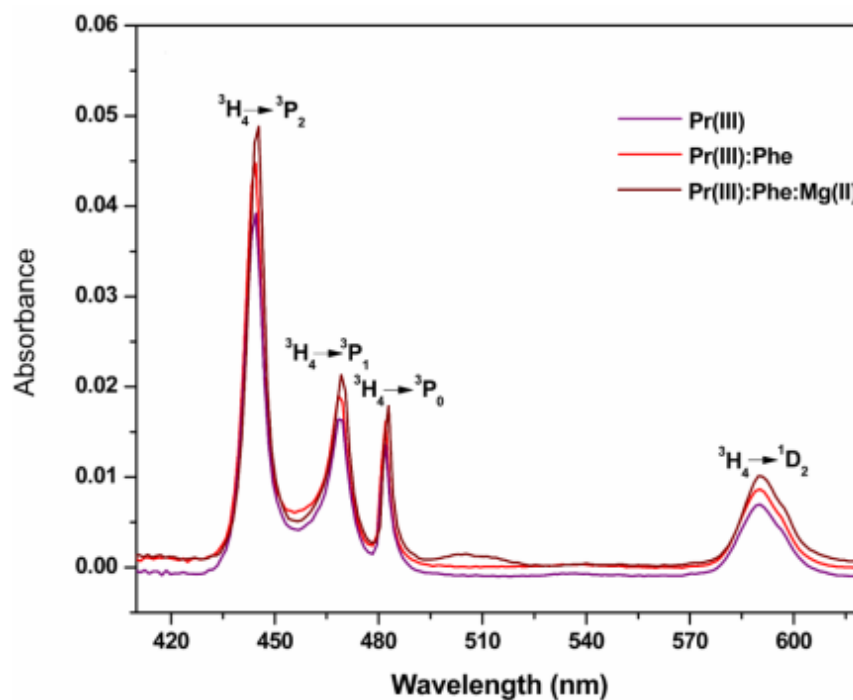


Fig. 3.5: UV-vis absorption spectra of the $4f-4f$ electronic transitions of Pr^{3+} , Pr(III):Phe and $\text{Pr(III):Phe:Mg(II)}$ complexes in Dioxane:Water (50% v/v) solvent.

Table 3.1. Computed values of the energy interaction parameters; percent covalency (δ), bonding ($b^{1/2}$), Nephelauxetic ratio (β), Racah parameters E_k , Lande Spin-orbit interactions ξ_{4f} (cm^{-1}), and Slater-Condon factor F_k (cm^{-1}) parameter of Pr^{3+} and its complexes in 50% (v/v) aquated solvents.

		METHANOL			DIOXAN			ACETONITRILE (ACN)			DIMETHYLFORMAMIDE (DMF)		
		Pr(III):Phe e:Mg(II)	Pr(III): Phe	Pr(III)	Pr(III):Ph e:Mg(II)	Pr(III): Phe	Pr(III)	Pr(III):Phe: Mg(II)	Pr(III):Phe	Pr(III)	Pr(III):Phe :Mg(II)	Pr(III):Phe	Pr(III)
		309.236	309.38	309.532	309.167	309.311	309.529	308.962	309.145	309.314	308.536	308.893	309.234
		42.690	42.711	42.731	42.680	42.700	42.730	42.652	42.677	42.700	42.593	42.642	42.689
		4.669	4.671	4.673	4.668	4.670	4.673	4.665	4.668	4.670	4.658	4.664	4.669
		722.680	722.50	722.568	722.102	722.203	721.958	722.043	722.550	722.765	718.585	719.389	720.599
		3511.26	3513.0	3514.63	3510.489	3512.12	3514.59	3508.161	3510.238	3512.15	3503.325	3507.372	3511.24
		23.761	23.773	23.784	23.756	23.767	23.783	23.740	23.754	23.767	23.707	23.735	23.761
		614.781	615.08	615.371	614.645	614.932	615.364	614.238	614.601	614.937	613.391	614.100	614.778
		0.947	0.947	0.947	0.946	0.946	0.947	0.946	0.946	0.947	0.9432	0.9443	0.9456
		0.162	0.162	0.162	0.163	0.163	0.162	0.164	0.163	0.162	0.1685	0.1669	0.1649
		5.593	5.581	5.553	5.648	5.617	5.600	5.686	5.617	5.573	6.0214	5.9011	5.7524

Table 3.2: Computed and observed values of energy (cm^{-1}) and RMS values for Pr^{3+} and its complexes in (50% v/v) aquated solvents.

		$^3\text{H}_4 \rightarrow ^3\text{P}_2$		$^3\text{H}_4 \rightarrow ^3\text{P}_1$		$^3\text{H}_4 \rightarrow ^3\text{P}_0$		$^3\text{H}_4 \rightarrow ^1\text{D}_2$		RMS
		E_{obs}	E_{cal}	E_{obs}	E_{cal}	E_{obs}	E_{cal}	E_{obs}	E_{cal}	
DIMETHYLFORMAMIDE (DMF)	Pr(III)	22523.54	22456.28	21363.68	21247.35	20758.78	20690.26	16909.42	17137.88	136.88
	Pr(III):Phe	22497.05	22430.19	21297.53	21221.42	20742.80	20666.18	16909.42	17120.60	123.22
	Pr(III):Phe: Mg(II)	22476.93	22399.02	21276.28	21190.46	20722.03	20637.47	16863.18	17099.96	138.43
ACETONITRILE (ACN)	Pr(III)	22518.47	22472.59	21356.43	21261.58	20753.09	20700.01	16971.02	17147.86	106.29
	Pr(III):Phe	22513.38	22460.09	21335.34	21248.88	20743.01	20687.74	16961.14	17139.47	106.27
	Pr(III):Phe: Mg(II)	22497.15	22445.18	21313.49	21234.05	20733.05	20673.94	16951.29	17129.58	105.23
DIOXAN	Pr(III)	22523.54	22483.03	21366.70	21273.41	20772.19	20713.54	16974.29	17155.38	107.91
	Pr(III):Phe	22520.15	22469.59	21352.56	21259.16	20756.09	20698.76	16961.14	17146.11	110.43
	Pr(III):Phe: e:Mg(II)	22516.12	22459.33	21334.93	21248.65	20747.06	20688.44	16953.85	17139.18	110.06
METHANOL	Pr(III)	22523.61	22486.32	21386.52	21276.06	20768.40	20714.93	16973.42	17157.30	112.09
	Pr(III):Phe	22520.15	22476.33	21373.26	21265.78	20759.08	20704.76	16963.76	17150.54	113.26
	Pr(III):Phe: e:Mg(II)	22513.29	22466.86	21364.71	21255.74	20747.47	20694.35	16956.45	17144.01	114.05

and Mg^{2+} in aquated solvents.

METHANOL				DIOXAN				ACETONITRILE (ACN)				DIMETHYLFORMAMIDE (DMF)					
Pr(III):Ph e; ₃ Mg(II)	Pr(III): Phe	Pr(III)	Pr(III):Phe :Mg(II)	Pr(III):P he	Pr(III)	³ H ₄ → ³ P ₂		³ H ₄ → ³ P ₁		³ H ₄ → ³ P ₀		³ H ₄ → ¹ D ₂		T ₂	T ₄	T ₆	
						Pobs	Pcal	Pobs	Pcal	Pobs	Pcal	Pobs	Pcal				
9.474	7.590	7.542	9.368	8.128	7.516	8.665	7.899	10.657	10.290	8.737	8.737	3.438	2.235	1.018	2.203	1.634	1.634
9.474	7.590	7.542	9.368	8.128	7.516	8.665	7.899	10.657	10.290	8.737	8.737	3.438	2.235	1.018	2.203	1.634	1.634
2.124	2.394	1.625	3.429	3.115	2.603	2.405	1.606	3.887	3.591	3.577	2.912	3.222	2.871	2.202	2.203	2.136	2.136
1.503	1.562	1.166	2.242	2.176	1.705	1.820	1.207	3.577	2.912	3.577	2.912	3.222	2.871	2.202	2.203	2.136	2.136
0.867	0.717	0.696	1.039	1.217	0.795	1.216	0.795	3.222	2.202	3.222	2.202	3.222	2.871	2.202	2.203	2.136	2.136
1.478	1.535	1.147	2.207	2.140	1.678	1.791	1.187	3.527	2.871	3.527	2.871	3.527	2.871	2.203	2.203	2.136	2.136
1.440	1.089	0.704	2.523	1.439	0.757	1.681	1.269	5.105	2.136	5.105	2.136	5.105	2.136	1.634	1.634	1.634	1.634
1.440	1.089	0.704	2.523	1.439	0.757	1.681	1.269	5.105	2.136	5.105	2.136	5.105	2.136	1.634	1.634	1.634	1.634
-299.4	-255.6	-338.5	-49.07	-213.3	-326.5	-151.1	-234.1	449.53	-200.4	449.53	-200.4	449.53	-200.4	-209.4	-209.4	-209.4	-209.4
4.122	4.281	3.196	6.157	5.972	4.676	4.998	3.311	9.851	8.012	9.851	8.012	9.851	8.012	6.143	6.143	6.143	6.143
29.957	23.731	23.859	29.063	25.043	23.38	29.708	27.071	32.361	31.618	32.361	31.618	32.361	31.618	26.989	26.989	26.989	26.989

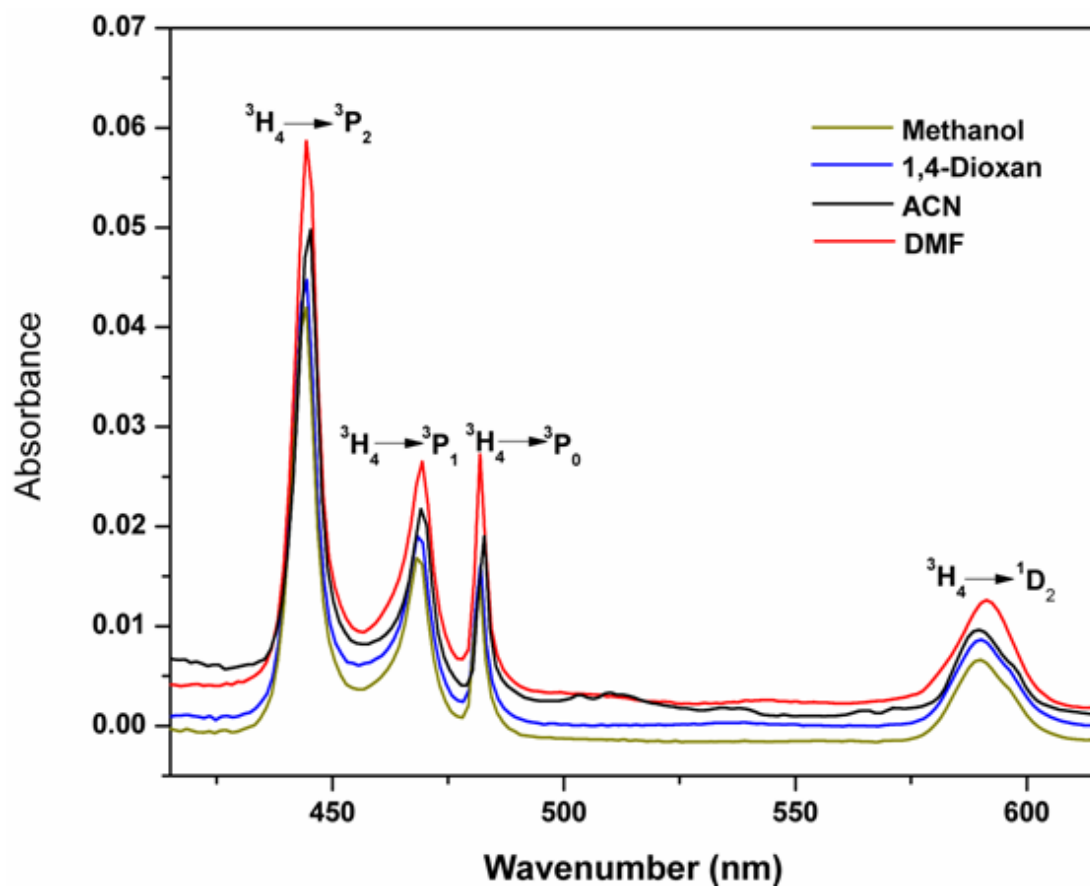


Fig. 3.6: Comparative UV-vis absorption spectra of Pr(III):Phe complex in different aquated solvents of C_3H_7NO , CH_3OH , $C_4H_8O_2$, and CH_3CN .

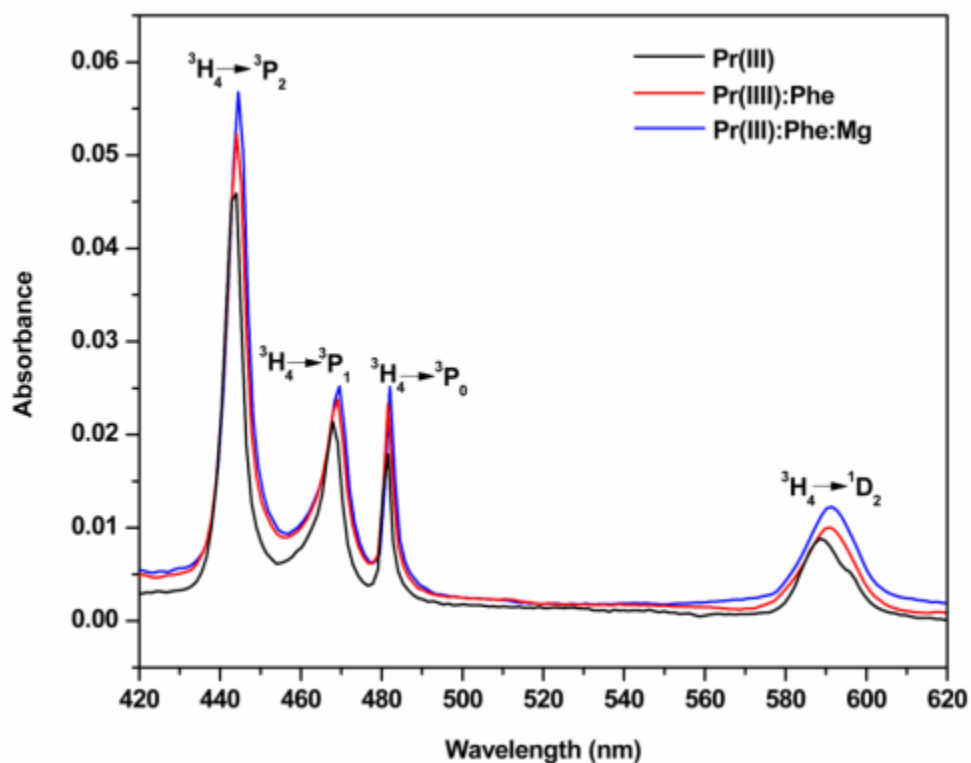


Fig. 3.7: UV-vis absorption spectra of $4f-4f$ electronic transitions of Pr^{3+} , Pr(III):Phe and Pr(III):Phe:Mg(II) complexes in 50% v/v aquated DMF solvent in different pH 4.

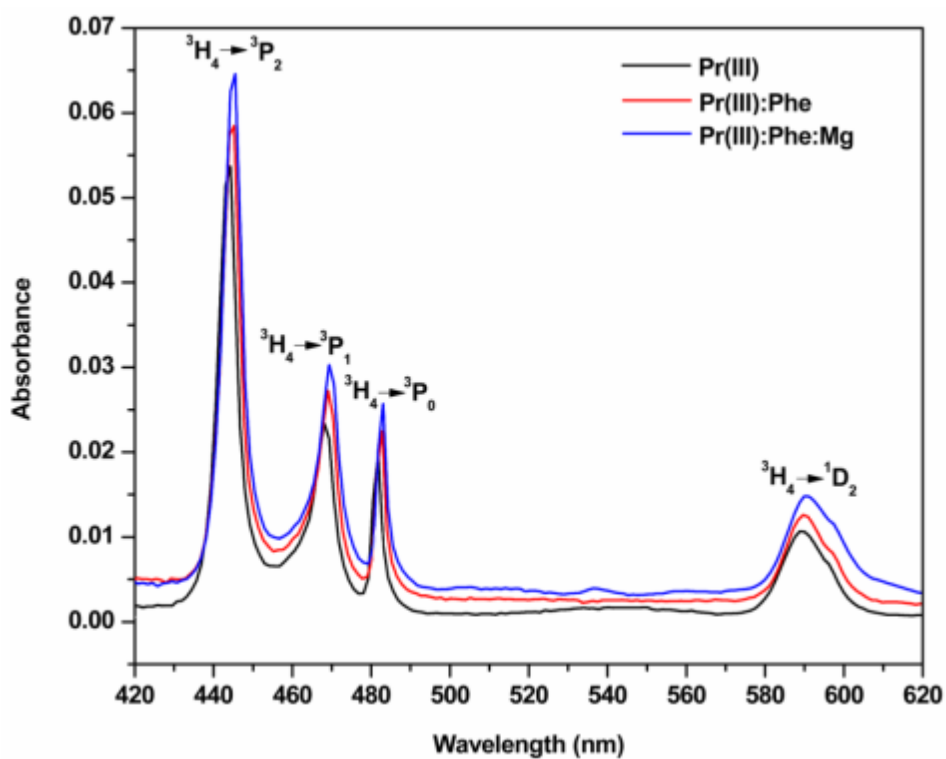


Fig. 3.8: UV-vis absorption spectra of $4f-4f$ electronic transitions of Pr^{3+} , Pr(III):Phe and Pr(III):Phe:Mg(II) complexes in 50% v/v aquated DMF solvent in different pH 6.

pH 6				pH 4			pH 2		
Pr(III):Phe: Mg(II)	Pr(III):Phe	Pr(III)	Pr(III):Phe: Mg(II)	Pr(III):Phe	Pr(III)	Pr(III):Phe: Mg(II)	Pr(III):Phe	Pr(III)	
8.693	6.279	5.201	7.082	5.883	3.958	5.003	4.109	3.205	
8.693	6.279	5.201	7.082	5.883	3.958	5.003	4.109	3.205	
4.186	3.313	2.265	3.029	2.686	1.643	2.129	1.968	1.492	
2.962	2.299	1.687	2.150	1.821	1.173	1.595	1.366	1.041	
1.712	1.266	1.093	1.253	0.942	0.693	1.043	0.751	0.579	
2.918	2.265	1.662	2.118	1.794	1.155	1.568	1.343	1.023	
2.599	1.992	1.661	2.070	1.481	1.201	1.476	1.200	0.999	
2.599	1.992	1.661	2.070	1.481	1.201	1.476	1.200	0.999	
9.630	32.521	30.156	-1.867	-55.68	8.934	1.669	-1.900	12.761	
8.120	6.303	4.626	5.895	4.993	3.216	4.377	3.747	2.853	
26.295	18.876	15.794	21.616	17.93	12.103	15.245	12.474	9.743	

Table 3.5: Computed value of energy interaction parameters Slater-Condon $F_K(\text{cm}^{-1})$, Spin-Orbit Interaction $\xi_{4f}(\text{cm}^{-1})$, Nephelauxetic ratio (β), bonding ($b^{1/2}$), and covalency (δ) parameters of Pr(III) with L-phenylalanine in presence/absence Mg^{2+} in aquated DMF solvent.

pH 6				pH 4			pH 2			
Pr(III):Phe :Mg(II)	Pr(III):Phe	Pr(III)	Pr(III):Phe :Mg(II)	Pr(III):Phe :Mg(II)	Pr(III):Phe	Pr(III)	Pr(III):Phe :Mg(II)	Pr(III):Phe	Pr(III)	
308.471	308.995	309.368	309.045	309.343	309.785	309.078	309.277	309.420	F_2	
42.584	42.656	42.708	42.663	42.704	42.765	42.668	42.695	42.715	F_4	
4.657	4.665	4.671	4.666	4.671	4.677	4.667	4.670	4.672	F_6	
721.992	722.236	723.541	718.357	719.154	721.207	722.140	722.702	722.982	ξ_{4f}	
3502.590	3508.537	3512.769	3509.108	3512.489	3517.504	3509.478	3511.736	3513.362	E_1	
23.702	23.742	23.771	23.746	23.769	23.803	23.749	23.764	23.775	E_2	
613.262	614.304	615.045	614.403	614.995	615.873	614.468	614.864	615.148	E_3	
0.945	0.946	0.947	0.943	0.944	0.946	0.946	0.947	0.947	β	
0.165	0.163	0.161	0.167	0.166	0.163	0.163	0.162	0.162	$b^{1/2}$	
5.770	5.666	5.505	5.955	5.845	5.615	5.660	5.584	5.539	δ	
113.23	113.92	114.34	130.34	126.00	106.97	114.36	105.09	103.52	RMS	

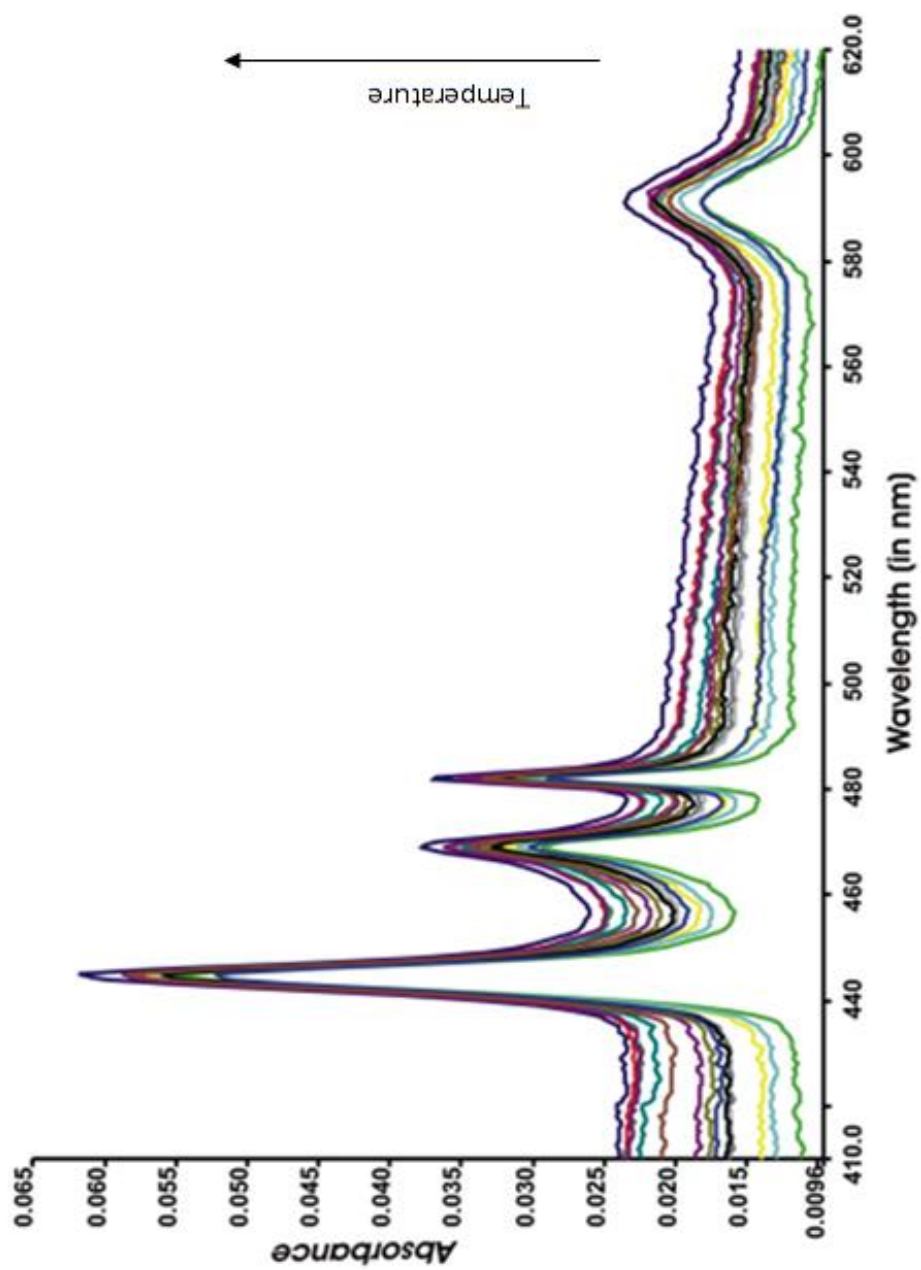


Fig. 3.9: Absorption spectra of Pr(III):Phe:Mg(II) complexation at 303 K and in different time intervals.

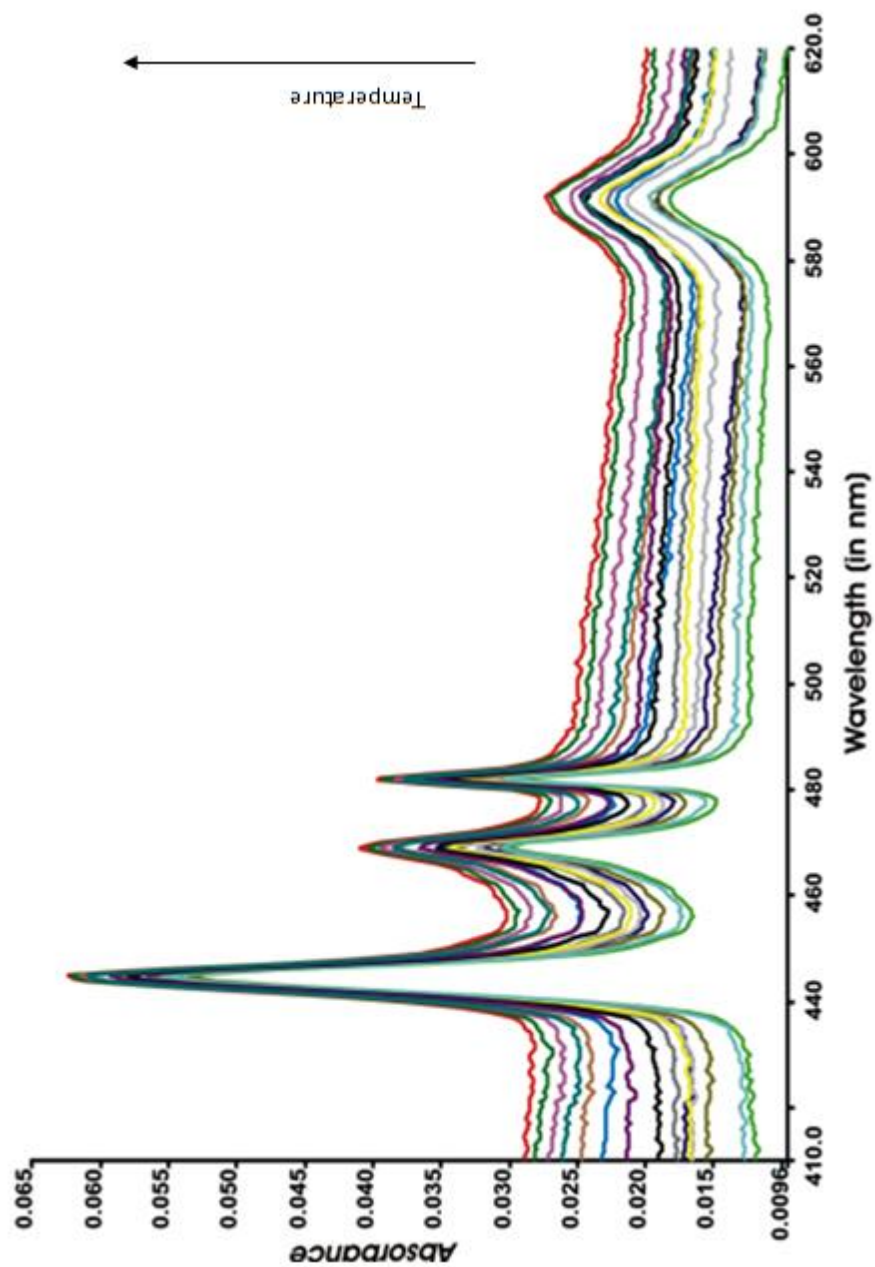


Fig. 3.10: Absorption spectra of Pr(III):Phe:Mg(II) complexation at 308K and in different time intervals.

Table 3.6: Observed and calculated oscillator strengths ($P \times 10^6$) and Judd-Ofelt intensity parameter (T_λ , $\lambda = 2, 4, 6 \times 10^{10} \text{ cm}^{-1}$) parameters for Pr(III):Phe:Mg(II) complex at 298 K and in different time intervals.

Time (inhr)	$^3\text{H}_4 \rightarrow ^3\text{P}_2$		$^3\text{H}_4 \rightarrow ^3\text{P}_1$		$^3\text{H}_4 \rightarrow ^3\text{P}_0$		$^3\text{H}_4 \rightarrow ^1\text{D}_2$		T_2	T_4	T_6
	Pobs	Pcal	Pobs	Pcal	Pobs	Pcal	Pobs	Pcal			
0	0.838	0.838	0.236	0.198	0.159	0.195	0.402	0.402	35.84	0.545	2.605
2	0.840	0.840	0.234	0.200	0.164	0.197	0.388	0.388	32.46	0.550	2.610
4	0.861	0.861	0.242	0.206	0.169	0.203	0.388	0.388	31.11	0.568	2.674
6	0.871	0.871	0.245	0.209	0.171	0.206	0.403	0.403	33.84	0.575	2.706
8	0.890	0.890	0.246	0.210	0.173	0.207	0.403	0.403	32.75	0.579	2.767
10	0.930	0.930	0.255	0.218	0.180	0.215	0.426	0.426	35.21	0.601	2.893
12	0.932	0.932	0.260	0.223	0.184	0.220	0.433	0.433	36.66	0.613	2.896
14	0.935	0.935	0.259	0.222	0.184	0.219	0.431	0.431	35.97	0.612	2.907
16	0.935	0.935	0.252	0.220	0.186	0.217	0.422	0.422	33.86	0.605	2.907
18	0.938	0.938	0.260	0.222	0.183	0.219	0.450	0.450	-40.134	0.612	2.915
20	0.943	0.943	0.263	0.223	0.182	0.220	0.429	0.429	34.905	0.615	2.930
22	0.946	0.946	0.259	0.223	0.186	0.220	0.430	0.430	34.967	0.615	2.943
24	1.035	1.035	0.291	0.250	0.207	0.246	0.459	0.459	35.730	0.688	3.213
26	1.036	1.036	0.286	0.245	0.202	0.241	0.459	0.459	35.498	0.674	3.222
28	1.041	1.041	0.286	0.247	0.206	0.243	0.464	0.464	-36.33	0.680	3.237
30	1.046	1.046	0.283	0.244	0.202	0.240	0.468	0.468	-37.05	0.670	3.255
32	1.050	1.050	0.281	0.245	0.207	0.241	0.463	0.463	35.62	0.674	3.267
34	1.061	1.066	0.297	0.255	0.211	0.251	0.484	0.484	-39.60	0.702	3.297

Table 3.7: Observed and calculated oscillator strengths ($P \times 10^6$) and Judd-Ofelt intensity parameter (T_λ , $\lambda = 2, 4, 6 \times 10^{10} \text{ cm}^{-1}$) parameters for Pr(III):Phe:Mg(II) complex at 303 K and in different time intervals.

Time (inhr)	$^3\text{H}_4 \rightarrow ^3\text{P}_2$		$^3\text{H}_4 \rightarrow ^3\text{P}_1$		$^3\text{H}_4 \rightarrow ^3\text{P}_0$		$^3\text{H}_4 \rightarrow ^1\text{D}_2$		T_2	T_4	T_6
	Pobs	Pcal	Pobs	Pcal	Pobs	Pcal	Pobs	Pcal			
0	0.885	0.885	0.240	0.209	0.177	0.206	0.177	0.177	-18.56	0.576	2.751
2	0.903	0.903	0.243	0.212	0.180	0.209	0.180	0.180	-19.00	0.584	2.807
4	0.919	0.919	0.240	0.213	0.184	0.210	0.184	0.184	-19.16	0.586	2.860
6	0.934	0.934	0.243	0.215	0.185	0.212	0.185	0.185	-19.90	0.591	2.909
8	0.983	0.983	0.259	0.226	0.191	0.223	0.191	0.191	-21.86	0.622	3.061
10	0.995	0.995	0.259	0.230	0.198	0.226	0.198	0.198	-21.05	0.632	3.097
12	1.003	1.003	0.266	0.234	0.200	0.231	0.200	0.200	-21.20	0.644	3.122
14	1.018	1.018	0.268	0.237	0.203	0.233	0.203	0.203	-21.39	0.651	3.168
16	1.038	1.038	0.272	0.239	0.203	0.235	0.203	0.203	-22.81	0.656	3.233
18	1.037	1.037	0.275	0.241	0.204	0.237	0.204	0.204	-22.49	0.662	3.227
20	1.046	1.546	0.279	0.245	0.208	0.241	0.208	0.208	-55.03	0.673	4.895
22	1.099	1.099	0.282	0.250	0.215	0.246	0.215	0.215	-24.11	0.687	3.424
24	1.102	1.102	0.292	0.258	0.221	0.254	0.221	0.221	-22.94	0.709	3.427
26	1.118	1.118	0.294	0.259	0.222	0.255	0.222	0.222	-23.78	0.713	3.480
28	1.128	1.128	0.293	0.261	0.227	0.257	0.227	0.227	-23.26	0.719	3.511
30	1.135	1.135	0.300	0.266	0.229	0.262	0.229	0.229	-23.34	0.731	3.531
32	1.151	1.151	0.299	0.266	0.230	0.262	0.230	0.230	-24.14	0.731	3.584
34	1.172	1.172	0.300	0.268	0.233	0.264	0.233	0.233	-24.82	0.737	3.650

Table 3.8: Observed and calculated oscillator strengths ($P \times 10^6$) and Judd-Ofelt intensity parameter (T_λ , $\lambda = 2, 4, 6 \times 10^{10} \text{ cm}^{-1}$) parameters for Pr(III):Phe:Mg(II) complex at 308 K and in different time intervals.

Time (in hr)	$^3\text{H}_4 \rightarrow ^3\text{P}_2$		$^3\text{H}_4 \rightarrow ^3\text{P}_1$		$^3\text{H}_4 \rightarrow ^3\text{P}_0$		$^3\text{H}_4 \rightarrow ^1\text{D}_2$		T_2	T_4	T_6
	Pobs	Pcal	Pobs	Pcal	Pobs	Pcal	Pobs	Pcal			
0	0.924	0.924	0.244	0.215	0.184	0.212	0.414	0.414	32.745	0.591	2.874
2	0.932	0.932	0.253	0.219	0.183	0.216	0.409	0.409	31.022	0.602	2.898
4	0.983	0.983	0.259	0.226	0.190	0.223	0.192	0.192	- 21.860	0.622	3.062
6	1.018	1.018	0.276	0.240	0.202	0.237	0.452	0.452	35.123	0.661	3.165
8	1.051	1.051	0.2700	0.242	0.210	0.238	0.451	0.451	32.962	0.663	3.269
10	1.087	1.087	0.282	0.251	0.218	0.247	0.472	0.472	35.125	0.691	3.384
12	1.081	1.081	0.275	0.246	0.214	0.242	0.498	0.498	-41.44	0.676	3.367
14	1.028	1.028	0.267	0.238	0.207	0.235	0.462	0.462	37.022	0.655	3.202
16	1.112	1.112	0.291	0.256	0.219	0.252	0.491	0.491	37.860	0.705	3.463
18	1.127	1.127	0.287	0.258	0.225	0.253	0.496	0.496	37.941	0.708	3.510
20	1.140	1.140	0.292	0.2262	0.231	0.258	0.497	0.497	-37.47	0.720	3.548
22	1.153	1.153	0.296	0.263	0.228	0.260	0.505	0.505	38.148	0.725	3.593
24	1.172	1.172	0.301	0.268	0.233	0.264	0.233	0.233	-24.20	0.737	3.651
26	1.203	1.203	0.625	0.452	0.275	0.445	0.719	0.719	82.890	1.240	3.609
28	1.218	1.218	0.442	0.410	0.371	0.403	0.519	0.519	84.407	1.243	3.713
30	1.233	1.233	0.662	0.473	0.277	0.465	0.767	0.767	91.36	1.296	3.693
32	1.254	1.254	0.692	0.494	0.291	0.486	0.8254	0.8254	103.22	1.237	3.713
34	1.274	1.724	0.301	0.452	0.275	0.445	0.719	0.719	82.890	1.240	3.650

Table 3.9: Observed and calculated oscillator strengths ($P \times 10^6$) and Judd-Ofelt intensity parameter (T_λ , $\lambda = 2, 4, 6 \times 10^{10} \text{ cm}^{-1}$) parameters for Pr(III):Phe:Mg(II) complex at 313 K and in different time intervals.

Time (in hr)	$^3\text{H}_4 \rightarrow ^3\text{P}_2$		$^3\text{H}_4 \rightarrow ^3\text{P}_1$		$^3\text{H}_4 \rightarrow ^3\text{P}_0$		$^3\text{H}_4 \rightarrow ^1\text{D}_2$		T_2	T_4	T_6
	Pobs	Pcal	Pobs	Pcal	Pobs	Pcal	Pobs	Pcal			
0	0.924	0.924	0.244	0.215	0.184	0.212	0.414	0.414	32.745	0.591	2.874
2	0.931	0.931	0.278	0.2787	0.214	0.362	0.486	0.486	37.38	0.602	2.898
4	0.931	0.931	0.278	0.2787	0.214	0.362	0.486	0.486	37.38	0.602	2.898
6	1.032	1.032	0.346	0.252	0.154	0.247	0.269	0.269	-7.505	0.688	3.196
8	1.047	1.047	0.279	0.246	0.211	0.242	0.485	0.485	-40.790	0.677	3.256
10	1.053	1.053	0.356	0.263	0.168	0.259	0.289	0.289	-1.650	0.739	3.236
12	1.092	1.092	0.518	0.367	0.214	0.362	0.486	0.486	-37.380	1.011	3.309
14	1.132	1.132	0.468	0.359	0.245	0.353	0.580	0.580	-38.819	0.685	3.454
16	1.163	1.163	0.484	0.369	0.249	0.363	0.535	0.535	43.907	1.012	3.541
18	1.187	1.187	0.515	0.385	0.252	0.380	0.423	0.423	46.852	1.058	3.605
20	1.195	1.195	0.583	0.421	0.2547	0.415	0.647	0.647	66.831	1.155	3.606
22	1.212	1.212	0.626	0.453	0.276	0.446	0.719	0.719	82.890	1.240	3.609
24	1.223	1.223	0.590	0.461	0.321	0.449	0.653	0.653	83.450	1.241	3.702
26	1.233	1.233	0.575	0.410	0.371	0.403	0.519	0.519	84.407	1.243	3.713
28	1.258	1.258	0.662	0.473	0.277	0.465	0.767	0.767	91.36	1.296	3.693
30	1.263	1.263	0.744	0.531	0.313	0.523	0.903	0.903	103.25	1.312	3.891
32	1.279	1.279	0.695	0.495	0.298	0.488	0.829	0.829	120.00	1.458	3.891
34	1.289	1.289	0.632	0.476	0.310	0.466	0.671	0.671	64.592	1.298	3.891

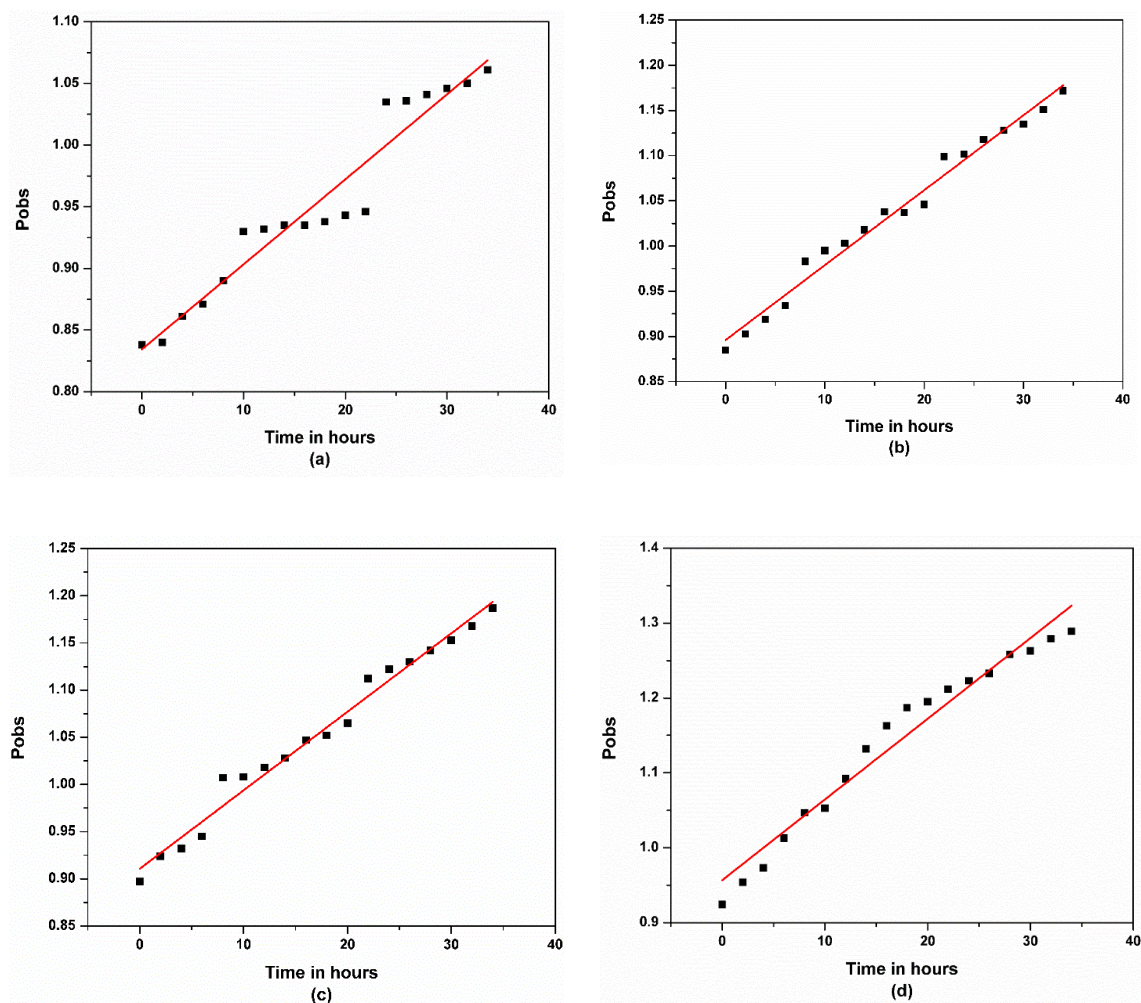


Fig. 3.11: Plot of P_{obs} and Time in hours for the $^3H_4 \rightarrow ^3P_2$ transition of Pr(III):Phe:Mg(II) at four different temperatures (a) 298 K, (b) 303 K, (c) 308 K, (d) 313 K.

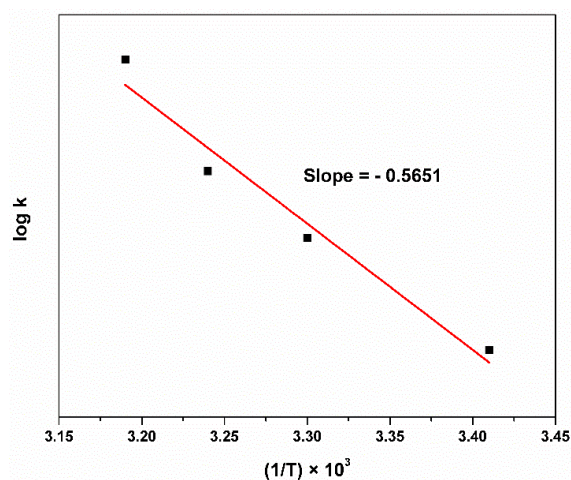


Fig. 3.12: Plot of $\log k$ versus $(1/T) \times 10^3$ for the complexation of Pr(III):Phe:Mg(II) in an aqueous medium.

Table 3.10: Rate Constants at different temperatures and Activation Energy for Pr(III):Phe:Mg(II) complex.

Temperature (K)	$1/T \times 10^3 \text{K}^{-1}$	Rate Constant (k) $\text{Mol L}^{-1} \text{h}^{-1}$	Rate Constant (k) $\text{Mol L}^{-1} \text{S}^{-1} \times 10^{-6}$	log k	Pre-exponential factor (A)	Activation Energy $\Delta E_a (\text{kJ/mol})$
298	3.41	0.0081	2.25	0.35	0.83	0.011
303	3.30	0.0086	2.41	0.38	0.89	
308	3.24	0.0090	2.50	0.40	0.93	
313	3.19	0.0092	2.56	0.48	0.96	

Table 3.11: Rate constants and thermodynamic parameters for Pr(III):Phe:Mg(II) complex at different temperatures.

Temperature (K)	Rate (k) $\text{Mol L}^{-1} \text{S}^{-1} \times 10^{-6}$	ΔH^0 (kJmol^{-1})	ΔG^0 ($\text{JK}^{-1} \text{mol}^{-1}$)	ΔS^0 (kJmol^{-1})
298	2.25	0.011	-1.99	0.0067
303	2.41		-2.20	0.0072
308	2.50		-2.30	0.0075
313	2.56		-2.46	0.0079

The $4f$ -electrons of lanthanides can give two types of transition; $f-d$ and $f-f$ transitions, out of which $f-f$ transitions are the observed spectral transitions of the lanthanide ions [16]. The $4f-4f$ transition band intensities are less affected by the coordination ambience since the filled $5s$ and $5p$ sub-shells firmly shield the $4f$ -subshell of Ln^{3+} and are regarded as non-hypersensitive transitions. On the other hand, some transitions show significantly high sensitivity with little changes in their coordination environment, and their band intensities become more intensified when a lanthanide ion gets complexed with ligands, and as such, they follow the selection rules, $\Delta S = 0$, $\Delta L \leq 2$ and $\Delta J = \leq 2$, known as hypersensitive transitions.

The solution spectral analysis of Pr^{3+} complexes reveals that some of the transition intensities of Pr^{3+} ions ($^3\text{H}_4 \rightarrow ^3\text{P}_2$, $^3\text{H}_4 \rightarrow ^3\text{P}_1$, $^3\text{H}_4 \rightarrow ^3\text{P}_0$, and $^3\text{H}_4 \rightarrow ^1\text{D}_2$) exhibit an exceptionally sensitive character towards minor changes in their coordination ambience even though they could not follow the selection rule. Such transitions are pseudoquadrupole in character and are known as Ligand Mediated Pseudohypersensitive transitions since their sensitivity is the inducing result of their coordination environment [17]. These Pseudo-hypersensitive transitions have been used extensively for the absorption spectral study to understand the nature of bonding and structural conformations of Pr(III) with ligands in solution study [18]. The interaction of Pr^{3+} with the ligand and their sensitivity towards the formation of the complex is shown vividly by the corresponding intensification of the pseudo hypersensitive transitions.

Amino acids generally possess $-\text{NH}_2$ and $-\text{COOH}$ functional groups and can modulate the size and dimensions of buoyant materials, while their -R group (side chains) remains intact [19]. For instance, in the case of Pr(III):Phe (L-Phenylalanine) complexation, the interaction essentially occurs via the carboxylic group of the ligand and their bonding is primarily electrostatic in nature. Fig. 3.13 depicts the possible reaction mechanism for the Pr(III):Phe complex in a lower pH medium. The preference for bonding lanthanide with the ligand will be through the donor sites such as oxygen atoms since lanthanides are hard metal ions and are strongly electro-positive in nature. Lanthanides show a preference for the donor atoms in the order $\text{O} > \text{N} > \text{S}$, which shows that lanthanide has a strong preference for oxygen donor atoms [20].

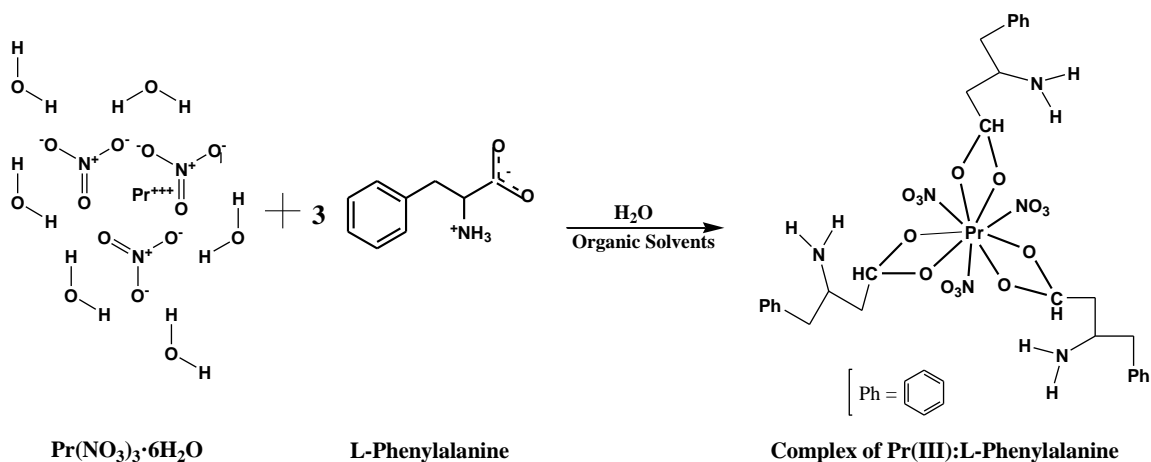


Fig. 3.13: The possible reaction mechanism for the formation of nona coordinated complex of Pr(III):L-Phenylalanine in an acidic medium.

Fig. 3.4 and 3.5 shows the comparative absorption spectra of different transitions of free Pr(III), Pr(III):Phe and Pr(III):Phe:Mg(II) in ACN:H₂O and in the UV-vis region. The variation of the band intensities is clearly visible as shown in the figures. The absorption bands get more intense when the ligand (L-phenylalanine) is added to the Pr³⁺ solution, and it further, gets more intensified on the addition of Mg²⁺ to the binary complex [Pr(III):Phe]. This firmly signifies the possibility of interaction of the metal Pr³⁺ with ligand L-Phenylalanine and Mg²⁺. The red-shift observed in figure 3.4 and 3.5 further substantiate the information of the possibility of the formation of Pr(III):Phe:Mg(II) complex [21].

The variations and the changes in the computed values of the energy interaction parameters: Slater-Condon factor ($F_k = 2, 4, 6$), Lande Spin-orbit interactions (ζ_{4f}), Racah parameters ($E_k = 1, 2, 3$), Nephelauxetic ratio (β), bonding ($b^{1/2}$) and percent covalency (δ) for Pr³⁺ and their complexes Pr(III):Phe and Pr(III):Phe:Mg(II) in aqueous solutions of Methanol, ACN, Dioxane and DMF (50% v/v) were presented in table 3.1. Comparing the values of energy interaction parameters of Pr³⁺ in its free

ionic state with that of the Pr(III):Phe and Pr(III):Phe:Mg(II) complexes in different solvents, it was found that there is a steady decrease in the computed values of the β , ξ_{4f} and F_k revealing the possibility of formation of complexes. Further, looking at the decreased value of (β), signifies the expansion of the orbital of the central metal ion thereby shortening the metal-ligand distance known as the nephelauxetic effect [22]. Consequently, the increase of percent covalency (δ) and the bonding parameter ($b^{1/2}$) followed by the nephelauxetic ratio (β) values, which were found to be less than unity, implies the possibility of the formation of covalent bond in the complexation of Pr(III) with L-phenylalanine [23]. The decrease in the values of β also conveys its correlation to the intensification of the various transition bands of Pr^{3+} ($^3\text{P}_2$, $^3\text{P}_1$, $^3\text{P}_0$, and $^1\text{D}_2$) as shown in figures 3.4 and 3.5. The accuracy of the estimated values of energy interaction parameters could be predicted by observing the root mean square (RMS) values (Table 3.2). On comparing the obtained values of the computed data, it was observed that the maximum values of $b^{1/2}$ and δ parameters are observed in the DMF:H₂O (50% v/v) system, this indicates the preference for covalent bond formation in the aquated DMF solvent which may be due to the presence of N-donor [24,25].

Judd-Ofelt parameters (T_λ) and Oscillator strength (P) for the ligand-mediated pseudohypersensitive transitions of free Pr^{3+} ion and Pr^{3+} in its complexes with L-Phenylalanine and Mg^{2+} was evaluated under various experimental ambiances. Its computed data shown in table 3.3 revealed that there is a remarkable change in the P values of $4f-4f$ bands which implies the possibility of the interaction between Pr^{3+} with L-phenylalanine [27]. The magnitude of T_λ ($\lambda = 2, 4, 6$) parameters increase significantly when Pr^{3+} interacts with the ligand in solution; this validates the possibility of the binding of L-phenylalanine to Pr^{3+} . Further, the intensification

increases when Mg^{2+} is added to the complex formed, Pr(III):Phe, which also may be due to the binding of Mg^{2+} to form a multimetal complex [19]. T_2 is correlated to the hypersensitive transition, $^3\text{H}_4 \rightarrow ^3\text{F}_3$, since this transition is beyond the UV-Visible region and its values are negative, thereby T_2 is ignored [28,29]. On the other hand, T_4 and T_6 are affected significantly and their values are positive and thus can be applied in the Judd-Ofelt theory of $4f-4f$ transitions. Both T_4 and T_6 parameters are related to changes in symmetry properties of the complex species [30] thus, the significant changes in the values of T_4 and T_6 suggest possible changes in their immediate coordination environment which induces to the changes in the complexation of Pr^{3+} with the ligands. When the values of P and their corresponding T_λ have significant variations, it indicates inner-sphere complexation while slight changes in the values of P and T_λ parameters indicate outer-sphere complexation of the metal with the ligand [31]. The significant changes in computed values of P and T_λ provide substantial evidence of the involvement of L-phenylalanine in the inner-sphere coordination of Pr^{3+} . The computed data reveals that among the three T_λ ($\lambda = 2, 4, 6$) parameters, T_6 is the best suited parameter to interpret the complexation of Pr^{3+} with L-phenylalanine and Mg^{2+} , and their order is $T_6 > T_4 > T_2$.

Figure 3.6 shows the comparative UV-Vis absorption spectra of Pr(III):Phe in various aquated binary solvents of Methanol, Dioxan, ACN, and DMF. The increase in the interaction between $4f$ orbitals of Pr^{3+} with that of the ligand is rendered by the intensification of the various $4f-4f$ transition bands. The higher intensification in the aquated DMF solvent depicts that there is a stronger influence of solvent over Pr^{3+} to form a complex with the ligand. This shows that DMF is the better solvent compared to the others in the formation of the complex of Pr^{3+} with phenylalanine. Such a

significant effect of DMF solvent in the complexation is due to its strong ability to donate oxygen atoms for the substitution of water molecules in the coordination sphere [26]. The $4f-4f$ absorption band intensities of the organic solvents have sensitivity in the order: DMF>CH₃CN>C₄H₈O₂>CH₃OH. Also, the values of oscillator strength (P) in the case of DMF solvent are higher compared to that of other solvents, indicating further that this solvent is the preferred one in the formation of the complex

Table 3.4 and 3.5 shows the computed results for the various energy interaction parameters: F_k ($k=2,4,6$), ζ_{4f} , E^k ($k=1,2,3$), β , $b^{1/2}$ and δ for Pr(III), Pr(III):Phe and Pr(III):Phe:Mg(II) at various pH values. The degree of protonation/deprotonation at Phenylalanine's binding sites is controlled by the pH value, which has a significant impact on its bonding capacity. From the observation, as the value of pH increases the computed values of β , ζ_{4f} and F_k show a steady decrease. This explains the increase in the interaction of metal with the ligand at higher pH. The computed data elucidates the deprotonation of the carboxylic group of L-phenylalanine at an acidic medium (lower pH), allowing the Pr(III) ion to bind through it [45]. Increases in percent covalency (δ) and bonding parameter ($b^{1/2}$) with increasing pH values indicate an increase in interaction and the probability of formation of covalent bonds, which could be related to an increase in deprotonation capacity as pH rises. The shortening of the metal-ligand distance is explained clearly by the decrease in the values of the nephelauxetic ratio (β). The change in the values of intensity parameters shown in tables 3.3 & 3.4 and the increase in the intensities of the four pseudohypersensitive transitions (figure 3.7 & 3.8) also demonstrate this effect. At high pH the amine group deprotonates, this is reflected by the T_λ , ($\lambda = 2, 4, 6$) values, which are found to be higher at higher pH.

For the kinetic study of the complexation of Pr(III) with L-phenylalanine and Mg(II), the absorption spectra were recorded in a binary solvent DMF:H₂O (50% v/v) at different temperatures of 303 K, 308 K, 313 K, and 318 K by maintaining a gap of two hours time interval. From the comparative absorption spectra (Fig. 3.9 & 3.10) at different temperatures and the observed changes in the computed values of P and T_λ parameters for the complex Pr(III):Phe:Mg(II), it is revealed that the transition $^3H_4 \rightarrow ^3P_2$ is the most sensitive $4f-4f$ transition as compared to that of $^3H_4 \rightarrow ^3P_1$, $^3H_4 \rightarrow ^3P_0$, and $^3H_4 \rightarrow ^1D_2$ transitions. The computed data (Tables 3.6, 3.7, 3.8 & 3.9) shows that the values of T_4 and T_6 were relatively more sensitive and they are found to increase proportionately with time and temperature; this trend signifies the rise in the rate constants of the complexation process of Pr(III) with the L-phenylalanine in the presence of Mg²⁺.

Fig. 3.11 shows the plot of P_{obs} vs time for the transition $^3H_4 \rightarrow ^3P_2$ at different temperatures. The values of the pre-exponential factor and slope obtained from the graphs were used in the calculation of rate constants as shown in table 3.10. From table 3.10, it is clearly seen that the rate constant for the formation of the Pr(III):Phe complex in presence of Mg(II) is enhanced by the rise in temperature in the order of $318\text{ K} > 313\text{ K} > 308\text{ K} > 303\text{ K}$ which is in accordant with the theoretical prediction of Arrhenius Reaction Rate. Also, the increase in the values of the Pre-exponential factor (A) with the rise in temperature shows the increase in the probability of collision of the molecules. The negligibly low value of the activation energy (E_a) indicates the possibility of the spontaneity of the reaction. In addition, fig. 3.12 presents the plot of $\log k$ vs $(1/T) \times 10^3$, and the values obtained from the graph were used for the determination of ΔH^0 , ΔG^0 , and ΔS^0 values (Table 3.11). The

endothermic reaction associated with complexation is shown by the positive values of ΔH^0 , whereas the spontaneity of the reaction process is indicated by the negative value of ΔG^0 . The positive values of ΔS^0 imply that the coordination reaction is entropy-driven and also that the complex is well-formed. Such kinetic studies based on absorption spectral analysis of the $4f-4f$ transition can be employed as an alternative approach for the theoretical study of the reaction dynamics and also for the prediction of possible thermodynamic behaviour involved in the Pr(III):Phe:Mg(II) complexation.

3.5 CONCLUSION

The interaction of Pr^{3+} with L-phenylalanine in the presence/absence of Mg^{2+} is revealed by the decrease in the values of ζ_{4f} , E^k , F_k , and the increase in the values of $b^{1/2}$ and δ . It is further substantiated by the increase in the interaction of $4f$ -orbitals which is interpreted through the intensification of absorption bands as well as the appearance of the redshift when the ligand is added to the pure Praseodymium ion. The increase in absorption bands of the $4f-4f$ transition of Pr^{3+} is associated with the shortening of the metal-ligand distance and lowering of the coordination number, shown by the decrease in the values of nephelauxetic ratio β . The significant variations in the computed values of P and T_λ could provide the formation of inner-sphere complexation as well as the strong binding effect in the complexation of Pr^{3+} with L-Phenylalanine and Mg^{2+} . The marked changes in the values of T_4 and T_6 suggests that there is a change in the symmetry of the complex formed. DMF was found to be the best-suited solvent for the complexation among the four solvents used. Based on the computed P and T_λ values, the stability of the complexes follows the order, $\text{Pr(III)} < \text{Pr(III):Phe} < \text{Pr(III):Phe:Mg(II)}$.

The discussions based upon the values of intensity parameters for the complexation at different time intervals and different temperatures vividly revealed that the rate constants for the formation of the Pr(III):Phe complex in presence of Mg(II) increases with time and temperature confirming the Arrhenius prediction of the reaction rate. The negligibly low value of Activation energy (E_a) conveys the possibility of spontaneity in the complexation of Pr^{3+} with L-phenylalanine and Mg^{2+} . The positive values of ΔH^0 imply the endothermic reaction associated with the complexation, and the negative value of ΔG^0 manifests the spontaneity of the reaction process and the favorable nature of the reaction in solution. Since, $T\Delta S^0 > \Delta H^0$, the present study of coordination reaction is found to be entropy-driven. The values of the pre-exponential factor (A) provide the empirical relationship between temperature and the reaction rate depending upon the probability of how often the molecules collide.

REFERENCES

- [1] I. Hemmilä, V. Laitala, Progress in lanthanides as luminescent probes, *J. Fluoresc.* 15 (2005) 529–542. <https://doi.org/10.1007/s10895-005-2826-6>.
- [2] D. Kang, E. Jeon, S. Kim, J. Lee, Lanthanide-Doped Upconversion Nanomaterials: Recent Advances and Applications, *Biochip J.* 14 (2020) 124–135. <https://doi.org/10.1007/s13206-020-4111-9>.
- [3] J.A. Cotruvo, The Chemistry of Lanthanides in Biology: Recent Discoveries, Emerging Principles, and Technological Applications, *ACS Cent. Sci.* 5, 9 (2019) 1496–1506. <https://doi.org/10.1021/acscentsci.9b00642>.
- [4] A.M. Măciucă, A.C. Munteanu, V. Uivarosi, Quinolone complexes with lanthanide ions: An insight into their analytical applications and biological activity, *Molecules.* 25(2020)1347. <https://doi.org/10.3390/molecules25061347>.
- [5] N. Bendangsenla, T. Moaienla, T. David Singh, C. Sumitra, N. Rajmuhon Singh, M. Indira Devi, Evaluation of intensity and energy interaction parameters for the complexation of Pr(III) with selected nucleoside and nucleotide through absorption spectral studies, *Spectrochim. Acta - Part A Mol. Biomol. Spectrosc.* 103 (2013) 160-166. <https://doi.org/10.1016/j.saa.2012.11.011>.
- [6] T.D. Singh, C. Sumitra, N. Yaiphaba, H.D. Devi, M.I. Devi, N.R. Singh, Comparison of energy interaction parameters for the complexation of Pr(III) with glutathione reduced (GSH) in absence and presence of Zn(II) in aqueous and aquated organic solvents using 4f-4f transition spectra as PROBE, *Spectrochim. Acta - Part A Mol. Biomol. Spectrosc.* 61 (2005) 1219–1225. <https://doi.org/10.1016/j.saa.2004.06.044>.
- [7] S.N. Misra, G. Ramchandriah, M.A. Gagnani, R.S. Shukla, M.I. Devi, Absorption spectral studies involving 4f-4f transitions as structural probe in chemical and biochemical reactions and compositional dependence of intensity parameters, *Appl. Spectrosc. Rev.* 38 (2003) 433-493. <https://doi.org/10.1081/ASR-120026330>.
- [8] J.D. Fernstrom, M.H. Fernstrom, Tyrosine, phenylalanine, and catecholamine synthesis and function in the brain, in: *J. Nutr.*, 137 (2007) 1539S-1547S. <https://doi.org/10.1093/jn/137.6.1539s>.
- [9] D.E. Matthews, An overview of phenylalanine and tyrosine kinetics in humans, in: *J. Nutr.*, 137(6) (2007) 1549S–1575S. <https://doi.org/10.1093/jn/137.6.1549s>.

- [10] M. Remko, D. Fitz, R. Broer, B.M. Rode, Effect of metal Ions (Ni $2+$, Cu $2+$ and Zn $2+$) and water coordination on the structure of L-phenylalanine, L-tyrosine, L-tryptophan and their zwitterionic forms, *J. Mol. Model.* 17 (2011) 3117–3128. <https://doi.org/10.1007/s00894-011-1000-0>.
- [11] R. Tan, J. Li, F. Liu, P. Liao, M. Ruiz, J. Dupuis, L. Zhu, Q. Hu, Phenylalanine induces pulmonary hypertension through calcium-sensing receptor activation, *Am. J. Physiol. - Lung Cell. Mol. Physiol.* (2020). <https://doi.org/10.1152/AJPLUNG.00215.2020>.
- [12] M.F. Bush, J. Oomens, R.J. Saykally, E.R. Williams, Effects of alkaline earth metal ion complexation on amino acid zwitterion stability: Results from infrared action spectroscopy, *J. Am. Chem. Soc.* 130 (2008) L1010-L1020. <https://doi.org/10.1021/ja711343q>.
- [13] F. Costanzo, R.G. Della Valle, V. Barone, MD simulation of the Na $^{+}$ -phenylalanine complex in water: Competition between cation- π interaction and aqueous solvation, *J. Phys. Chem. B.* 109 (2005) 23016-23. <https://doi.org/10.1021/jp055271g>.
- [14] A.L. Sobolewski, D. Shemesh, W. Domcke, Computational studies of the photophysics of neutral and zwitterionic amino acids in an aqueous environment: Tyrosine-(H $_2$ O) $_2$ and tryptophan-(H $_2$ O) $_2$ clusters, *J. Phys. Chem. A.* 113 (2009) 542-550. <https://doi.org/10.1021/jp8091754>.
- [15] J.C.G. Bünzli, C. Piguet, Lanthanide-containing molecular and supramolecular polymetallic functional assemblies, *Chem. Rev.* (2002). <https://doi.org/10.1021/cr010299j>.
- [16] S. Purohit, N. Bhojak, The Absorption Spectra of Some Lanthanide (III) Ions, *J. Chem.* 2 (2013) 10–12.
- [17] M.S. N., S.S. O, Absorption Spectra of Lanthanide Complexes in Solution, *Appl. Spectrosc. Rev.* 26 (1991) 151–202. <https://doi.org/10.1080/05704929108050880>.
- [18] N. Yaiphaba, Comparative 4f-4f absorption spectral study for the interactions of Pr(III) with selected urea and thiourea: Energy and electric dipole intensity parameters, *J. Chem. Pharm. Res.* 5 (2013) 377-385.
- [19] K.K. Gangu, S. Maddila, S.N. Maddila, S.B. Jonnalagadda, Nanostructured samarium doped fluorapatites and their catalytic activity towards synthesis of

- 1,2,4-triazoles, *Molecules*. 21 (2016) 121. <https://doi.org/10.3390/molecules21101281>.
- [20] S.N. Misra, M.I. Devi, The synthesis and determination of the octacoordinated structure of Pr(III) and Nd(III) complexes with β -diketones and diols in non aqueous solutions: Evidence of some participation of π -electron density of diols with Pr(III) and Nd(III) in complexation, *Spectrochim. Acta - Part A Mol. Biomol. Spectrosc.* (1997). [https://doi.org/10.1016/S1386-1425\(97\)00064-4](https://doi.org/10.1016/S1386-1425(97)00064-4).
- [21] Z.A. Taha, A.K. Hijazi, W.M. Al Momani, Lanthanide complexes of the tridentate Schiff base ligand salicylaldehyde-2- picolinoylhydrazone: Synthesis, characterization, photophysical properties, biological activities and catalytic oxidation of aniline, *J. Mol. Struct.* 1220 (2020) 128712. <https://doi.org/10.1016/j.molstruc.2020.128712>.
- [22] S.N. Misra, K. John, Difference and Comparative Absorption Spectra and Ligand Mediated Pseudohypersensitivity for 4f-4f Transitions of Pr (III) and Nd (III) Difference and Comparative Absorption Spectra and Ligand Mediated Pseudo hypersensi tivi ty for 4f-4f Transitions o, 4928 (2016). <https://doi.org/10.1080/05704929308018115>.
- [23] N. Bendangsenla, T. Moaienla, T. David Singh, C. Sumitra, N. Rajmuhon Singh, M. Indira Devi, Evaluation of intensity and energy interaction parameters for the complexation of Pr(III) with selected nucleoside and nucleotide through absorption spectral studies, *Spectrochim. Acta - Part A Mol. Biomol. Spectrosc.* 103 (2013) 160–166. <https://doi.org/10.1016/j.saa.2012.11.011>.
- [24] N. Ranjana Devi, B. Huidrom, N. Rajmuhon Singh, Studies on the complexation of Pr(III) and Nd(III) with glycyl-glycine (gly-gly) using spectral analysis of 4f-4f transitions and potentiometric titrations, *Spectrochim. Acta - Part A Mol. Biomol. Spectrosc.* 96 (2012) 370–379. <https://doi.org/10.1016/j.saa.2012.05.038>.
- [25] C.V. Devi, N.R. Singh, Absorption spectroscopic probe to investigate the interaction between Nd(III) and calf-thymus DNA, *Spectrochim. Acta - Part A Mol. Biomol. Spectrosc.* 78 (2011) 1180–1186. <https://doi.org/10.1016/j.saa.2010.12.078>.
- [26] C. Sumitra, T. David Singh, M. Indira Devi, N.R. Singh, Calculation of electric dipole intensity parameters of 4f-4f transitions of Pr(III) and glutathione reduced (GSH) complex in presence and absence of Zn(II), *Spectrochim. Acta - Part A Mol. Biomol. Spectrosc.* 66 (4-5) (2007) 1333-9.

<https://doi.org/10.1016/j.saa.2006.06.023>.

- [27] C. Victory Devi, N. Rajmuhon Singh, Spectrophotometric study of kinetics and associated thermodynamics for the complexation of Pr(III) with L-proline in presence of Zn(II), Arab. J. Chem. 10 (2017) S2124–S2131. <https://doi.org/10.1016/j.arabjc.2013.07.044>.
- [28] T. Moaienla, T.D. Singh, N.R. Singh, M.I. Devi, Computation of energy interaction parameters as well as electric dipole intensity parameters for the absorption spectral study of the interaction of Pr(III) with l-phenylalanine, l-glycine, l-alanine and l-aspartic acid in the presence and absence of Ca²⁺, Spectrochim. Acta - Part A Mol. Biomol. Spectrosc. 74 (2009) 434–440. <https://doi.org/10.1016/j.saa.2009.06.039>.
- [29] N. Bendangsenla, T. Moainla, J. Sanchu, M.I. Devi, Computation of Energy, Intensity and Thermodynamic Parameters for the Interaction of Ln(III) with Nucleic Acid: Analysis of Structural Conformations, Chemical Kinetics and Thermodynamic Behaviour through 4f-4f Transition Spectra as Probe, J. Mater. Sci. Chem. Eng. 6 (2018) 169–183. <https://doi.org/10.4236/msce.2018.67018>.
- [30] A.A. Khan, H.A. Hussain, K. Iftikhar, 4f-4f absorption spectra and hypersensitivity in nine-coordinate Ho(III) and Er(III) complexes in different environments, Spectrochim. Acta - Part A Mol. Biomol. Spectrosc. 60(8-9) (2004) 2087–92. <https://doi.org/10.1016/j.saa.2003.10.042>.
- [31] T. Moaienla, N. Bendangsenla, T. David Singh, C. Sumitra, N. Rajmuhon Singh, M. Indira Devi, Comparative 4f-4f absorption spectral study for the interactions of Nd(III) with some amino acids: Preliminary thermodynamics and kinetic studies of interaction of Nd(III):glycine with Ca(II), Spectrochim. Acta - Part A Mol. Biomol. Spectrosc. 87 (2012) 142–150. <https://doi.org/10.1016/j.saa.2011.11.028>.

CHAPTER- 4

Complexation of Pr^{3+} with L-methionine in the presence/absence of Mg^{2+} : their reaction dynamics and thermodynamic properties

In this chapter, the 4f-4f transition spectra of Praseodymium (Pr^{3+}) were used as a probe to analyze the interaction of Pr(III) ion with L-methionine in presence/absence of Mg(II) in 50%v/v aquated organic solvents. The nature of the complexation was studied by the changes in the theoretically computed data of the energy interaction parameters whereas the changes in the computed values of intensity parameters (Oscillator strength, P and Judd-Ofelt T_{λ}) were calculated to study and scrutinized the possibility of the inner and outer sphere complexation. The thermodynamic behavior was studied by computing the parameters like specific rate constant/rate constant (k), pre-exponential factor (A), ΔH° , ΔS° , and ΔG° .

The text of this chapter has been published as:

Z. Thakro, J. Sanchu, C. Imsong, M.I. Devi, **Complexation of Pr^{3+} with L-methionine in the presence/absence of Mg^{2+} : Their reaction dynamics and thermodynamic properties**, Chem. Phys. Impact. 4 (2022) 100078. <https://doi.org/10.1016/j.chphi.2022.100078>.

4.1 INTRODUCTION

The 15 elements from lanthanum (La) to lutetium (Lu) are termed lanthanides and they correspond to the gradual filling of the 4f electronic shell, which is shielded by the outer $5s^2 5p^6$ subshells [1]. Lanthanide complexes have been investigated for their intriguing and crucial features such as their ability to bind oxygen reversibly, structural probes in biological systems, and catalytic activity in the hydrogenation of olefins [2–4]. The coordination chemistry of Lanthanide in solution is emerging rapidly due to the increasing usage of lanthanides as probes in biomolecular reactions to explore their structural functions. It is mainly due to their similarities and ability to substitute Ca(II) ions [5–7]. Lanthanide ions possess the properties of antitumor, antibacterial, and antiviral agents when they coordinate with organic ligands and participate effectively in many important biochemical activities [8–10].

4.1.1 Methionine

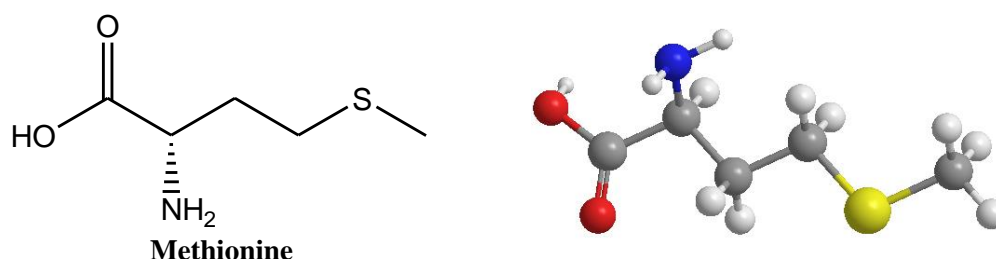


Fig. 4.1: 2D and 3d structures of L-methionine.

Methionine, also known as 2-amino-4-(methylthio)butanoic acid (Figure 4.1), is a sulfur-containing aliphatic essential amino acid that is indispensable for many physiological and biochemical metabolism. Supplementing or restricting methionine can affect an organism's natural antioxidant capacity by causing the synthesis of

endogenous enzymes that reduce oxidative stress and, as a result, DNA damage, neuropsychiatric disorders, cardiovascular disease, cancer, and neurodegenerative illnesses [11]. Functional groups ($-\text{NH}_2$ & $-\text{COOH}$) in amino acids can be used to modify the size and dimensions of propitious materials, while their side chains ($-\text{R}$ group) remain intact [12]. In physiological conditions, amino acids and peptides are common bimolecular molecules that function as binding sites. Peptides are well-known simple amino acid building blocks with significant biological value in the therapeutic field, making peptide research one of the rapidly emerging fields of research in recent times [13]. Thus, employing the $4f-4f$ transition spectrum of Pr^{3+} as a probe to explore the interaction of metal with L-methionine, a biologically active amino acid, would be an exciting new field in current research.

4.1.2 Bonding nature of L-methionine with Praseodymium

Lanthanides are categorized as class A/hard acceptors, and hence prefer to bind with the hard donor sites of the ligand (in the order $\text{O} > \text{N} > \text{S}$ and $\text{F} > \text{Cl}$) for complex formation. In general, coordination numbers of lanthanide ion ranges from 6 to 12, with 8 or 9 being biologically significant coordination numbers. As a result, the complexes could have a wide range of geometrical conformations [14]. When amino acids are in the gaseous phase, they exist in their neutral state [15]. However, they occur in zwitterionic form when they are in the aqueous solution [16–18]. Bonding of the ligand with the metal relies on the pH values and it plays an important role in formation of the complex (Figure 4.2 & 4.3) [19].

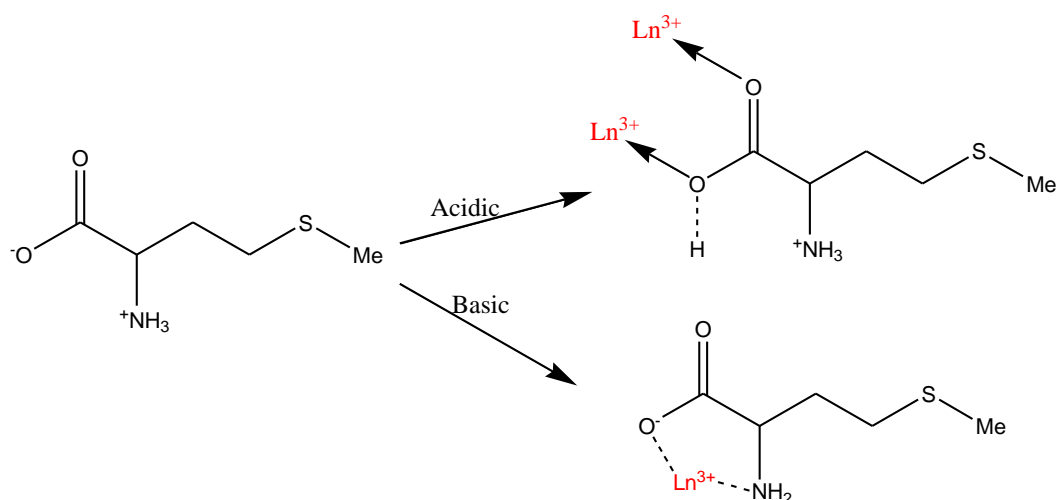


Fig 4.2: Bonding nature of the zwitterions L-methionine under different pH mediums.

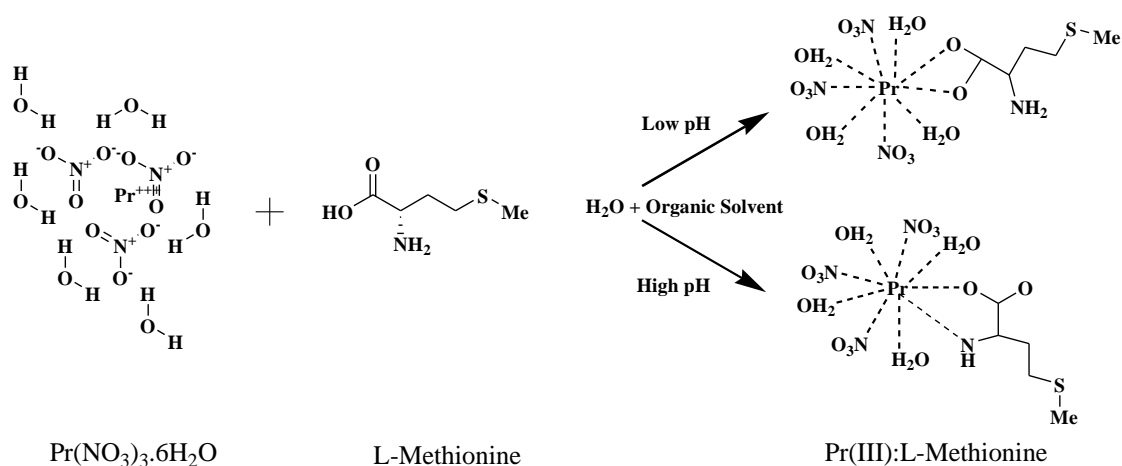


Fig 4.3: Possible reaction of Pr(III) with L-methionine under different pH medium

The current study uses the $4f-4f$ transition spectra of Pr^{3+} as a probe to analyze the interaction of Pr(III) ion with L-methionine in the presence/absence of Mg(II) in 50% v/v aquated organic solvents ($\text{C}_4\text{H}_8\text{O}_2$, DMF, CH_3CN , and CH_3OH). The nature of the complexation was studied by the changes in the theoretically computed data of the energy interaction parameters: percentage covalency (δ), bonding parameter ($b^{1/2}$), Nephelauxetic ratio (β), Spin-orbit interaction (ζ_{4f}), Racah energy (E_k), and Slater-

Condon (F_k). The changes in the computed values of intensity parameters: oscillator strengths (P) and Judd-Ofelt (T_λ , $\lambda=2, 4, 6$) electric dipole intensity parameters were calculated to study and scrutinized the possibility of the inner and outer sphere complexation of metal with the L-methionine. The complexation of Pr^{3+} with L-methionine in presence/absence of Mg(II) at different pH (2,4,6) mediums was done in 50% v/v aquated DMF solvent. The kinetic and thermodynamic parameters like specific rate constant/rate constant (k), pre-exponential factor (A), ΔH° , ΔS° , and ΔG° were evaluated to analyze systematically, the nature of the chemical reaction pathways.

4.2 EXPERIMENTAL SECTION

4.2.1 Materials and Methods

Praseodymium (III) nitrate hexahydrate of 99.9% purity and 2-amino-4-(methylthio)butanoic acid were purchased from Sigma-Aldrich and HiMedia respectively. 99.5% purity organic solvents; N,N-Dimethylformamide, Acetonitrile, Methanol, and 1,4-Dioxan was purchased from Merck. For recording spectra, concentrations of Pr(III) , 2-amino-4-(methylthio)butanoic acid (Methionine), and Mg(II) were kept at 5×10^{-3} M in (50% v/v) of aquated organic solvents (ACN, Dioxane, MeOH & DMF). The complexation of Praseodymium (Pr^{3+}) with L-methionine in presence and absence of Mg^{2+} at various pH (2, 4, 6) was studied particularly in a 50% v/v aquated DMF medium. UV/Vis spectrophotometer (Perkin Elmer Lambda 365) was used for recording the absorption spectra. Eutech pH 700 digital pH meter was used for the pH measurements.

4.3 CALCULATIONS

The following equations are used for the calculations of different parameters. The details of the calculations have been discussed in chapter 2.

4.3.1 Energy parameters

Nephelauxetic ratio ' β '

$$\beta = \frac{F_K^C}{F_K^f} \text{ or } \frac{E_C^K}{E_f^K} \quad (1)$$

Slater–Condon ' F_k ' and Lande spin-orbit parameters ' ξ_{4f} '

$$F_k = F_k^0 + \Delta F_k \quad (2)$$

$$\xi_{4f} = \xi_{4f}^0 + \Delta \xi_{4f} \quad (3)$$

Racah parameter

$$E^1 = \frac{70F_2 + 231F_4 + 20.02F_6}{9} \quad (4)$$

$$E^2 = \frac{F_2 - 3F_4 + 7F_6}{9} \quad (5)$$

$$E^3 = \frac{5F_2 + 6F_4 - 9F_6}{9} \quad (6)$$

Bonding parameter ($b^{1/2}$) and covalent percentage (δ)

$$b^{1/2} = \left[\frac{1-\beta}{2} \right]^{1/2} \quad (7)$$

$$\delta = \left[\frac{1-\beta}{\beta} \right] \times 100 \quad (8)$$

4.3.2 Intensity parameters

Oscillator strength

$$P_{\text{obs}} = 4.6 \times 10^{-9} \times \epsilon_{\text{max}} \bar{\nu}_{1/2} \quad (9)$$

Judd-Ofelt parameters (T_λ)

$$\frac{P_{\text{obs}}}{\nu} = [(U)^2]^2 \cdot T_2 + [(U)^4]^2 \cdot T_4 + [(U)^6]^2 \cdot T_6 \quad (10)$$

4.3.3 Reaction dynamics/thermodynamics theory

$$\log k = \log A - \frac{E_a}{2.303R} \frac{1}{T} \quad (11)$$

$$E_a = -\text{slope} \times 2.303 \times R \quad (12)$$

$$\log k = -\frac{\Delta H^\circ}{R} \left[\frac{1}{T} \right] + \frac{\Delta S^\circ}{R} \quad (13)$$

4.4 RESULTS AND DISCUSSIONS

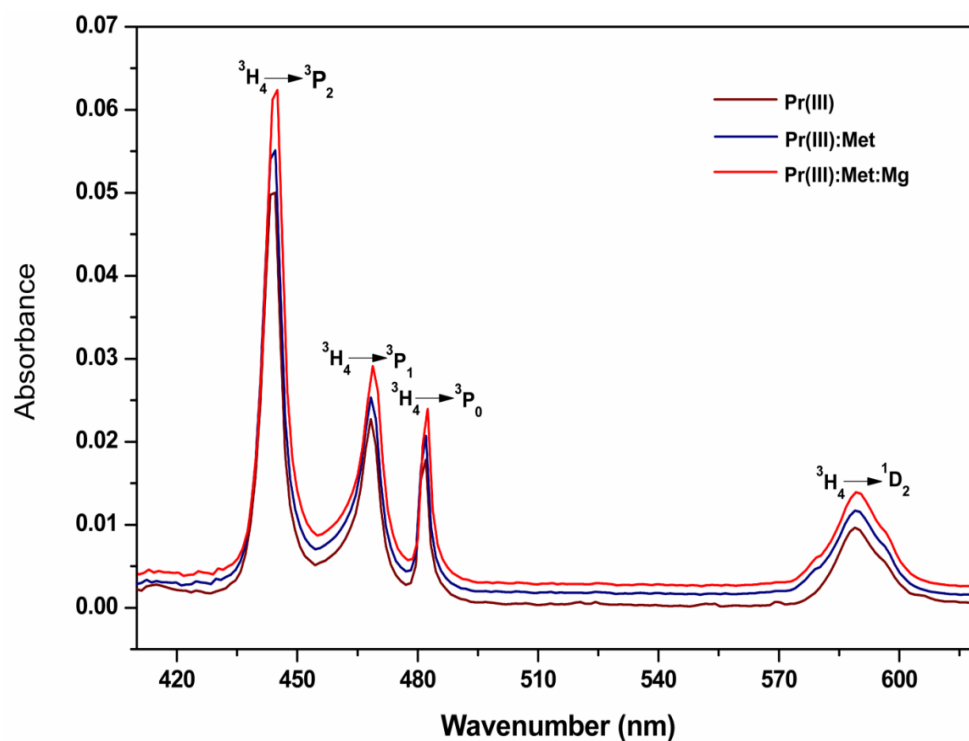


Fig. 4.4: UV-vis absorption spectra of $4f-4f$ electronic transitions of Pr^{3+} , Pr(III):Met and $\text{Pr(III):Met:Mg(II)}$ complexes in 50% v/v aquated ACN solvent.

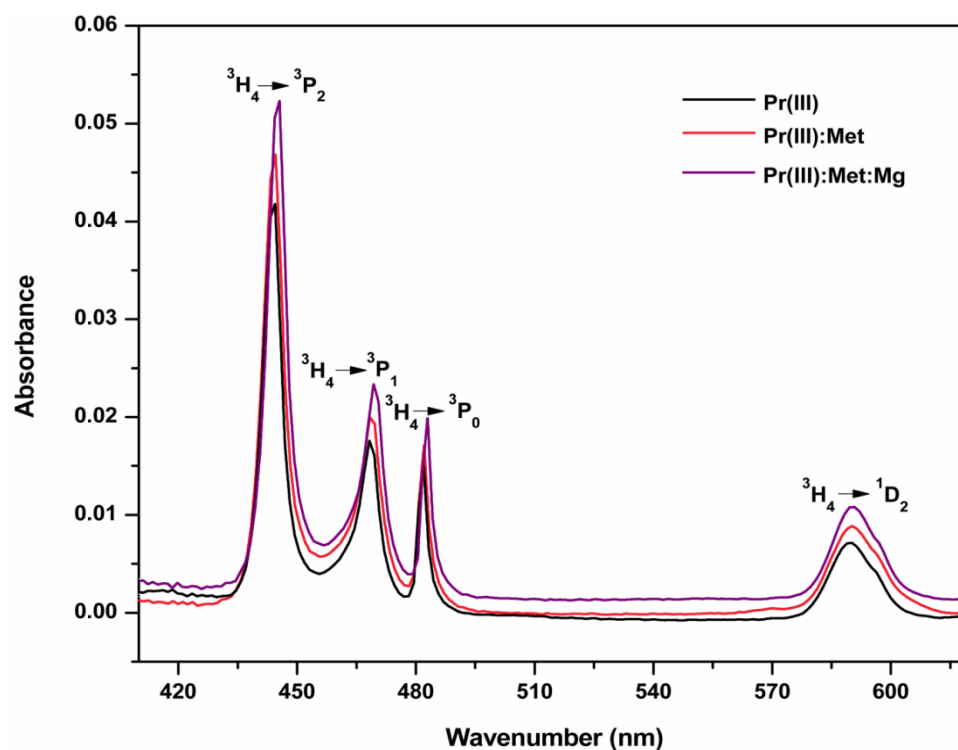


Fig. 4.5: UV-vis absorption spectra of the $4f-4f$ electronic transitions of Pr^{3+} , Pr(III):Met and $\text{Pr(III):Met:Mg(II)}$ complexes in 50% v/v aquated Dioxane solvent.

Table 4.1: Observed and calculated values of oscillator strengths ($P \times 10^6$) and Judd-Olfelt intensity parameter [T_λ , ($\lambda = 2, 4, 6$) $\times 10^{10} \text{ cm}^{-1}$] of Pr^{3+} with L-methionine in presence/absence of Mg^{2+} in various aquated organic solvent (50% v/v).

Methanol:Water			Dioxane:Water			ACN:Water			DMF:Water			T_2	T_4	T_6
Pr(III): Met:Mg	Pr(III): Met	Pr(III)	Pr(III):M et:Mg(II)	Pr(III) :Met	Pr(III)	Pr(III):M et:Mg(II)	Pr(III) :Met	Pr(III)	Pr(III) :Met	Pr(III) :Met	Pr(III): Met			
5.4821	4.2585	3.8144	7.4745	4.2748	3.676	7.4745	6.6085	3.6919	8.0232	6.6085	5.0595			
5.4821	4.2585	3.8144	7.4745	4.2748	3.676	7.4745	6.6085	3.6919	8.0232	6.6085	5.0595			
2.4903	1.2805	1.198	2.7263	2.237	1.4742	2.7263	1.9764	1.4645	2.9536	2.3665	1.8385			
1.7637	0.9811	0.8054	2.0175	1.4629	1.0016	2.0185	1.3874	1.0036	2.1968	1.6697	1.2601			
1.0203	0.6706	0.4061	1.2903	0.6774	0.5202	1.2903	0.7852	0.5338	1.4208	0.9603	0.6718			
1.7351	0.9652	0.7922	1.9891	1.4388	0.9848	1.9871	1.3646	0.9871	2.1675	1.648	1.2419			
1.8549	0.3996	0.3342	2.4756	1.621	1.347	2.4756	1.9537	1.3257	2.0289	1.6197	1.2107			
1.8549	0.3996	0.3342	2.4756	1.621	1.347	2.4756	1.9537	1.3257	2.0289	1.6197	1.2107			
54.688	-192.1	-177.1	65.158	82.748	61.168	63.543	5.2723	54.998	-72.12	-70.57	-60.67			
4.842	2.6932	2.2097	5.5381	4.0074	2.7401	5.5523	3.8096	2.7514	6.0493	4.5932	3.4598			
16.694	13.249	11.912	23.014	12.923	11.288	23.1	20.641	11.365	24.731	20.455	15.657			

Table 4.2: Computed value of energy interaction parameters Slater-Condon $F_K(\text{cm}^{-1})$, Spin-Orbit Interaction $\xi_{4f}(\text{cm}^{-1})$, Nephelauxetic ratio (β), bonding ($b^{1/2}$), and covalency (δ) parameters of Pr^{3+} free ion, Pr(III) with Methionine in presence and absence of Mg^{2+} in various aquated organic solvents.

Methanol:Water			Dioxane:Water			ACN:Water			DMF:Water			
Pr(III):Me t:Mg(II)	Pr(III): Met	Pr(III)	Pr(III):M et:Mg(II)	Pr(III): Met	Pr(III)	Pr(III):Met :Mg(II)	Pr(III): Met	Pr(III)	Pr(III):Met :Mg(II)	Pr(III): Met	Pr(III)	
309.113	309.178	309.320	309.469	309.636	309.983	308.645	308.967	309.441	308.712	309.100	309.432	F_2
42.673	42.682	42.701	42.722	42.745	42.793	42.608	42.653	42.718	42.617	42.671	42.705	F_4
4.667	4.668	4.670	4.673	4.675	4.680	4.660	4.665	4.672	4.661	4.667	4.671	F_6
722.976	723.405	724.021	720.320	722.329	722.988	721.528	722.585	722.761	718.476	718.176	719.627	ξ_{4f}
3509.870	3510.61	3512.22	3513.908	3515.80	3519.76	3504.555	3508.22	3513.60	3505.316	3509.73	3512.50	E_1
23.751	23.757	23.766	23.779	23.792	23.818	23.715	23.740	23.777	23.721	23.750	23.769	E_2
614.537	614.667	614.948	615.244	615.577	616.268	613.607	614.249	615.190	613.740	614.512	614.998	E_3
0.947	0.947	0.948	0.945	0.947	0.948	0.945	0.946	0.947	0.943	0.944	0.945	β
0.163	0.162	0.161	0.165	0.162	0.160	0.165	0.163	0.162	0.169	0.168	0.165	$b^{1/2}$
5.590	5.557	5.477	5.735	5.555	5.447	5.778	5.644	5.553	6.001	5.960	5.808	δ
97.71	93.49	91.84	114.09	115.48	112.23	99.37	102.30	104.70	126.99	128.98	124.49	RMS

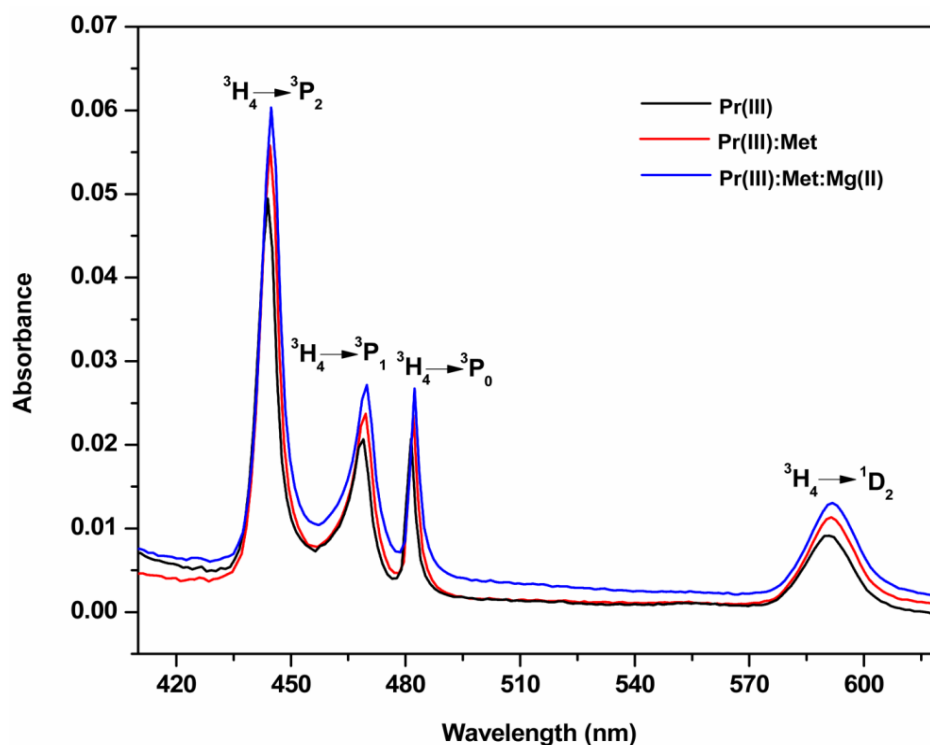


Fig. 4.6: UV-vis absorption spectra of the $4f-4f$ electronic transitions of Pr^{3+} , Pr(III):Met & $\text{Pr(III):Met:Mg(II)}$ complex in 50% v/v aquated DMF solvent at pH 4.

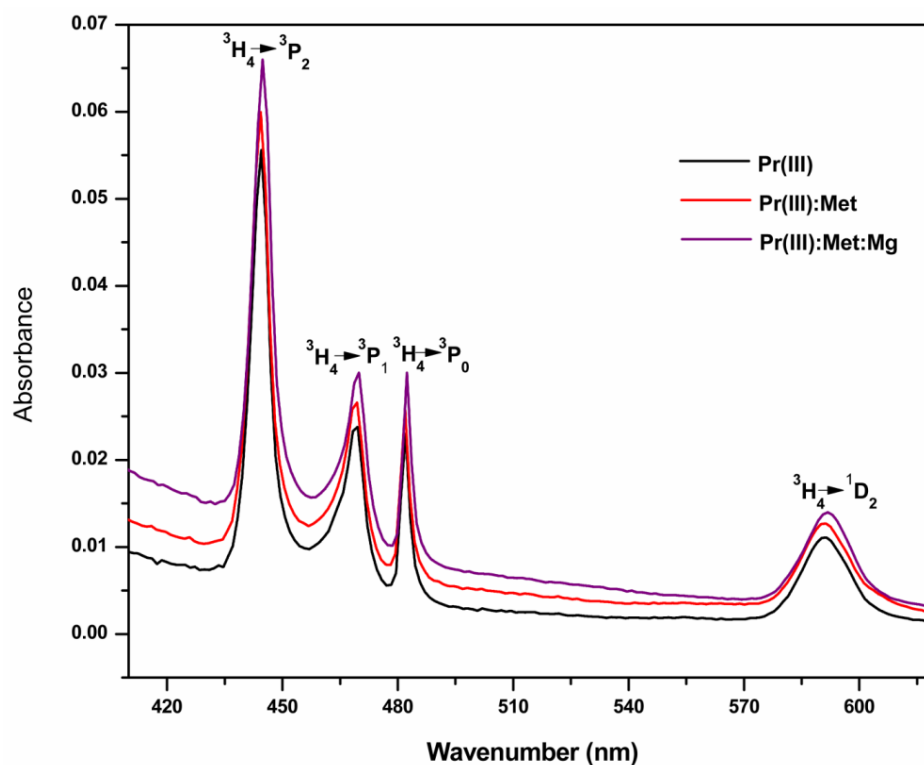


Fig. 4.7: UV-vis absorption spectra of the $4f-4f$ electronic transitions of Pr^{3+} , Pr(III):Met & $\text{Pr(III):Met:Mg(II)}$ complex in 50% v/v aquated DMF solvent at pH 6.

Table 4.3: Observed and calculated oscillator strengths ($P \times 10^6$) and Judd-Ofelt intensity parameters [T_λ , ($\lambda = 2, 4, 6$) $\times 10^{10} \text{ cm}^{-1}$] of Pr^{3+} with L-methionine in presence/absence of Mg^{2+} in different pH in aquated DMF solvent.

pH 6				pH 4			pH 2			
Pr(III):Me t:Mg(II)	Pr(III):Met	Pr(III)	Pr(III):Me t:Mg(II)	Pr(III):Met	Pr(III)	Pr(III):Met: Mg(II)	Pr(III):Met	Pr(III)		
8.179	6.371	5.329	6.937	5.699	4.341	6.871	5.633	4.080	$^3\text{H}_4\rightarrow^3\text{P}_2$	
8.170	6.371	5.329	6.936	5.699	4.341	6.871	5.633	4.080		
3.401	2.397	1.785	3.128	2.218	1.878	2.202	2.181	1.875	$^3\text{H}_4\rightarrow^3\text{P}_1$	
2.777	1.768	1.281	2.612	1.648	1.279	1.528	1.499	0.972		
2.122	1.122	0.765	2.067	1.063	0.669	0.842	0.806	0.067	$^3\text{H}_4\rightarrow^3\text{P}_0$	
2.737	1.742	1.262	2.577	1.625	1.260	1.507	1.478	0.957		
2.150	1.893	1.573	2.119	1.892	1.400	1.173	1.394	1.136	$^3\text{H}_4\rightarrow^1\text{D}_2$	
2.150	1.893	1.573	2.119	1.892	1.400	1.173	1.394	1.136		
-57.04	6.4789	4.277	18.451	50.988	29.556	-189.5	-57.97	-13.06	T ₂	
7.645	4.863	3.519	7.192	4.534	3.514	4.204	4.121	2.668	T ₄	
24.823	19.606	16.518	20.856	17.486	13.275	21.42	17.36	12.659	T ₆	

Table 4.4: Computed value of energy interaction parameters Slater-Condon $F_K(\text{cm}^{-1})$, Spin-Orbit Interaction $\xi_{4f}(\text{cm}^{-1})$, Nephelauxetic ratio (β), bonding ($b^{1/2}$), and covalency (δ) parameters of Pr^{3+} with Methionine in presence/absence Mg^{2+} in different pH in aquated DMF solvent.

pH 6				pH 4			pH 2			
Pr(III):M et:Mg(II)	Pr(III):Met	Pr(III)	Pr(III):M et:Mg(II)	Pr(III):Met	Pr(III)	Pr(III):M et:Mg(II)	Pr(III):Met	Pr(III)	F ₂	F ₄
308.6089	308.8926	309.1770	307.806	308.715	309.169	309.069	309.285	309.437	F ₆	ξ_{4f}
42.6035	42.6426	42.6819	42.492	42.618	42.680	42.667	42.696	42.717	E ₁	E ₂
4.6600	4.6643	4.6686	4.647	4.661	4.668	4.667	4.670	4.672	E ₃	β
719.739	720.343	720.372	708.733	718.499	721.496	719.973	721.051	721.539	b ^{1/2}	δ
3504.146	3507.367	3510.596	3495.029	3505.350	3510.51	3509.377	3511.825	3513.55	RMS	
23.713	23.735	23.756	23.651	23.721	23.756	23.748	23.765	23.776		
613.535	614.099	614.664	611.938	613.745	614.650	614.451	614.879	615.182		
0.944	0.944	0.945	0.935	0.943	0.946	0.944	0.946	0.946		
0.167	0.165	0.165	0.179	0.168	0.164	0.165	0.164	0.163		
5.920	5.828	5.779	6.906	5.998	5.694	5.827	5.709	5.647		
120.68	116.02	123.51	127.17	229.59	118.18	110.01	104.83	100.85		

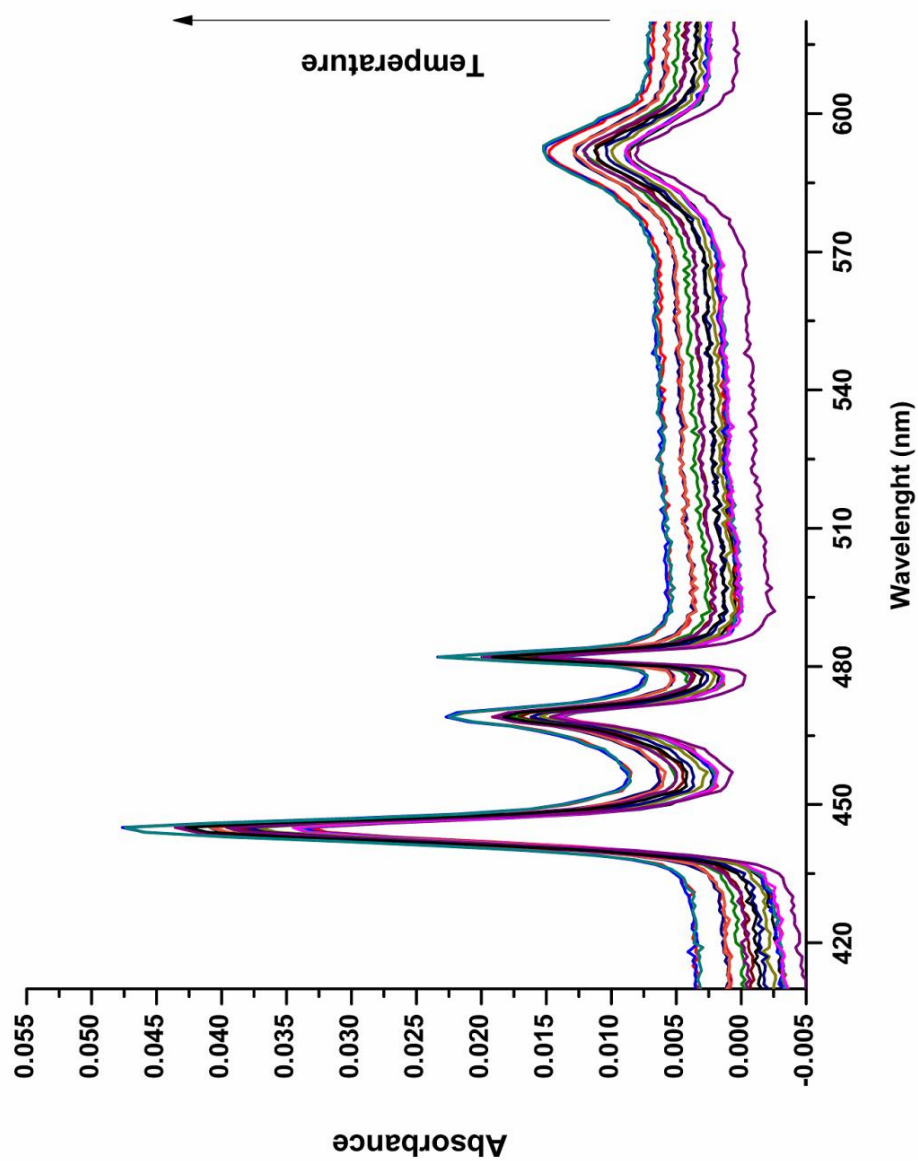


Fig. 4.8: Absorption spectra of $\text{Pr(III):Met:Mg(II)}$ complexation at 298 K and in different time intervals.

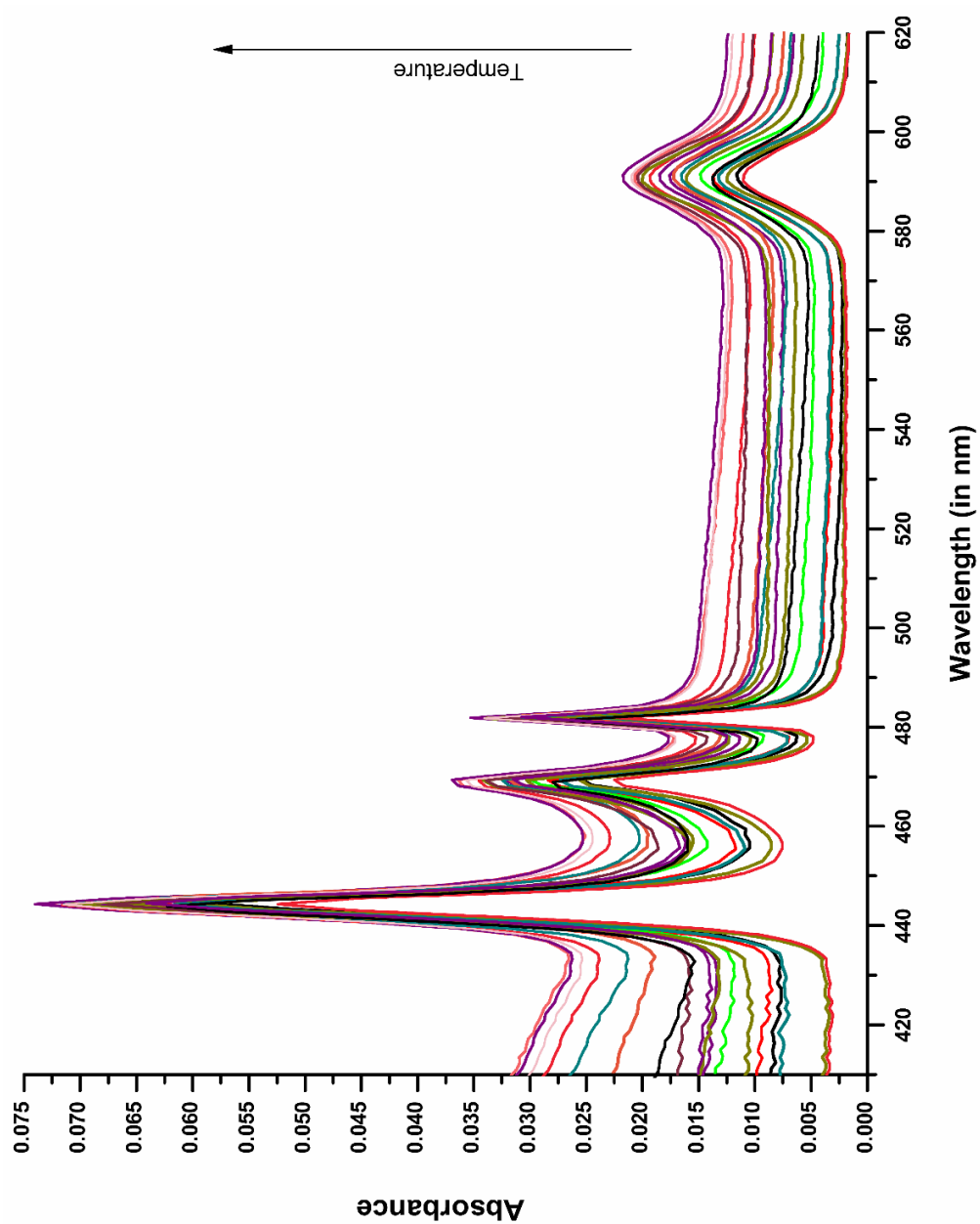


Fig. 4.9: Absorption spectra of $\text{Pr(III):Met:Mg(II)}$ complexation at 313 K and in different time intervals.

Table 4.5: Observed and calculated oscillator strengths ($P \times 10^6$) and Judd-Ofelt intensity parameters [T_λ ($\lambda = 2, 4, 6$) $\times 10^{10} \text{ cm}^{-1}$]: At 298 K and in various time intervals for Pr(III):Met:Mg(II) complex.

Time	$^3\text{H}_4 \rightarrow ^3\text{P}_2$		$^3\text{H}_4 \rightarrow ^3\text{P}_1$		$^3\text{H}_4 \rightarrow ^3\text{P}_0$		$^3\text{H}_4 \rightarrow ^1\text{D}_2$		T_2	T_4	T_6
	Pobs	Pcal	Pobs	Pcal	Pobs	Pcal	Pobs	Pcal			
0	4.623	4.623	2.515	1.851	1.169	1.825	1.702	1.702	78.091	5.092	13.79
2	4.843	4.843	2.595	1.916	1.220	1.889	1.768	1.768	78.372	5.273	14.461
4	5.023	5.023	2.628	1.950	1.253	1.922	1.787	1.787	70.868	5.365	15.028
6	5.130	5.130	2.647	1.969	1.272	1.941	1.902	1.902	89.818	5.417	15.363
8	5.405	5.405	2.742	2.055	1.347	2.025	1.987	1.986	90.806	5.653	16.201
10	5.550	5.550	2.900	2.137	1.354	2.106	2.381	2.381	170.76	5.879	16.615
12	5.591	5.591	2.932	2.163	1.373	2.132	2.526	2.526	201.00	5.950	16.733
14	5.675	5.675	2.949	2.187	1.405	2.156	2.579	2.579	207.31	6.018	16.99
16	5.991	5.991	2.942	2.202	1.441	2.171	2.678	2.678	209.22	6.058	18.013
18	6.182	6.182	3.041	2.285	1.507	2.252	2.742	2.742	210.95	6.286	18.578
20	6.183	6.183	3.170	2.367	1.541	2.333	3.001	3.001	269.37	6.511	18.521
22	6.223	6.223	3.310	2.447	1.561	2.412	3.029	3.029	272.86	6.732	18.594
24	6.487	6.487	3.458	2.603	1.724	2.566	3.083	3.083	267.43	7.163	19.345
26	6.529	6.529	3.658	2.720	1.758	2.682	3.169	3.168	283.77	7.485	19.393
28	6.582	6.582	3.797	2.795	1.768	2.755	3.297	3.297	309.3	7.689	19.514
30	6.647	6.647	3.854	2.834	1.789	2.794	3.480	3.480	346.43	7.798	19.697
32	6.708	6.708	3.878	2.917	1.928	2.875	3.559	3.559	360.22	8.026	19.836
34	6.846	6.846	4.020	3.034	2.019	2.991	3.822	3.822	410.57	8.347	20.204

Table 4.6: Observed and calculated oscillator strengths ($P \times 10^6$) and Judd-Ofelt intensity parameter [T_λ ($\lambda = 2, 4, 6$) $\times 10^{10} \text{ cm}^{-1}$] parameters: At 303 K and in various time intervals for Pr(III):Met:Mg(II) complex.

Time	$^3\text{H}_4 \rightarrow ^3\text{P}_2$		$^3\text{H}_4 \rightarrow ^3\text{P}_1$		$^3\text{H}_4 \rightarrow ^3\text{P}_0$		$^3\text{H}_4 \rightarrow ^1\text{D}_2$		T_2	T_4	T_6
	Pobs	Pcal	Pobs	Pcal	Pobs	Pcal	Pobs	Pcal			
0	5.318	5.318	0.983	0.889	0.783	0.876	2.486	2.486	216.65	2.445	16.63
2	5.725	5.725	1.391	1.137	0.871	1.121	2.592	2.592	205.61	3.129	18.16
4	6.611	6.611	3.173	2.164	1.140	2.135	1.110	1.110	-187.8	5.961	20.07
6	6.661	6.661	3.241	2.233	1.208	2.203	1.179	1.179	-175.7	6.151	20.18
8	6.712	6.712	2.738	1.993	1.232	1.966	1.243	1.243	-163.6	5.490	20.53
10	6.726	6.726	2.758	2.015	1.255	1.988	1.309	1.309	-149.5	5.549	20.56
12	6.763	6.763	2.779	2.042	1.288	2.015	1.374	1.374	-137.3	5.625	20.66
14	6.942	6.942	2.791	2.069	1.329	2.042	1.411	1.411	-140.7	5.700	21.22
16	7.015	7.015	3.075	2.254	1.415	2.224	1.467	1.467	-133.2	6.210	21.33
18	7.195	7.195	3.237	2.354	1.452	2.323	1.945	1.945	-36.74	6.485	21.84
20	7.296	7.296	3.404	2.448	1.473	2.416	2.065	2.065	-16.34	6.744	22.11
22	7.549	7.549	3.443	2.527	1.589	2.493	2.116	2.116	-21.57	6.961	22.87
24	7.627	7.627	3.509	2.567	1.604	2.533	2.193	2.193	-9.305	7.072	23.10
26	7.806	7.806	3.632	2.658	1.661	2.623	2.485	2.485	45.19	7.322	23.62
28	7.880	7.880	3.708	2.713	1.696	2.677	2.564	2.564	58.185	7.474	23.82
30	8.355	8.355	4.432	3.093	1.730	3.051	2.739	2.739	65.657	8.519	25.10
32	8.502	8.502	5.171	3.481	1.768	3.435	2.791	2.791	66.552	9.589	25.30
34	8.570	8.570	3.916	2.871	1.802	2.833	3.048	3.048	122.65	7.909	25.97

Table 4.7: Observed and calculated oscillator strengths ($P \times 10^6$) and Judd-Ofelt intensity parameter [T_λ ($\lambda = 2, 4, 6$) $\times 10^{10} \text{ cm}^{-1}$]: At 308 K and in various time intervals for Pr(III):Met:Mg(II) complex.

Time	$^3\text{H}_4 \rightarrow ^3\text{P}_2$		$^3\text{H}_4 \rightarrow ^3\text{P}_1$		$^3\text{H}_4 \rightarrow ^3\text{P}_0$		$^3\text{H}_4 \rightarrow ^1\text{D}_2$		T_2	T_4	T_6
	Pobs	Pcal	Pobs	Pcal	Pobs	Pcal	Pobs	Pcal			
0	6.640	6.640	2.751	1.709	0.656	1.678	1.148	1.148	-179.6	4.683	20.51
2	6.667	6.667	2.776	1.768	0.746	1.735	1.163	1.163	-178.1	4.843	20.56
4	6.747	6.747	3.171	2.002	0.816	1.964	1.186	1.186	-178.7	5.483	20.64
6	6.822	6.822	3.329	2.110	0.874	2.070	1.660	1.660	-76.14	5.780	20.81
8	6.927	6.927	3.343	2.139	0.918	2.099	1.858	1.858	-38.14	5.860	21.13
10	7.031	7.031	3.356	2.155	0.935	2.114	1.869	1.869	-42.43	5.902	21.46
12	7.202	7.202	3.363	2.189	0.995	2.147	1.911	1.911	-44.29	5.995	22.00
14	7.286	7.286	3.379	2.202	1.004	2.160	1.951	1.951	-40.69	6.031	22.26
16	7.365	7.365	3.411	2.221	1.011	2.179	1.572	1.572	-132.3	6.084	22.51
18	7.490	7.490	3.450	2.251	1.033	2.209	2.355	2.355	37.662	6.167	22.90
20	7.644	7.644	3.555	2.325	1.073	2.281	2.440	2.440	46.82	6.367	23.35
22	7.722	7.722	3.810	2.469	1.108	2.423	2.551	2.551	66.484	6.765	23.50
24	8.007	8.007	3.809	2.469	1.109	2.423	2.552	2.552	48.041	6.766	24.43
26	8.085	8.085	3.787	2.471	1.133	2.425	2.654	2.654	66.011	6.769	24.68
28	8.097	8.097	3.943	2.554	1.142	2.505	2.749	2.749	86.822	6.995	24.66
30	8.494	8.494	4.094	2.633	1.149	2.586	2.888	2.888	91.849	7.213	25.91
32	8.596	8.596	4.159	2.679	1.176	2.629	2.953	2.953	100.03	7.339	26.21
34	8.829	8.829	4.308	2.764	1.197	2.712	3.019	3.019	99.44	7.571	26.91

Table 4.8: Observed and calculated oscillator strengths ($P \times 10^6$) and Judd-Ofelt intensity parameter [T_λ ($\lambda = 2, 4, 6$) $\times 10^{10} \text{ cm}^{-1}$]: At 313 K and in various time intervals for Pr(III):Met:Mg(II) complex.

Time	$^3\text{H}_4 \rightarrow ^3\text{P}_2$		$^3\text{H}_4 \rightarrow ^3\text{P}_1$		$^3\text{H}_4 \rightarrow ^3\text{P}_0$		$^3\text{H}_4 \rightarrow ^1\text{D}_2$		T_2	T_4	T_6
	Pobs	Pcal	Pobs	Pcal	Pobs	Pcal	Pobs	Pcal			
0	6.521	6.521	1.861	1.643	1.406	1.619	2.793	2.793	201.93	4.521	20.18
2	6.654	6.654	1.997	1.821	1.621	1.795	2.861	2.861	208.03	5.010	20.49
4	6.816	6.816	2.131	1.901	1.647	1.874	3.135	3.135	259.45	5.230	20.96
6	7.041	7.041	2.195	1.971	1.720	1.942	3.245	3.245	269.43	5.420	21.65
8	7.334	7.334	2.331	2.058	1.759	2.028	3.306	3.306	263.82	5.662	22.54
10	7.563	7.563	2.354	2.112	1.843	2.082	3.383	3.383	266.23	5.809	23.25
12	7.806	7.806	3.632	2.658	1.661	2.622	2.485	2.485	45.19	7.321	23.62
14	7.956	7.956	2.392	2.169	1.916	2.138	3.396	3.396	243.07	5.966	24.50
16	8.085	8.085	3.787	2.471	1.133	2.424	2.654	2.654	66.011	6.769	24.68
18	8.209	8.209	2.463	2.252	2.011	2.219	3.593	3.593	270.91	6.194	25.27
20	8.495	8.495	4.094	2.633	1.149	2.583	2.887	2.887	91.849	7.213	25.91
22	8.544	8.544	2.796	2.523	2.216	2.486	3.713	3.713	275.43	6.939	26.17
24	8.685	8.685	2.864	2.595	2.292	2.557	3.934	3.933	315.91	7.138	26.58
26	8.737	8.737	3.438	2.235	1.018	2.203	1.634	1.634	-209.4	6.143	26.989
28	8.831	8.831	4.308	2.764	1.196	2.712	3.019	3.019	99.44	7.571	26.91
30	9.474	9.474	2.124	1.503	0.867	1.478	1.440	1.440	-299.4	4.122	29.95
32	9.635	9.635	3.803	2.725	1.620	2.678	2.168	2.168	-151.1	7.476	29.71
34	10.07	10.07 9	2.989	2.731	2.437	2.692	4.083	4.083	258.23	7.512	31.05

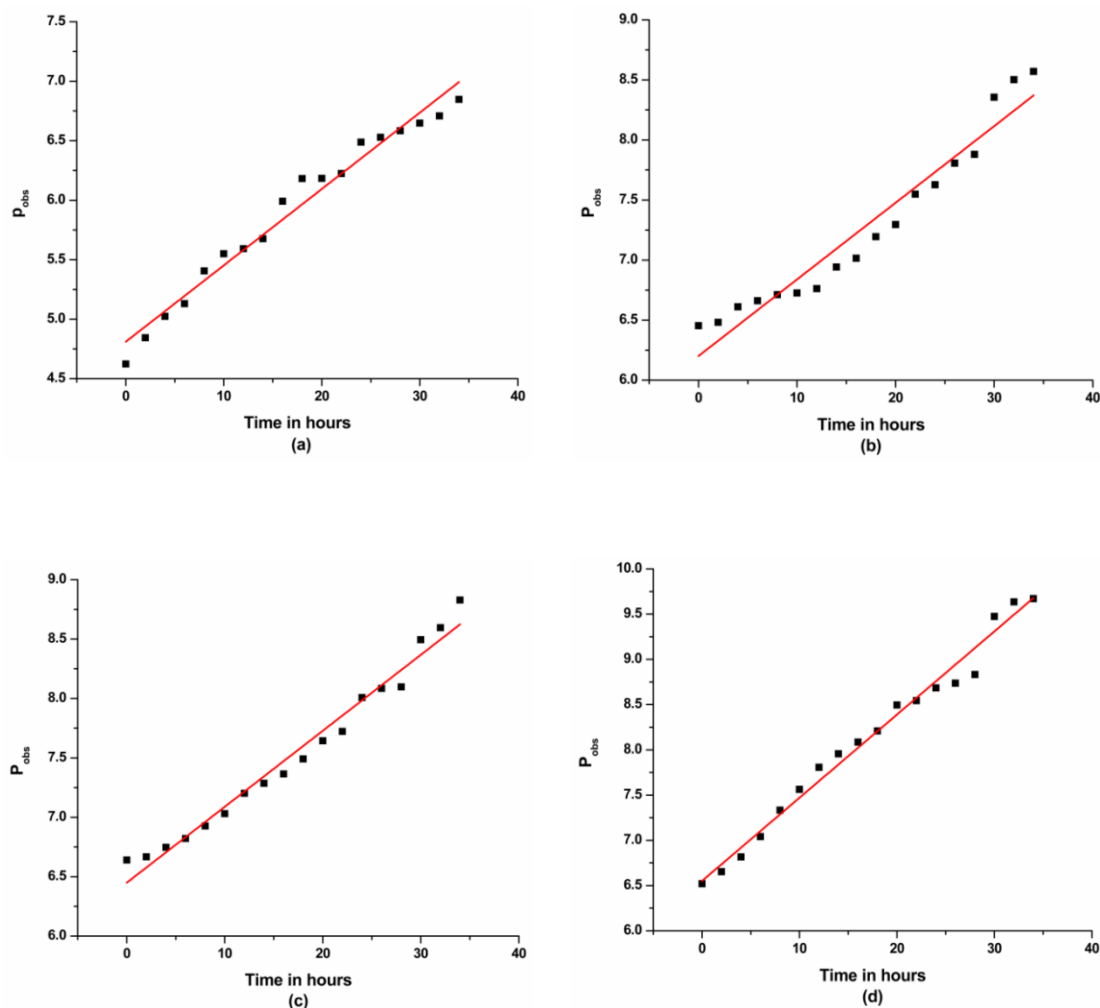


Fig. 4.10: P_{obs} vs Time in hours at various temperatures: (a) 298 K, (b) 303 K, (c) 308 K, (d) 313 K for the $^3\text{H}_4 \rightarrow ^3\text{P}_2$ transition of $\text{Pr(III):Met:Mg(II)}$.

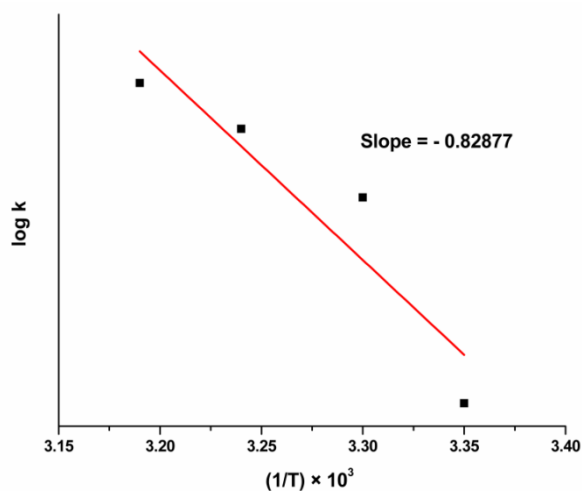


Fig. 4.11: $\log k$ vs $(1/T) \times 10^3$ for $\text{Pr(III):Met:Mg(II)}$ complex in 50% v/v aquated DMF medium.

Table 4.9: Rate Constants and Activation Energy for Pr(III):Met:Mg(II) complex at various temperatures.

Temperature (K)	$1/T \times 10^3 \text{K}^{-1}$	Rate Constant (k) $\text{Mol L}^{-1} \text{h}^{-1}$	Rate Constant (k) $\text{Mol L}^{-1} \text{S}^{-1} \times 10^{-6}$	log k	Pre-exponential factor (A)	Activation Energy $\Delta E_a (\text{kJ/mol})$
298	3.35	0.045	12.77	1.11	4.81	0.016
303	3.30	0.058	16.12	1.20	6.20	
308	3.24	0.062	17.35	1.23	6.44	
313	3.19	0.065	18.07	1.25	6.55	

Table 4.10: Rate constants and thermodynamic parameters for Pr(III):Met:Mg(II) complex at various temperatures.

Temperature (K)	Rate (k) $\text{Mol L}^{-1} \text{S}^{-1} \times 10^{-6}$	ΔH^0 (kJmol^{-1})	ΔG^0 ($\text{JK}^{-1} \text{mol}^{-1}$)	ΔS^0 (kJmol^{-1})
298	12.77	0.016	-6.33	0.021
303	16.12		-6.96	0.023
308	17.35		-7.25	0.024
313	18.07		-7.49	0.024

The presence of a highly detailed internal f-electron transition, as well as Lanthanide's sensitivity to the coordination environment and geometry of the complex, formed with various ligands in easily accessible spectral regions, have paved the way for a broad approach to using absorption spectrophotometry as an emerging tool for studying lanthanide chemistry, especially in solutions in both aqueous and non-aqueous solvents [20–22]. The absorption spectra for the $4f-4f$ transitions of Ln^{3+} ions are used to determine the strength of Ln^{3+} in the interaction with ligand, coordination geometry, the structure of metal-ligand complex formed, and chelate-solvent interactions [23].

$4f-4f$ transitions of lanthanide ions occur deep within the metal's core shell and they are generally insensitive to the coordination environment and are referred to as non-hypersensitive [24]. The hypersensitive transitions, on the other hand, follow the selection rules, $\Delta S = 0$, $\Delta L \leq 2$ and $\Delta J \leq 2$ and are highly sensitive to changes in their coordination environment and their band intensities become more intensified when a lanthanide ion gets complexed with ligands [25]. Through investigations, it is revealed that some transition intensities of Pr^{3+} ($^3\text{H}_4 \rightarrow ^3\text{P}_2$, $^3\text{H}_4 \rightarrow ^3\text{P}_1$, $^3\text{H}_4 \rightarrow ^3\text{P}_0$ and $^3\text{H}_4 \rightarrow ^1\text{D}_2$) do not follow the selection rule but they could exhibit an exceptionally sensitive character towards minor changes in their coordination environment. Such transitions, pseudoquadrupole in character are known as Ligand Mediated Pseudohypersensitive transitions since their sensitivity is the inducing result of their coordination environment [26–28]. This Pseudohypersensitive transition has been used extensively for the absorption study to understand the nature of bonding and structural conformations of Pr^{3+} with ligand in solution study. The interaction of Pr^{3+} with the ligand and their sensitivity towards the formation of the complex is shown vividly by the corresponding intensification of the pseudo-hypersensitive transitions.

The intensity parameters; Judd-Ofelt parameters (T_λ) and Oscillator strength (P) for the ligand-mediated pseudohypersensitive transitions ($^3\text{H}_4 \rightarrow ^3\text{P}_2$, $^3\text{H}_4 \rightarrow ^3\text{P}_1$, $^3\text{H}_4 \rightarrow ^3\text{P}_0$, and $^3\text{H}_4 \rightarrow ^1\text{D}_2$) of free Pr^{3+} ion and Pr^{3+} in its complexes with L-methionine and Mg^{2+} was evaluated under various experimental ambience. The remarkable changes in the P values of $4f-4f$ bands shown in table 4.1 imply the possibility of the interaction between Pr^{3+} with L-methionine [29]. The amplitude of T_λ ($\lambda = 2, 4, 6$) parameters increases significantly when Pr^{3+} interacts with the ligand in solution; this validates the possibility of the binding of L-methionine to Pr^{3+} . Further, addition of Mg^{2+} to the

of Pr(III):Met complex enhances the intensity, which could be attributed to binding of Mg^{2+} to form a multimetal complex [12]. The evaluated values of T_4 and T_6 show large variations and their values are positive and thus can be applied in the Judd-Ofelt theory of $4f-4f$ transitions. Both T_4 and T_6 parameters are related to changes in symmetry properties of the complex species [30]. Thus, significant changes in the values of T_4 and T_6 suggest the change in their immediate coordination domain which induces changes in the complexation of Pr^{3+} with the ligands. On the other hand, T_2 is correlated to the hypersensitive transition, $^3\text{H}_4 \rightarrow ^3\text{F}_3$, since this transition is beyond the UV-Visible region and its values are negative, thereby T_2 is ignored [31]. The inner-sphere complexation is indicated by the significant variations in P and their corresponding T_λ values while a slight variation of P and T_λ values suggests the outer-sphere complexation of metal with the ligand [32]. The significant changes in P and T_λ values could provide fundamental evidence that L-methionine is involved in the inner-sphere coordination with Pr^{3+} in its ambience. The computed data reveals that among the three T_λ ($\lambda = 2, 4, 6$) parameters, T_6 is the best suited parameter to interpret the interaction of L-methionine with Pr^{3+} in presence of Mg^{2+} , and the order in which they appear is $T_6 > T_4 > T_2$.

Table 4.2 reflects the computed data of different energy interaction parameters: F_k ($k=2,4,6$), ζ_{4f} , E^k ($k=1,2,3$), β , $b^{1/2}$ and δ . From the variation and changes in the values of energy interaction parameters of Pr^{3+} (free ion) and their complexes [Pr(III):Met & $\text{Pr(III):Met:Mg(II)}$] in 50% v/v aquated organic solvents (ACN, DMF, Dioxane and Methanol), the detailed nature of bonding could be studied. When the computed values of energy interaction parameters β , ζ_{4f} , and F_k for Pr^{3+} in its free ionic state are compared with that of the Pr(III):Met and $\text{Pr(III):Met:Mg(II)}$ complexes in various

solvents, there is a steady decrease in the values which indicate the possibility of complex formation. The increase of percent covalency (δ) and the bonding parameter ($b^{1/2}$) followed by the values of the nephelauxetic ratio (β), which were found to be less than unity, implies the possibility of the formation of covalent bond in the complexation of Pr(III) with L-methionine [33]. The decreased value of β explained the expansion of the orbital of the central metal ion thereby shortening the distance between the metal and the ligand known as the nephelauxetic effect [34]. The root mean square (RMS) values predict the accuracy of the estimated values of energy interaction parameters.

From the computed data, the intensity parameters (P , T_λ) and energy interaction parameters ($F_k, \zeta_{4f}, E^k, \beta, b^{1/2}$ & δ) shown in table 4.1 & 4.2 respectively, the intensified magnitude in the intensity parameters and the variations in the energy parameters of the various $4f-4f$ transition bands predict the possibility of the increase in the interaction between $4f$ orbitals of Pr^{3+} with that of the ligand. The significant variations and the higher magnitude in the intensity parameters in the aquated DMF solvent imply that there is a stronger influence of solvent over Pr^{3+} to form a complex with the ligand [35]. This shows that DMF is the better solvent compared to the others in the formation of the complex of Pr^{3+} with L-methionine. Furthermore, the oscillator strength (P) values in the case of DMF solvent are higher than in the case of other solvents, indicating that this solvent is preferred in the formation of the complex. On comparing the obtained computed data, it was observed that the maximum values of $b^{1/2}$ and δ parameters are observed in the DMF:H₂O (50% v/v) system, this indicates the preference for covalent bond formation in DMF solvent which may be due to the

presence of N-donor [20]. The sensitivity of the organic solvents is in the order of DMF>CH₃CN>C₄H₈O₂>CH₃OH.

The absorption bands of Pr³⁺ solution get more intense with the addition of ligand (L-methionine) and further, with the addition of Mg²⁺ to Pr(III):Met complex the intensification increases. This firmly signifies the possibility of interaction of the metal Pr³⁺ with ligand L-methionine and Mg²⁺. The redshift observed in figures 4.4 and 4.5 further adds evidence to the possibility of forming a complex [Pr(III):Met:Mg(II)] in solution [36].

The computed results for the various energy interaction parameters: F_k ($k=2,4,6$), ζ_{4f} , E^k ($k=1,2,3$), β , $b^{1/2}$ and δ for Pr(III), Pr(III):Met and Pr(III):Met:Mg(II) at various pH values are shown in table 4.4. The degree of protonation/deprotonation at Methionine's binding sites is controlled by the pH value, which has a significant impact on its bonding capacity. From the observation, as the value of pH increases the computed values of β , ζ_{4f} and F_k show a steady decrease. This explains the increase in the interaction of metal with the ligand at higher pH. Since hard metal ions prefer hard donor sites, the interaction of lanthanide ions with the carboxylic group is the primary mode of bonding for Pr(III):Met complex. The computed data elucidates the deprotonation of the carboxylic group of L-methionine at an acidic medium (lower pH), allowing the Pr(III) ion to bind through it [37]. Increases in percent covalency (δ) and bonding parameter ($b^{1/2}$) with increasing pH values indicate an increase in interaction and the probability of formation of covalent bonds, which could be related to an increase in deprotonation capacity as pH rises. The shortening of the metal-ligand distance is explained clearly by the decrease in the values of the nephelauxetic

ratio (β). The change in the values of intensity parameters shown in table 4.3 and the increase in the intensities of the four pseudohypersensitive transitions (figure 4.6 & 4.7) also demonstrate this effect. At high pH, the amine group deprotonates, this is reflected by the T_λ , ($\lambda = 2, 4, 6$) values, which are found to be higher at higher pH.

The absorption spectra of Pr(III):Met:Mg(II) at different temperatures of 298K, 303 K, 308 K, and 313 K were recorded in aquated organic solvent DMF:H₂O (50% v/v) at an interval two-hour to study the kinetic of the complexation. Figure 4.8 and 4.9 shows the comparative absorption spectra of the complex at 298 K, and 313 K. From the spectra we could observe that the intensity increases with respect to time and temperature. From the variations in the computed data of P and T_λ parameters at different temperatures for the complex Pr(III):Met:Mg(II) shown in tables 4.5, 4.6, 4.7 & 4.8, the pseudohypersensitive transition $^3H_4 \rightarrow ^3P_2$ is observed to be the most sensitive $4f-4f$ transition compared to the other $^3H_4 \rightarrow ^3P_1$, $^3H_4 \rightarrow ^3P_0$, and $^3H_4 \rightarrow ^1D_2$ transitions. The computed data demonstrates that the values of T_4 and T_6 were relatively more sensitive and their values increase proportionately with time and temperature. This trend signifies the rise in the rate constant of the complexation process of Pr(III) with L-methionine in presence of Mg^{2+} .

Fig. 4.10 shows the plot of P_{obs} vs time for the transition $^3H_4 \rightarrow ^3P_2$ at different temperatures. The values of slope and pre-exponential factor obtained from the graphs were used in the calculation of rate constants as shown in table 4.9. From the table, rate constant values of complexation are enhanced by the rise in temperature in the order of $313\text{ K} > 308\text{ K} > 313\text{ K} > 298\text{ K}$ which is in accord with the theoretical prediction of the Arrhenius Reaction Rate. Again, the increase in the values of the Pre-

exponential factor (A) with the rise in temperature shows the increase in the probability of collision of the molecules. The negligibly low value of the activation energy (E_a) indicates the possibility of the spontaneity of the reaction. In addition, fig. 4.11 presents the plot of $\log k$ vs $(1/T) \times 10^3$, and the values obtained from the graph were used for the determination of ΔH^0 , ΔG^0 , and ΔS^0 values (table 4.10). The endothermic reaction associated with complexation is shown by the positive values of ΔH^0 , whereas the spontaneity of the reaction process is indicated by the negative value of ΔG^0 . The positive values of ΔS^0 imply that the coordination reaction is entropy-driven and also that the complex is well-formed. Such kinetic studies based on absorption spectral analysis of the $4f-4f$ transition can be employed as an alternative approach for the theoretical study of the reaction dynamics and also for the prediction of possible thermodynamic behavior involved in the *Pr(III):Met:Mg(II)* complexation.

4.5 CONCLUSION

The significant variations in the computed values of P and T_λ could provide the formation of inner-sphere complexation as well as the strong binding effect in the complexation of Pr^{3+} with L-methionine in the presence and absence of Mg^{2+} . The marked changes in the values of T_4 and T_6 suggests that there is a change in the symmetry of the complex formed. The increase in the values of $b^{1/2}$, δ and the steady decrease in the values of ζ_{4f} , E^k , F_k suggests that there is an interaction between the metal ion with the ligand. It is further substantiated by the increase in the interaction of $4f$ -orbitals which is interpreted through the intensification of absorption bands as well as the appearance of the redshift when the ligand is added to the pure Praseodymium ion. The increase in absorption bands of the $4f-4f$ transition of Pr^{3+} is associated with the shortening of the metal-ligand distance and lowering of the

coordination number, shown by the decrease in the values of nephelauxetic ratio (β). DMF was found to be the best-suited solvent for the complexation among the four solvents used. Based on the computed P and T_λ values, the stability of the complexes follows the order, $\text{Pr(III)} < \text{Pr(III):Met} < \text{Pr(III):Met:Mg(II)}$. The increase in the interaction of metal with the ligand at higher pH is explained by the steady decrease in the computed values of β , ζ_{4f} , and F_k as the value of pH increases. The increase in interaction and possibility of the formation of a covalent bond with an increase in the pH is depicted by the values of percent covalency (δ) and the bonding parameter ($b^{1/2}$). The deprotonation of the amine group at higher pH values is explained by the intensity parameters (T_λ , $\lambda = 2, 4, 6$) values, which are higher at higher pH values.

The discussions based upon the values of intensity parameters for the complexation at various time intervals and temperatures vividly demonstrated that the rate of complexation elevates proportionately with an increase in time and temperature confirming the Arrhenius prediction of the reaction rate. The negligibly low value of Activation energy (E_a) conveys the possibility of spontaneity in the complexation of Pr^{3+} with L-methionine in the presence of Mg^{2+} . The positive values of ΔH^0 imply an endothermic reaction associated with the complexation. The reaction's spontaneity and the favorable character of the reaction in solution are reflected in the negative value of ΔG^0 . Since, $T\Delta S^0 > \Delta H^0$, the present study of coordination reaction is found to be entropy-driven. The values of the pre-exponential factor (A) provide the empirical relationship between temperature and the reaction rate depending upon the probability of how often the molecules collide.

REFERENCES

- [1] J.G. Bu, Ä.P. Fe, Benefiting from the Unique Properties of Lanthanide Ions, 39 (2006) 53–61. <https://doi.org/10.1021/ar0400894>.
- [2] S.N. Misra, M.I. Devi, The synthesis and determination of the octacoordinated structure of Pr(III) and Nd(III) complexes with β -diketones and diols in non aqueous solutions: Evidence of some participation of π -electron density of diols with Pr(III) and Nd(III) in complexation, Spectrochim. Acta - Part A Mol. Biomol. Spectrosc. 53 (1997) 1941–1946. [https://doi.org/10.1016/S1386-1425\(97\)00064-4](https://doi.org/10.1016/S1386-1425(97)00064-4).
- [3] X.M. Qiao, C.X. Zhang, Y.K. Kong, Y.Y. Zhang, A Mononuclear Lanthanide Metal Compounds Based on the Nitronyl Nitroxide Radicals: Synthesis, Crystal Structure, and Magnetic Properties, Synth. React. Inorganic, Met. Nano-Metal Chem. 46 (2016) 841–846. <https://doi.org/10.1080/15533174.2014.989594>.
- [4] E.M. Stephens, S. Davis, M.F. Reid, F.S. Richardson, Empirical Intensity Parameters for the $4f \rightarrow 4f$ Absorption Spectra of Nine-Coordinate Neodymium(III) and Holmium(III) Complexes in Aqueous Solution, Inorg. Chem. 23 (1984) 4607–4611. <https://doi.org/10.1021/ic00194a040>.
- [5] N. Bendangsenla, T. Moaienla, T. David Singh, C. Sumitra, N. Rajmuhon Singh, M. Indira Devi, Evaluation of intensity and energy interaction parameters for the complexation of Pr(III) with selected nucleoside and nucleotide through absorption spectral studies, Spectrochim. Acta - Part A Mol. Biomol. Spectrosc. 15 (2013) 160–6. <https://doi.org/10.1016/j.saa.2012.11.011>.
- [6] T.D. Singh, C. Sumitra, N. Yaiphaba, H.D. Devi, M.I. Devi, N.R. Singh, Comparison of energy interaction parameters for the complexation of Pr(III) with glutathione reduced (GSH) in absence and presence of Zn(II) in aqueous and aquated organic solvents using $4f$ - $4f$ transition spectra as PROBE, Spectrochim. Acta - Part A Mol. Biomol. Spectrosc. 61 (2005) 1219–1225. <https://doi.org/10.1016/j.saa.2004.06.044>.
- [7] S.N. Misra, G. Ramchandriah, M.A. Gagnani, R.S. Shukla, M.I. Devi, Absorption spectral studies involving $4f$ - $4f$ transitions as structural probe in chemical and biochemical reactions and compositional dependence of intensity parameters, Appl. Spectrosc. Rev. (2003). <https://doi.org/10.1081/ASR-120026330>.
- [8] K.B. Gudasi, V.C. Havanur, S.A. Patil, B.R. Patil, Antimicrobial study of newly synthesized lanthanide(III) complexes of 2-[2-hydroxy-3-methoxyphenyl] - 3 - [2 - hydroxy - 3 - methoxybenzylamino]-1, 2-dihydroquin

- azolin -4 (3H) -one, Met. Based. Drugs. 2007 (2007) 37348. <https://doi.org/10.1155/2007/37348>.
- [9] S. Alghool, M.S. Zoromba, H.F.A. El-Halim, Lanthanide amino acid Schiff base complexes: Synthesis, spectroscopic characterization, physical properties and in vitro antimicrobial studies, J. Rare Earths. 31 (2013) 715–721. [https://doi.org/10.1016/S1002-0721\(12\)60347-0](https://doi.org/10.1016/S1002-0721(12)60347-0).
- [10] M.P. Cabral Campello, E. Palma, I. Correia, P.M.R. Paulo, A. Matos, J. Rino, J. Coimbra, J.C. Pessoa, D. Gambino, A. Paulo, F. Marques, Lanthanide complexes with phenanthroline-based ligands: insights into cell death mechanisms obtained by microscopy techniques, Dalt. Trans. 48 (2019) 4611–4624. <https://doi.org/10.1039/c9dt00640k>.
- [11] Y. Martínez, X. Li, G. Liu, P. Bin, W. Yan, D. Más, M. Valdivié, C.A.A. Hu, W. Ren, Y. Yin, The role of methionine on metabolism, oxidative stress, and diseases, Amino Acids. 49 (2017) 2091–2098. <https://doi.org/10.1007/s00726-017-2494-2>.
- [12] K.K. Gangu, S. Maddila, S.N. Maddila, S.B. Jonnalagadda, Nanostructured samarium doped fluorapatites and their catalytic activity towards synthesis of 1,2,4-triazoles, Molecules. 21 (2016) 1281. <https://doi.org/10.3390/molecules21101281>.
- [13] N. Ranjana Devi, B. Huidrom, N. Rajmuhon Singh, Studies on the complexation of Pr(III) and Nd(III) with glycyl-glycine (gly-gly) using spectral analysis of 4f-4f transitions and potentiometric titrations, Spectrochim. Acta - Part A Mol. Biomol. Spectrosc. 96 (2012) 370–379. <https://doi.org/10.1016/j.saa.2012.05.038>.
- [14] A.M. Măciucă, A.C. Munteanu, V. Uivarosi, Quinolone complexes with lanthanide ions: An insight into their analytical applications and biological activity, Molecules. 25 (2020) 1347. <https://doi.org/10.3390/molecules25061347>.
- [15] M.F. Bush, J. Oomens, R.J. Saykally, E.R. Williams, Effects of alkaline earth metal ion complexation on amino acid zwitterion stability: Results from infrared action spectroscopy, J. Am. Chem. Soc. 130 (2008) 6463–6471. <https://doi.org/10.1021/ja711343q>.
- [16] M. Remko, D. Fitz, R. Broer, B.M. Rode, Effect of metal Ions (Ni^{2+} , Cu^{2+} and Zn^{2+}) and water coordination on the structure of L-phenylalanine, L-tyrosine, L-tryptophan and their zwitterionic forms, J. Mol. Model. 17 (2011) 3117–3128.

<https://doi.org/10.1007/s00894-011-1000-0>.

- [17] F. Costanzo, R.G. Della Valle, V. Barone, MD simulation of the Na⁺-phenylalanine complex in water: Competition between cation- π interaction and aqueous solvation, *J. Phys. Chem. B.* 109 (2005) 23016-23. <https://doi.org/10.1021/jp055271g>.
- [18] A.L. Sobolewski, D. Shemesh, W. Domcke, Computational studies of the photophysics of neutral and zwitterionic amino acids in an aqueous environment: Tyrosine-(H₂O)₂ and tryptophan-(H₂O)₂ clusters, *J. Phys. Chem. A.* 113 (2009) 543-550. <https://doi.org/10.1021/jp8091754>.
- [19] J.C.G. Bünzli, C. Piguet, Lanthanide-containing molecular and supramolecular polymetallic functional assemblies, *Chem. Rev.* 102 (2002) 1897-1928. <https://doi.org/10.1021/cr010299j>.
- [20] Z. Ahmed, K. Iftikhar, Synthesis and visible light luminescence of mononuclear nine-coordinate lanthanide complexes with 2,4,6-tris(2-pyridyl)-1,3,5-triazine, *Inorg. Chem. Commun.* 13 (2010) 1253-1258. <https://doi.org/10.1016/j.inoche.2010.07.009>.
- [21] Y.F. Zhao, H. Bin Chu, F. Bai, D.Q. Gao, H.X. Zhang, Y.S. Zhou, X.Y. Wei, M.N. Shan, H.Y. Li, Y.L. Zhao, Synthesis, crystal structure, luminescent property and antibacterial activity of lanthanide ternary complexes with 2,4,6-tri(2-pyridyl)-s-triazine, *J. Organomet. Chem.* 716 (2012) 167-174. <https://doi.org/10.1016/j.jorganchem.2012.06.031>.
- [22] L. Sorace, C. Benelli, D. Gatteschi, Lanthanides in molecular magnetism: Old tools in a new field, *Chem. Soc. Rev.* 40 (2011) 3092-3104. <https://doi.org/10.1039/c0cs00185f>.
- [23] C. Sumitra, T.D. Singh, M.I. Devi, N.R. Singh, Absorption spectral studies of 4f-4f transitions for the complexation of Pr(III) and Nd(III) with glutathione reduced (GSH) in presence of Zn(II) in different aquated organic solvents and kinetics for the complexation of Pr(III):GSH with Zn(II), *J. Alloys Compd.* 451 (2008) 365-371. <https://doi.org/10.1016/j.jallcom.2007.04.153>.
- [24] N. Bendangsenla, T. Moaienla, T. David Singh, C. Sumitra, N. Rajmuhon Singh, M. Indira Devi, Evaluation of intensity and energy interaction parameters for the complexation of Pr(III) with selected nucleoside and nucleotide through absorption spectral studies, *Spectrochim. Acta - Part A Mol. Biomol. Spectrosc.* 103(2013)160-166. <https://doi.org/10.1016/j.sa.2012.11.011>.

- [25] T. Moaienla, N. Bendangsenla, T. David Singh, C. Sumitra, N. Rajmuhon Singh, M. Indira Devi, Comparative 4f-4f absorption spectral study for the interactions of Nd(III) with some amino acids: Preliminary thermodynamics and kinetic studies of interaction of Nd(III):glycine with Ca(II), *Spectrochim. Acta - Part A Mol. Biomol. Spectrosc.* 87 (2012) 142–150. <https://doi.org/10.1016/j.saa.2011.11.028>.
- [26] J.B. Gruber, G.W. Burdick, S. Chandra, D.K. Sardar, Analyses of the ultraviolet spectra of Er^{3+} in Er_2O_3 and Er^{3+} in Y_2O_3 , *J. Appl. Phys.* 108 (2010). <https://doi.org/10.1063/1.3465615>.
- [27] R.D. Peacock, The intensities of lanthanide $f \leftrightarrow f$ transitions, in: *Rare Earths*, 22 (2007) 83-122. <https://doi.org/10.1007/bfb0116556>.
- [28] W.T. Carnall, P.R. Eieids, K. Rajnak, Electronic energy levels of the trivalent lanthanide aquo ions. II. Gd^{3+} , *J. Chem. Phys.* 49 (1968) 4407–4411. <https://doi.org/10.1063/1.1669894>.
- [29] C. Victory Devi, N. Rajmuhon Singh, Spectrophotometric study of kinetics and associated thermodynamics for the complexation of Pr(III) with L-proline in presence of Zn(II), *Arab. J. Chem.* 10 (2017) S2124–S2131. <https://doi.org/10.1016/j.arabjc.2013.07.044>.
- [30] A.A. Khan, H.A. Hussain, K. Iftikhar, 4f-4f absorption spectra and hypersensitivity in nine-coordinate Ho(III) and Er(III) complexes in different environments, *Spectrochim. Acta - Part A Mol. Biomol. Spectrosc.* 60 (2004) 2087-2092. <https://doi.org/10.1016/j.saa.2003.10.042>.
- [31] T. Moaienla, T.D. Singh, N.R. Singh, M.I. Devi, Computation of energy interaction parameters as well as electric dipole intensity parameters for the absorption spectral study of the interaction of Pr(III) with l-phenylalanine, l-glycine, l-alanine and l-aspartic acid in the presence and absence of Ca^{2+} , *Spectrochim. Acta - Part A Mol. Biomol. Spectrosc.* 74 (2009) 434-40. <https://doi.org/10.1016/j.saa.2009.06.039>.
- [32] N. Bendangsenla, T. Moainla, J. Sanchu, M.I. Devi, Computation of Energy, Intensity and Thermodynamic Parameters for the Interaction of Ln(III) with Nucleic Acid: Analysis of Structural Conformations, Chemical Kinetics and Thermodynamic Behaviour through 4f-4f Transition Spectra as Probe, *J. Mater. Sci. Chem. Eng.* 6 (2018) 169-183. <https://doi.org/10.4236/msce.2018.67018>.
- [33] S.N. Misra, K. John, Difference and Comparative Absorption Spectra and Ligand Mediated Pseudohypersensitivity for 4f-4f Transitions of Pr (III) and

Nd (III) Difference and Comparative Absorption Spectra and Ligand Mediated Pseudo hypersensitivity for 4f-4f Transitions o, 4928 (2016) 285-325. <https://doi.org/10.1080/05704929308018115>.

- [34] C. Sumitra, T. David Singh, M. Indira Devi, N.R. Singh, Calculation of electric dipole intensity parameters of 4f-4f transitions of Pr(III) and glutathione reduced (GSH) complex in presence and absence of Zn(II), Spectrochim. Acta - Part A Mol. Biomol. Spectrosc. 66 (2007) 1333-9. <https://doi.org/10.1016/j.saa.2006.06.023>.
- [35] C.V. Devi, N.R. Singh, Absorption spectroscopic probe to investigate the interaction between Nd(III) and calf-thymus DNA, Spectrochim. Acta - Part A Mol. Biomol. Spectrosc. 78 (2011) 1180–1186. <https://doi.org/10.1016/j.saa.2010.12.078>.
- [36] Z.A. Taha, A.K. Hijazi, W.M. Al Momani, Lanthanide complexes of the tridentate Schiff base ligand salicylaldehyde-2- picolinoylhydrazone: Synthesis, characterization, photophysical properties, biological activities and catalytic oxidation of aniline, J. Mol. Struct. 1220 (2020) 128712. <https://doi.org/10.1016/j.molstruc.2020.128712>.
- [37] M. Ziekhri, Z. Thakro, C. Imsong, J. Sanchu, M.I. Devi, Computation of energy interaction and intensity parameters for the complexation of Pr (III) with glutathione at different pH in the presence / absence of Mg²⁺: 4f-4f transition spectra as a probe, 200 (2021). <https://doi.org/10.1016/j.poly.2021.115099>.

CHAPTER- 5

Absorption spectral analysis for the complexation of Pr^{3+} with L-leucine in the presence/absence of Mg^{2+} : 4f-4f transition as a probe

In this chapter, 4f-4f spectra of the fascinating lanthanide (Pr^{3+}) were used as a spectral and structural tool to investigate the reaction when Pr(III) ion interacts with L-leucine [Pr(III):Leu] in the presence/absence of Mg^{2+} in aquated organic solvents. The various energy interaction parameters and intensity parameters were employed to explore the various 4f-4f transitions under varied conditions. Thermodynamic parameters such as rate constant (k), frequency/pre-exponential factor (A), ΔH^0 , ΔS^0 & ΔG^0 were evaluated.

The text of this chapter has been communicated as:

Absorption spectral analysis for the complexation of Pr^{3+} with L-leucine in the presence/absence of Mg^{2+} : 4f-4f transition as a probe

Zevivonü Thakro^a, Chubazenba Imsong^a, Juliana Sanchu^a, M. Indira Devi^{a*}

^aDepartment of Chemistry, Nagaland University, Lumami, Nagaland, India

*E-mail- cam_indira@yahoo.co.in

5.1 INTRODUCTION

The *f*-electron based lanthanide (4*f*) binary compounds have piqued interest in the last few decades from both a fundamental and applied standpoints [1,2]. Numerous experimental and theoretical studies were carried out to bring forth a better understanding of the role of *f*-electrons in this area [3,4]. Although there are other oxidation states accessible, under normal conditions lanthanides are predominantly in their +3 state [5–7]. Lanthanide biochemistry is largely influenced by their 4*f*-electrons. Hence, the 4*f* electrons serve as a weak barrier against rising nuclear charge for the outer shells since 4*f*-orbitals have a radial probability distribution nearer to the nucleus as compared to 5*p* and 6*s* electrons [8].

5.1.1 Leucine



Fig. 5.1: 2D and 3D structure of L-leucine

It is well understood that amino acids perform numerous biological functions and are essential in biological systems. L-leucine (figure 5.1) functions as a substrate for protein synthesis and is an essential mineral for modulating protein metabolism [9]. Physiologically, peptides and amino acids can act as effective metal binding sites. Peptides are considered the simple building blocks of amino acids. In addition to their biological importance, peptides are among the most actively researched molecules today because of their medicinal properties [10,11]. The functional groups, –COOH

and $-\text{NH}_2$ are present in L-leucine and they have the ability to change the dimensions and size of favorable materials while maintaining the integrity of their -R group [12]. In the gaseous phase, L-leucine appears neutral, and in an aqueous solution, they appear as zwitterions [13–16].

In the present study, $4f-4f$ spectra of the fascinating lanthanide (Pr^{3+}) were used as spectral and structural tool to investigate the reaction when Pr(III) ion interacts with L-leucine [Pr(III):Leu] in the presence/absence of Mg^{2+} in aquated organic solvents. Aquated organic solvents ratio (CH_3CN , CH_3OH , $\text{C}_4\text{H}_8\text{O}_2$, & DMF) was 50% v/v. Differences in the theoretical values for the various energy interaction parameters: bonding parameters ($b^{1/2}$), percentage covalency (δ), Nephelauxetic ratio (β), Slater-Condon (F_k), Racah energy (E_k), and Spin-orbit interaction (ζ_{4f}) were employed to look into the insight of the complexation. To explore the various $4f-4f$ transitions under varied conditions, the intensity parameters, Judd-Ofelt (T_λ , $\lambda=2, 4, 6$) and oscillator strengths (P) were determined. The mechanism of Pr^{3+} interaction with L-leucine and magnesium for various pH (2, 4, 6) was studied in DMF:Water medium. Thermodynamic behavior such as rate constant (k), frequency/pre-exponential factor (A), ΔH^0 , ΔS^0 & ΔG^0 were evaluated.

5.2 MATERIALS AND METHODS

$\text{Pr(III)(NO}_3)_3 \cdot 6\text{H}_2\text{O}$ (99.9%) was acquired from Sigma-Aldrich, 2-Amino-4-methylpentanoic acid from HiMedia, and solvents (1,4-Dioxan, Acetonitrile, N,N-Dimethylformamide, and Methanol, 99.5% from Merck. A concentration of 5×10^{-3} M for Pr(III), L-leucine (2-Amino-4-methylpentanoic acid), and Magnesium ion (+2) was maintained for recording spectra. 50% vol/vol of four different aquated organic

solvents [Dioxane, Acetonitrile (ACN), Methanol (MeOH) & Dimethylformamide (DMF)] was used for the preparations of the solution. A Perkin Elmer Lambda 365 UV/Vis spectrophotometer was utilized to record the absorption spectra. For the measurements of pH, the digital pH meter Eutech pH 700 was utilized.

5.3 METAL COMPLEXES OF LANTHANIDE WITH AMINO ACIDS

The pH values affect how the ligand binds to the metal; for example, in acidic medium, only the oxygen atom attaches to the metal, while in basic medium, nitrogen and oxygen atoms are both bonded to the metal (Figure 5.2) [17].

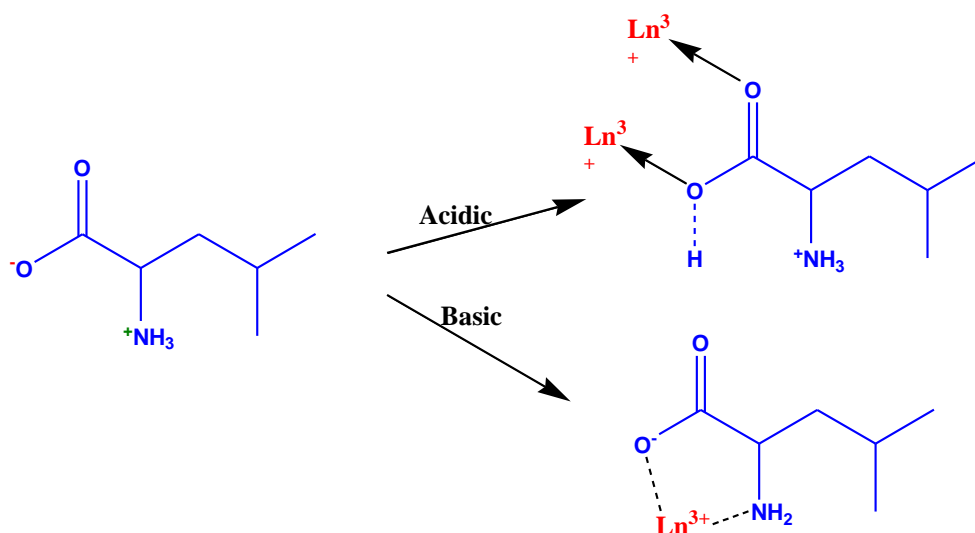


Fig 5.2: Bonding properties of L-leucine at various pH medium.

When it comes to complex formation, lanthanides are regarded as hard acceptors or class A, and thus favor hard acceptor or class A ligands (in the order $\text{Cl} < \text{F} < \text{S} < \text{N} < \text{O}$). Coordination numbers are typically between six and twelve, but biologically relevant coordination numbers are eight or nine. Hence, complexes are capable of various geometrical configurations (Figure 5.3) [18].

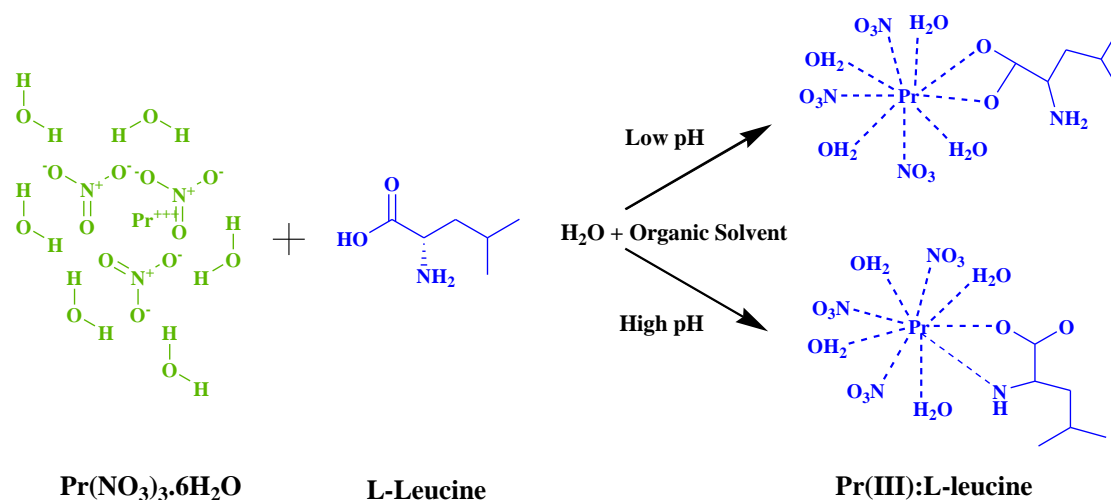


Fig 5.3: Possible interaction between Pr^{3+} and L-leucine in acidic media.

5.4 CALCULATIONS

The following equations are used for the calculations of different parameters. The details of the calculations have been discussed in chapter 2.

5.4.1 Energy parameters

Nephelauxetic ratio ' β '

$$\beta = \frac{F_K^C}{F_K^f} \text{ or } \frac{E_C^K}{E_f^K} \quad (1)$$

Slater–Condon ' F_k ' and Lande spin-orbit parameters ' ξ_{4f} '

$$F_k = F_k^0 + \Delta F_k \quad (2)$$

$$\xi_{4f} = \xi_{4f}^0 + \Delta \xi_{4f} \quad (3)$$

Racah parameter

$$E^1 = \frac{70F_2 + 231F_4 + 20.02F_6}{9} \quad (4)$$

$$E^2 = \frac{F_2 - 3F_4 + 7F_6}{9} \quad (5)$$

$$E^3 = \frac{5F_2 + 6F_4 - 9F_6}{9} \quad (6)$$

Bonding parameter ($b^{1/2}$) and covalent percentage (δ)

$$b^{1/2} = \left[\frac{1-\beta}{2} \right]^{1/2} \quad (7)$$

$$\delta = \left[\frac{1-\beta}{\beta} \right] \times 100 \quad (8)$$

5.4.2 Intensity parameters

Oscillator strength

$$P_{\text{obs}} = 4.6 \times 10^{-9} \times \epsilon_{\text{max}} \bar{\nu}^{1/2} \quad (9)$$

Judd-Ofelt parameters (T_λ)

$$\frac{P_{\text{obs}}}{\nu} = [(U)^2]^2 \cdot T_2 + [(U)^4]^2 \cdot T_4 + [(U)^6]^2 \cdot T_6 \quad (10)$$

5.4.3 Reaction dynamics/Thermodynamics theory

$$\log k = \log A - \frac{E_a}{2.303RT} \quad (11)$$

$$E_a = -\text{slope} \times 2.303 \times R \quad (12)$$

$$\log k = -\frac{\Delta H^\circ}{R} \left[\frac{1}{T} \right] + \frac{\Delta S^\circ}{R} \quad (13)$$

5.5 RESULTS AND DISCUSSIONS

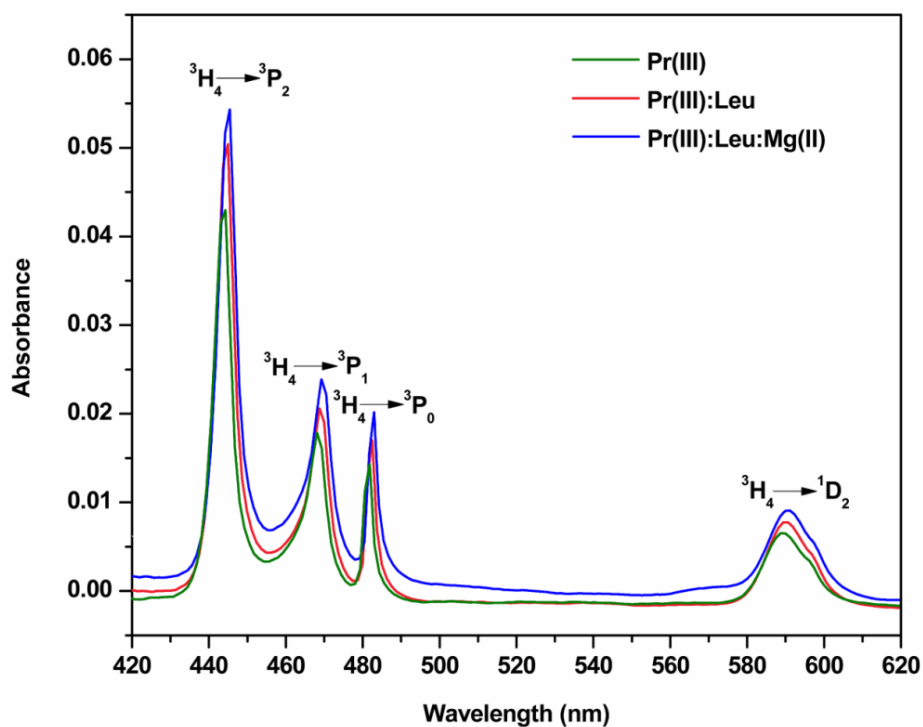


Fig. 5.4: 4f-4f electronic transition absorption spectra (UV-vis) of Pr^{3+} , Pr(III):Leu & $\text{Pr(III):Leu:Mg(II)}$ complex in aquated dioxane (50% v/v)

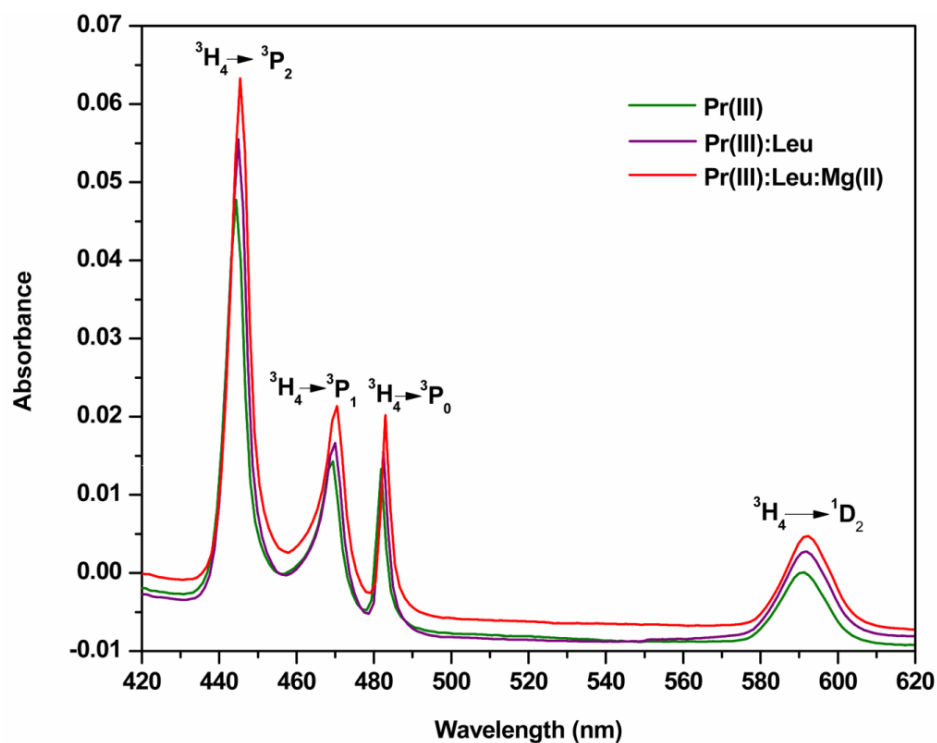


Fig. 5.5: 4f-4f electronic transition absorption spectra (UV-vis) of Pr^{3+} , Pr(III):Leu & $\text{Pr(III):Leu:Mg(II)}$ complex in aquated DMF(50% v/v).

Table 5.1: Observed and calculated P and T_λ (T_λ , $\lambda = 2, 4, 6 \times 10^{10} \text{ cm}^{-1}$) intensity parameters of Pr(III) with L-leucine in presence and absence of Mg^{2+} in different aquated organic solvents.

Methanol:Water			Dioxane:Water			ACN:Water			DMF:Water			T ₂	T ₄	T ₆
Pr(III):Leu:Mg(II)	Pr(III):Leu	Pr(III)	Pr(III):Leu:Mg(II)	Pr(III):Leu	Pr(III)	Pr(III):Leu:Mg(II)	Pr(III):Leu	Pr(III)	Pr(III):Leu:Mg(II)	Pr(III):Leu	Pr(III)			
5.120	4.309	3.468	6.894	5.869	3.710	8.361	6.770	4.348	8.803	7.838	5.355	-147.4	3.544	16.618
5.120	4.309	3.468	6.894	5.869	3.715	8.3618	6.770	4.348	8.803	7.838	5.355	-265.5	5.614	24.242
2.615	1.587	1.489	2.737	1.761	1.122	3.067	2.353	1.726	3.884	2.991	1.826	-235.4	7.662	26.916
1.767	1.094	0.852	1.646	1.341	0.841	2.202	1.827	1.289	2.780	2.038	1.288	-70.03	3.535	13.32
0.905	0.591	0.211	0.546	0.905	0.549	1.315	1.280	0.837	1.651	1.071	0.739	-193.5	5.017	20.889
1.739	1.077	0.838	1.619	1.317	0.825	2.166	1.797	1.267	2.738	2.010	1.270	-150.0	6.053	25.86
1.885	1.342	1.202	0.781	0.429	0.020	1.789	1.132	0.967	1.548	1.125	0.915	-241.5	2.302	11.552
1.885	1.342	1.202	0.782	0.429	0.020	1.789	1.133	0.967	1.548	1.125	0.915	-291.8	3.677	18.256
86.352	18.246	-283.6	-280.5	-291.8	-241.5	-150.0	-193.5	-70.03	-235.4	-265.5	-147.4	-283.6	2.335	10.745
4.855	3.003	2.335	4.522	3.677	2.302	6.053	5.017	3.535	7.662	5.614	3.544	3.003	3.003	13.338
15.518	13.338	10.745	21.43	18.256	11.552	25.86	20.889	13.32	26.916	24.242	16.618	10.745	10.745	10.745

Table 5.2: Computed value of $F_K(\text{cm}^{-1})$, $\xi_{4f}(\text{cm}^{-1})$, β , $b^{1/2}$, and δ parameters of Pr(III) free ion, Pr(III) with L-leucine in the presence and absence of Mg^{2+} .

Methanol:Water			Dioxane:Water			ACN:Water			DMF:Water			
Pr(III):Leu: u:Mg(II)	Pr(III): Leu	Pr(III)	Pr(III):Leu: u:Mg(II)	Pr(III): Leu	Pr(III)	Pr(III):Leu: u:Mg(II)	Pr(III): Leu	Pr(III)	Pr(III):Leu: u:Mg(II)	Pr(III): Leu	Pr(III)	
308.955	309.213	309.419	308.794	309.157	309.466	308.602	308.957	309.209	308.112	308.592	308.895	F_2
42.651	42.686	42.715	42.629	42.679	42.721	42.602	42.651	42.686	42.535	42.601	42.643	F_4
4.665	4.669	4.672	4.662	4.668	4.672	4.659	4.665	4.669	4.653	4.659	4.664	F_6
720.444	720.995	721.556	721.657	723.446	724.099	721.918	722.256	722.420	719.934	719.767	719.965	ξ_{4f}
3508.078	3511.006	3513.344	3506.251	3510.37	3513.87	3504.068	3508.11	3510.95	3498.50	3503.95	3507.39	E_1
23.739	23.759	23.775	23.727	23.755	23.779	23.713	23.740	23.759	23.675	23.712	23.735	E_2
614.223	614.736	615.145	613.9036	614.625	615.239	613.521	614.229	614.728	612.547	613.502	614.104	E_3
0.944	0.945	0.947	0.945	0.947	0.948	0.943	0.944	0.946	0.942	0.943	0.944	β
0.167	0.164	0.163	0.1648	0.1621	0.1607	0.166	0.164	0.163	0.168	0.167	0.166	$b^{1/2}$
5.810	5.725	5.649	5.743	5.547	5.447	5.754	5.670	5.617	5.987	5.921	5.856	δ
120.55	114.65	113.30	118.97	113.65	108.47	113.70	110.64	111.79	123.16	121.20	122.50	RMS

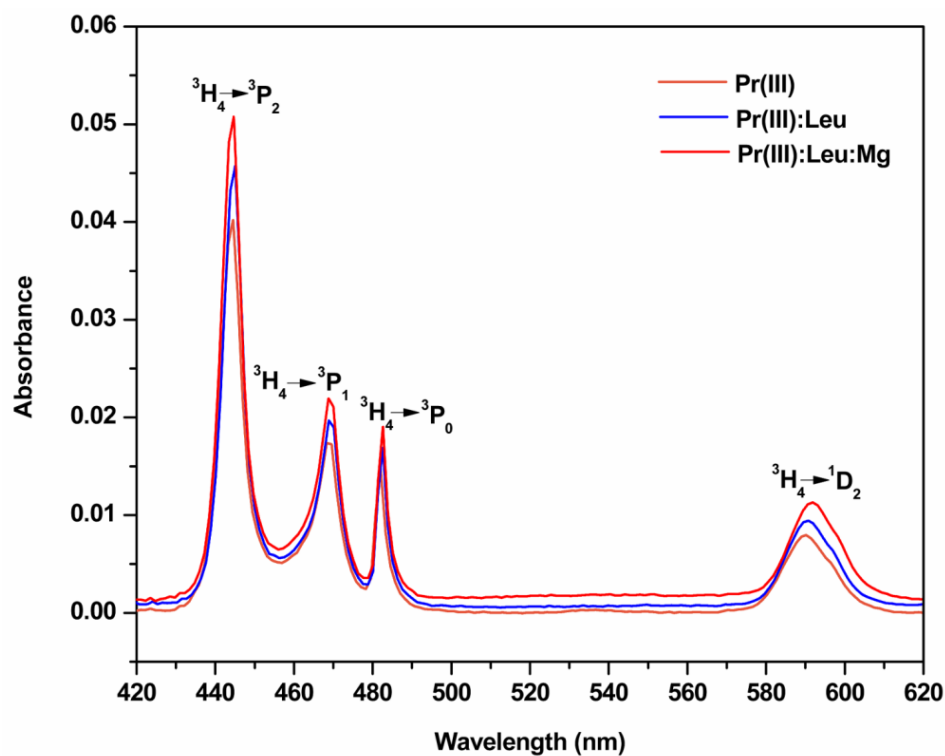


Fig. 5.6: 4f-4f electronic transition absorption spectra (UV-vis) of Pr³⁺, Pr(III):Leu & Pr(III):Leu:Mg(II) complex at pH 4.

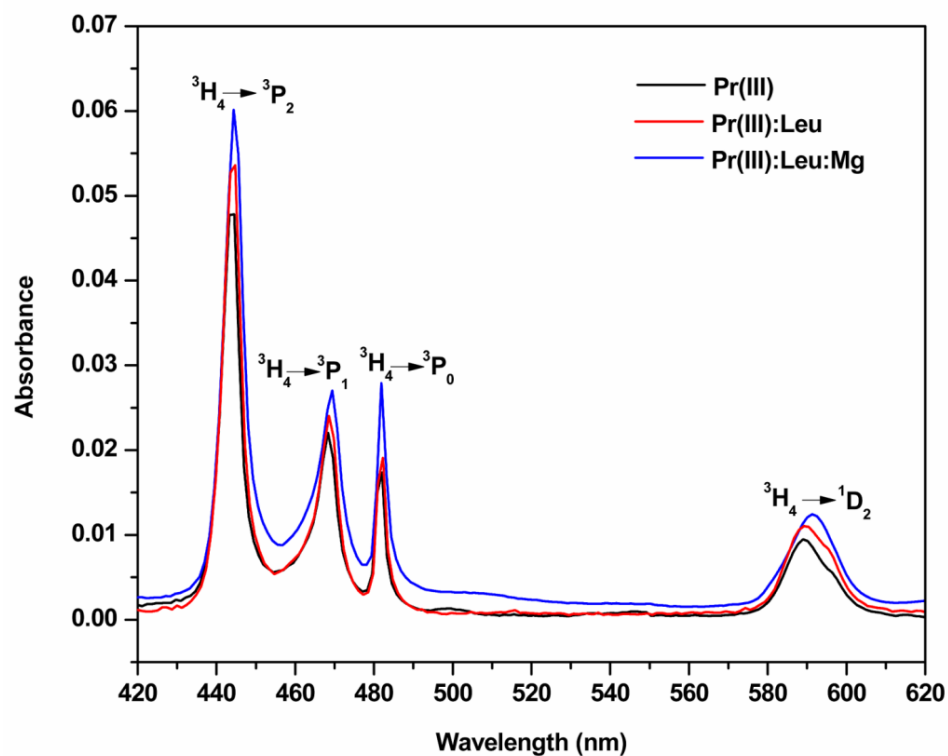


Fig. 5.7: 4f-4f electronic transition absorption spectra (UV-vis) of Pr³⁺, Pr(III):Leu & Pr(III):Leu:Mg(II) complex at pH 6.

Table 5.3: Computed value of $F_K(\text{cm}^{-1})$, $\xi_{4f}(\text{cm}^{-1})$, β , $b^{1/2}$, and δ parameters of Pr(III) free ion, Pr(III) with L-leucine in the presence and absence of Mg^{2+} at various pH.

pH 6				pH 4			pH 2			
Pr(III):Leu:Mg(II)	Pr(III):Leu	Pr(III)	Pr(III):Leu:Mg(II)	Pr(III):Leu:Mg(II)	Pr(III):Leu	Pr(III)	Pr(III):Leu:Mg(II)	Pr(III):Leu	Pr(III)	
308.819	309.255	309.602	308.493	308.875	309.106	308.739	309.083	309.329	F_2	
42.632	42.692	42.740	42.587	42.640	42.672	42.621	42.668	42.702	F_4	
4.663	4.669	4.675	4.658	4.664	4.667	4.662	4.667	4.670	F_6	
718.724	720.746	722.578	721.073	721.901	722.661	721.276	721.301	721.783	ξ_{4f}	
3506.536	3511.488	3515.423	3502.834	3507.176	3509.790	3505.626	3509.529	3512.324	E_1	
23.729	23.762	23.789	23.704	23.733	23.751	23.723	23.749	23.768	E_2	
613.953	614.820	615.509	613.305	614.065	614.523	613.794	614.477	614.967	E_3	
0.943	0.945	0.947	0.944	0.946	0.946	0.945	0.946	0.946	β	
0.167	0.164	0.162	0.166	0.164	0.163	0.165	0.163	0.163	$b^{1/2}$	
5.964	5.737	5.541	5.837	5.711	5.615	5.781	5.646	5.646	δ	
117.66	115.01	113.27	124.48	122.53	116.32	108.53	105.73	103.42	RMS	

Table 5.4: Observed and calculated P and T_λ ($\lambda = 2, 4, 6 \times 10^{10} \text{ cm}^{-1}$) intensity parameter of Pr(III) with L-leucine in the presence and absence of Mg^{2+} in different pH mediums.

pH 6			pH 4			pH 2				
Pr(III):Leu:Mg(II)	Pr(III):Leu	Pr(III)	Pr(III):Leu:Mg(II)	Pr(III):Leu	Pr(III)	Pr(III):Leu:Mg(II)	Pr(III):Leu	Pr(III)	Pr(III):Leu:Mg(II)	Pr(III)
7.094	5.215	4.305	6.247	4.787	3.456	4.682	3.755	3.384	$^3\text{H}_4\rightarrow^3\text{P}_2$	
									Pobs	Pcal
7.094	5.215	4.305	6.247	4.787	3.456	4.682	3.755	3.384	$^3\text{H}_4\rightarrow^3\text{P}_1$	
									Pobs	Pcal
3.350	2.414	2.199	2.521	1.994	1.371	2.081	1.785	1.504	$^3\text{H}_4\rightarrow^3\text{P}_0$	
									Pobs	Pcal
2.503	1.892	1.546	1.915	1.440	1.029	1.417	1.187	0.987	$^3\text{H}_4\rightarrow^1\text{D}_2$	
									Pobs	Pcal
1.633	1.350	0.879	1.288	0.871	0.676	0.741	0.579	0.463		
									Pobs	Pcal
2.468	1.863	1.521	1.884	1.416	1.012	1.394	1.168	0.972		
									Pobs	Pcal
2.317	1.870	1.967	1.994	1.498	1.169	1.157	1.267	1.012		
									Pobs	Pcal
2.317	1.870	1.967	1.994	1.498	1.169	1.157	1.267	1.012		
									Pobs	Pcal
52.304	76.123	159.05	31.954	21.617	35.548	-49.71	37.198	4.068	T_2	
									T_4	
6.886	5.194	4.238	5.266	3.954	2.824	3.895	3.259	2.710	T_6	
21.482	15.724	12.957	19.128	14.650	10.575	14.350	11.448	10.378		

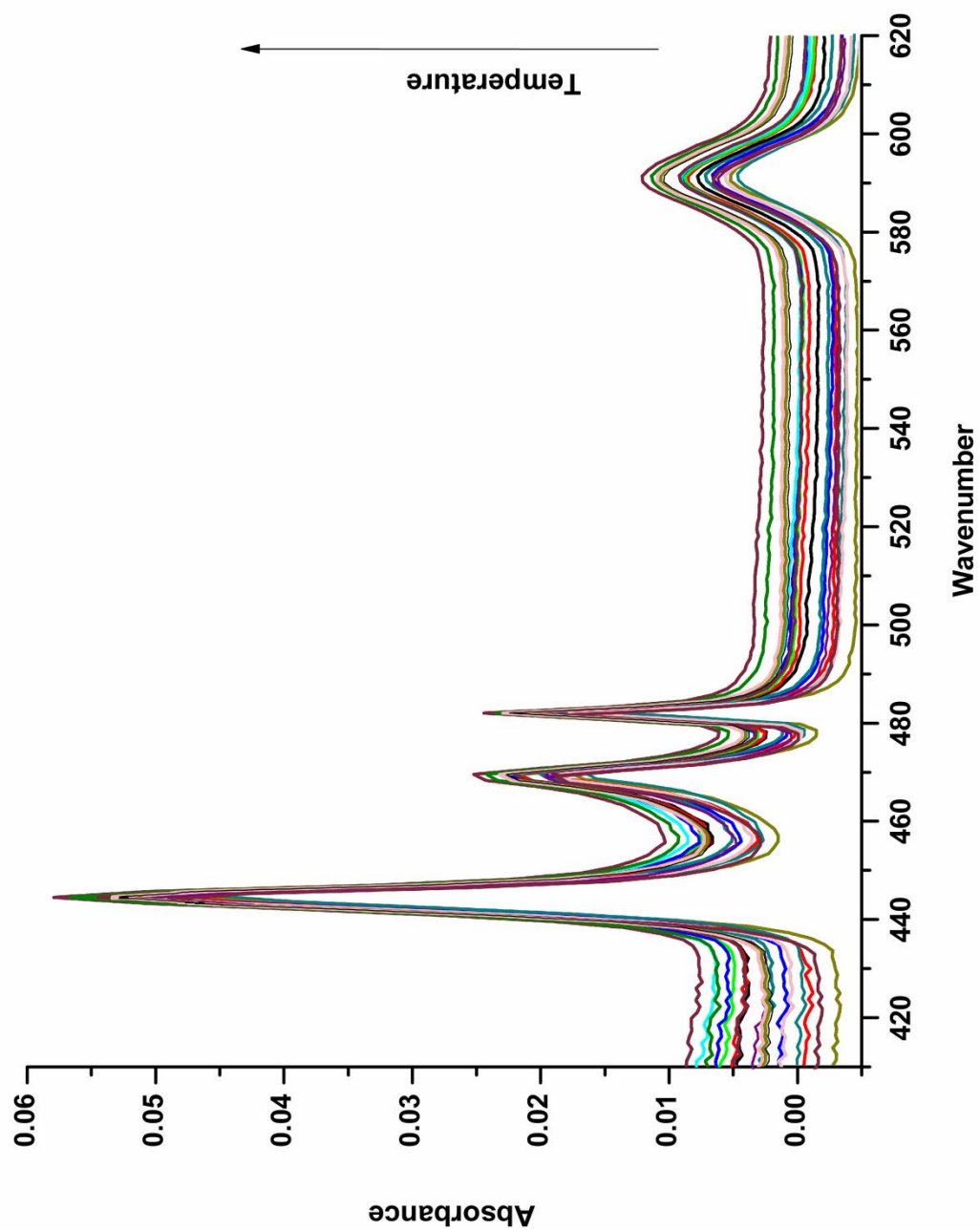


Fig. 5.8: Absorption spectra of $\text{Pr(III):Leu:Mg(II)}$ complexation at 298 K and in different time

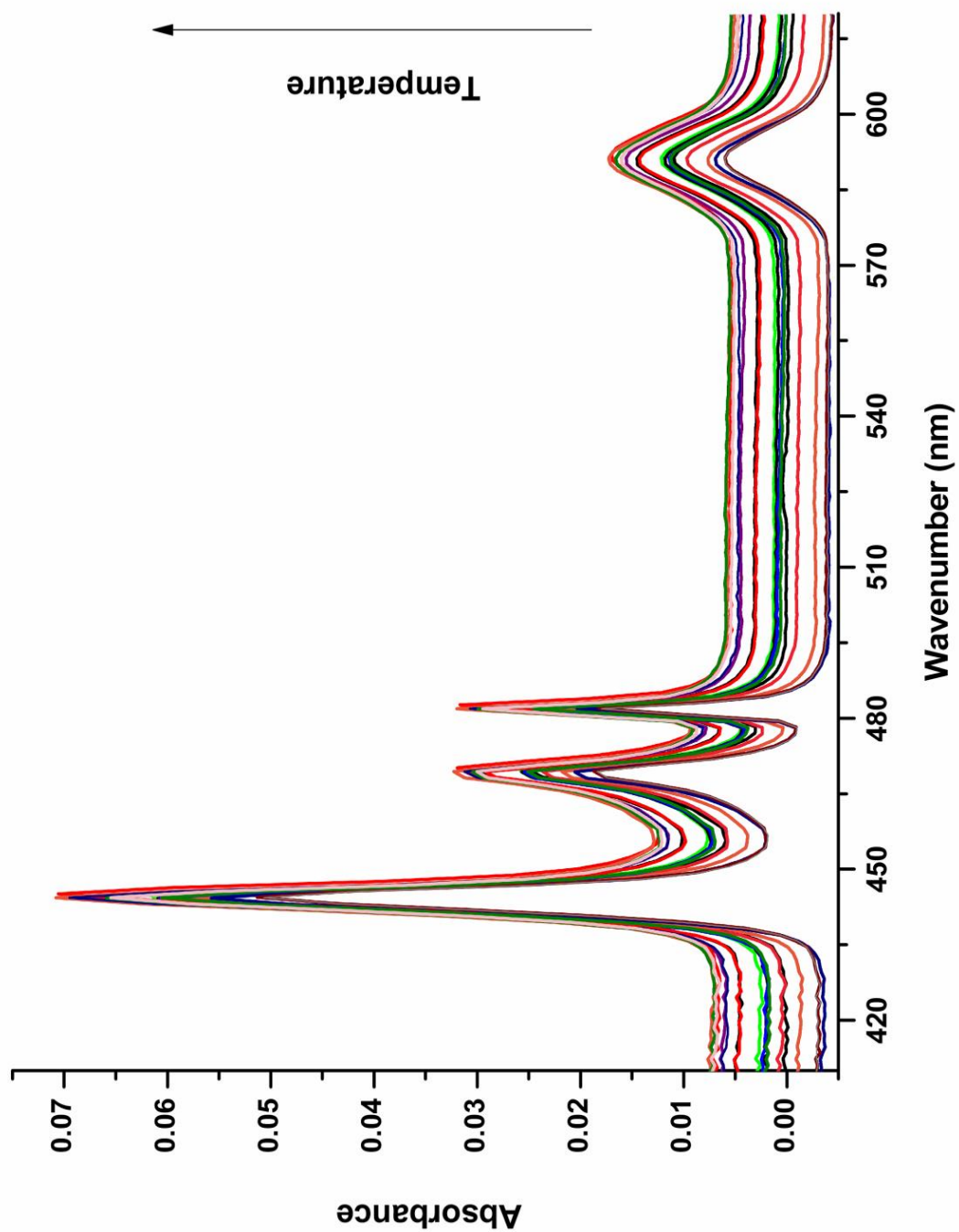


Fig. 5.9: Absorption spectra of $\text{Pr(III):Leu:Mg(II)}$ complexation at 303 K and in different time intervals.

Table 5.5: Observed and calculated P and T_λ , ($\lambda = 2, 4, 6$) at 298 K and in various time intervals for the complex Pr(III):Leu:Mg(II).

Time	$^3\text{H}_4 \rightarrow ^3\text{P}_2$		$^3\text{H}_4 \rightarrow ^3\text{P}_1$		$^3\text{H}_4 \rightarrow ^3\text{P}_0$		$^3\text{H}_4 \rightarrow ^1\text{D}_2$		T_2	T_4	T_6
	Pobs	Pcal	Pobs	Pcal	Pobs	Pcal	Pobs	Pcal			
0	5.068	5.068	1.638	1.229	0.808	1.212	0.969	0.969	-116.2	3.379	15.723
2	5.093	5.093	1.653	1.241	0.816	1.223	1.054	1.054	-98.61	3.410	15.797
4	5.204	5.205	1.671	1.265	0.848	1.248	1.168	1.168	-80.17	3.479	16.145
6	5.286	5.286	1.685	1.277	0.857	1.259	1.334	1.334	-47.65	3.512	16.403
8	5.453	5.453	1.693	1.284	0.864	1.267	2.907	2.907	298.79	3.532	16.947
10	5.514	5.514	1.716	1.303	0.878	1.285	1.803	1.803	43.81	3.582	17.132
12	5.569	5.569	1.757	1.333	0.897	1.315	1.885	1.885	58.63	3.666	17.292
14	5.651	5.651	1.768	1.343	0.906	1.324	1.959	1.959	70.28	3.693	17.552
16	6.017	6.017	1.787	1.361	0.922	1.342	2.055	2.055	67.86	3.742	18.739
18	6.159	6.159	1.832	1.394	0.943	1.375	2.111	2.111	71.26	3.833	19.182
20	6.271	6.271	1.86	1.419	0.961	1.399	2.166	2.166	76.29	3.902	19.530
22	6.357	6.357	1.884	1.439	0.980	1.419	2.215	2.215	81.62	3.956	19.799
24	6.581	6.581	1.914	1.463	0.997	1.442	2.231	2.231	70.551	4.022	20.514
26	6.702	6.702	2.590	1.970	1.331	1.942	2.727	2.727	173.76	5.415	20.539
28	6.985	6.985	2.743	2.099	1.435	2.070	2.845	2.845	181.54	5.771	21.375
30	7.065	7.065	2.812	2.156	1.480	2.126	2.949	2.949	199.71	5.929	21.596
32	7.178	7.178	3.021	2.277	1.513	2.246	3.072	3.072	219.96	6.261	21.875
34	7.347	7.347	3.150	2.382	1.592	2.349	3.073	3.073	208.64	6.549	22.353

Table 5.6: Observed and calculated P and T_λ , ($\lambda = 2, 4, 6$) at 303 K and in various time intervals for the complex Pr(III):Leu:Mg(II).

Time	$^3\text{H}_4 \rightarrow ^3\text{P}_2$		$^3\text{H}_4 \rightarrow ^3\text{P}_1$		$^3\text{H}_4 \rightarrow ^3\text{P}_0$		$^3\text{H}_4 \rightarrow ^1\text{D}_2$		T_2	T_4	T_6
	Pobs	Pcal	Pobs	Pcal	Pobs	Pcal	Pobs	Pcal			
0	5.724	5.724	2.197	1.595	0.980	1.573	1.286	1.286	-88.52	4.387	17.61
2	5.741	5.741	2.289	1.680	1.057	1.657	1.360	1.360	-73.02	4.620	17.59
4	5.778	5.778	2.466	1.788	1.094	1.763	1.413	1.413	-63.75	4.915	17.64
6	5.938	5.938	2.577	1.887	1.181	1.861	1.679	1.679	-14.07	5.188	18.09
8	6.033	6.033	2.613	1.937	1.243	1.910	1.908	1.908	31.59	5.326	18.36
10	6.160	6.161	2.648	1.969	1.273	1.942	1.921	1.921	25.95	5.414	18.76
12	6.274	6.274	2.726	2.012	1.280	1.984	2.257	2.257	94.93	5.532	19.104
14	6.302	6.302	2.777	2.056	1.317	2.028	2.292	2.292	100.84	5.653	19.16
16	6.495	6.495	3.073	2.215	1.339	2.185	2.371	2.371	105.59	6.091	19.68
18	6.777	6.777	3.427	2.415	1.384	2.381	2.434	2.434	100.69	6.639	20.46
20	7.119	7.119	3.591	2.535	1.459	2.500	2.496	2.496	92.03	6.970	21.49
22	7.178	7.178	3.676	2.593	1.489	2.557	2.580	2.580	107.02	7.129	21.64
24	7.255	7.255	3.738	2.636	1.513	2.599	2.625	2.625	112.09	7.247	21.86
26	7.290	7.290	3.781	2.706	1.608	2.668	2.692	2.692	124.74	7.439	21.92
28	7.349	7.349	3.847	2.762	1.653	2.724	2.747	2.747	133.25	7.593	22.08
30	7.422	7.422	3.871	2.813	1.731	2.774	2.804	2.804	141.22	7.734	22.28
32	7.471	7.471	3.907	2.860	1.788	2.821	2.841	2.841	146.08	7.863	22.41
34	7.573	7.573	3.983 1	2.919	1.830	2.879	2.888	2.888	150.07	8.025	22.69

Table 5.7: Observed and calculated P and T_λ , ($\lambda = 2, 4, 6$) at 308 K and in various time intervals for the complex Pr(III):Leu:Mg(II).

Time	$^3\text{H}_4 \rightarrow ^3\text{P}_2$		$^3\text{H}_4 \rightarrow ^3\text{P}_1$		$^3\text{H}_4 \rightarrow ^3\text{P}_0$		$^3\text{H}_4 \rightarrow ^1\text{D}_2$		T_2	T_4	T_6
	Pobs	Pcal	Pobs	Pcal	Pobs	Pcal	Pobs	Pcal			
0	6.191	6.190	1.703	1.367	1.017	1.348	0.854	0.854	-216.4	3.759	19.304
2	6.315	6.315	1.830	1.453	1.061	1.432	1.371	1.372	-107.3	3.994	19.651
4	6.415	6.415	1.912	1.498	1.069	1.477	1.519	1.519	-80.44	4.119	19.947
6	6.524	6.524	2.180	1.678	1.161	1.655	1.573	1.573	-75.99	4.614	20.17
8	6.612	6.612	2.461	1.846	1.213	1.820	2.034	2.034	22.401	5.074	20.336
10	6.649	6.649	2.587	1.923	1.242	1.897	2.091	2.091	32.849	5.288	20.401
12	7.022	7.021	2.635	1.957	1.261	1.929	2.154	2.154	22.676	5.379	21.597
14	7.118	7.118	2.878	2.098	1.301	2.069	2.303	2.303	49.514	5.769	21.812
16	7.118	7.118	2.878	2.098	1.300	2.069	2.303	2.303	49.514	5.769	21.812
18	7.290	7.290	3.005	2.190	1.357	2.160	2.443	2.443	69.853	6.022	22.307
20	7.362	7.362	3.045	2.221	1.378	2.190	2.526	2.526	83.97	6.106	22.521
22	7.431	7.431	3.085	2.245	1.385	2.214	2.568	2.568	88.82	6.172	22.731
24	7.459	7.459	3.212	2.320	1.408	2.287	2.641	2.641	103.23	6.377	22.768
26	7.532	7.532	3.329	2.387	1.425	2.354	2.696	2.696	110.86	6.563	22.958
28	8.088	8.088	3.331	2.396	1.441	2.363	2.771	2.771	91.341	6.588	24.775
30	8.344	8.344	3.336	2.408	1.461	2.375	2.817	2.817	84.946	6.621	25.605
32	8.356	8.356	3.341	2.417	1.473	2.383	2.854	2.854	92.552	6.645	25.637
34	8.386	8.386	3.348	2.431	1.493	2.397	2.909	2.909	103.13	6.684	25.727

Table 5.8: Observed and calculated P and T_λ , ($\lambda = 2, 4, 6$) at 313 K and in various time intervals for the complex Pr(III):Leu:Mg(II).

Time	$^3\text{H}_4 \rightarrow ^3\text{P}_2$		$^3\text{H}_4 \rightarrow ^3\text{P}_1$		$^3\text{H}_4 \rightarrow ^3\text{P}_0$		$^3\text{H}_4 \rightarrow ^1\text{D}_2$		T_2	T_4	T_6
	Pobs	Pcal	Pobs	Pcal	Pobs	Pcal	Pobs	Pcal			
0	6.525	6.525	1.780	1.302	0.811	1.283	1.236	1.236	-151.30	3.580	20.45
2	6.730	6.730	1.998	1.467	0.922	1.445	1.529	1.529	-98.90	4.034	21.01
4	6.974	6.974	2.264	1.623	0.966	1.599	1.810	1.810	-51.57	4.462	21.69
6	7.127	7.127	2.507	1.782	1.041	1.755	2.066	2.066	-3.96	4.899	22.07
8	7.297	7.297	2.530	1.823	1.101	1.796	2.253	2.253	27.35	5.015	22.61
10	7.591	7.591	2.647	1.945	1.224	1.916	2.434	2.434	48.82	5.348	23.48
12	7.772	7.772	2.880	2.088	1.277	2.057	2.619	2.619	78.38	5.743	23.96
14	7.914	7.914	3.001	2.162	1.303	2.130	2.812	2.812	112.73	5.944	24.38
16	8.121	8.121	3.080	2.219	1.338	2.186	2.957	2.957	132.05	6.103	25.02
18	8.232	8.232	3.193	2.324	1.434	2.290	3.137	3.137	165.17	6.391	25.31
20	8.467	8.467	3.269	2.377	1.463	2.342	3.343	3.343	196.47	6.537	26.04
22	8.643	8.643	3.337	2.426	1.492	2.390	3.385	3.385	194.38	6.670	26.58
24	8.692	8.692	3.390	2.480	1.547	2.443	3.576	3.576	234.29	6.819	26.70
26	8.832	8.832	3.437	2.522	1.583	2.485	3.653	3.653	242.37	6.935	27.13
28	8.908	8.908	3.463	2.552	1.617	2.514	3.727	3.727	254.21	7.018	27.35
30	8.959	8.959	3.507	2.589	1.646	2.550	3.794	3.794	266.04	7.118	27.49
32	9.046	9.046	3.644	2.668	1.666	2.628	3.844	3.844	271.29	7.336	27.72
34	9.109	9.109	3.663	2.686	1.684	2.646	3.897	3.897	279.16	7.386	27.91

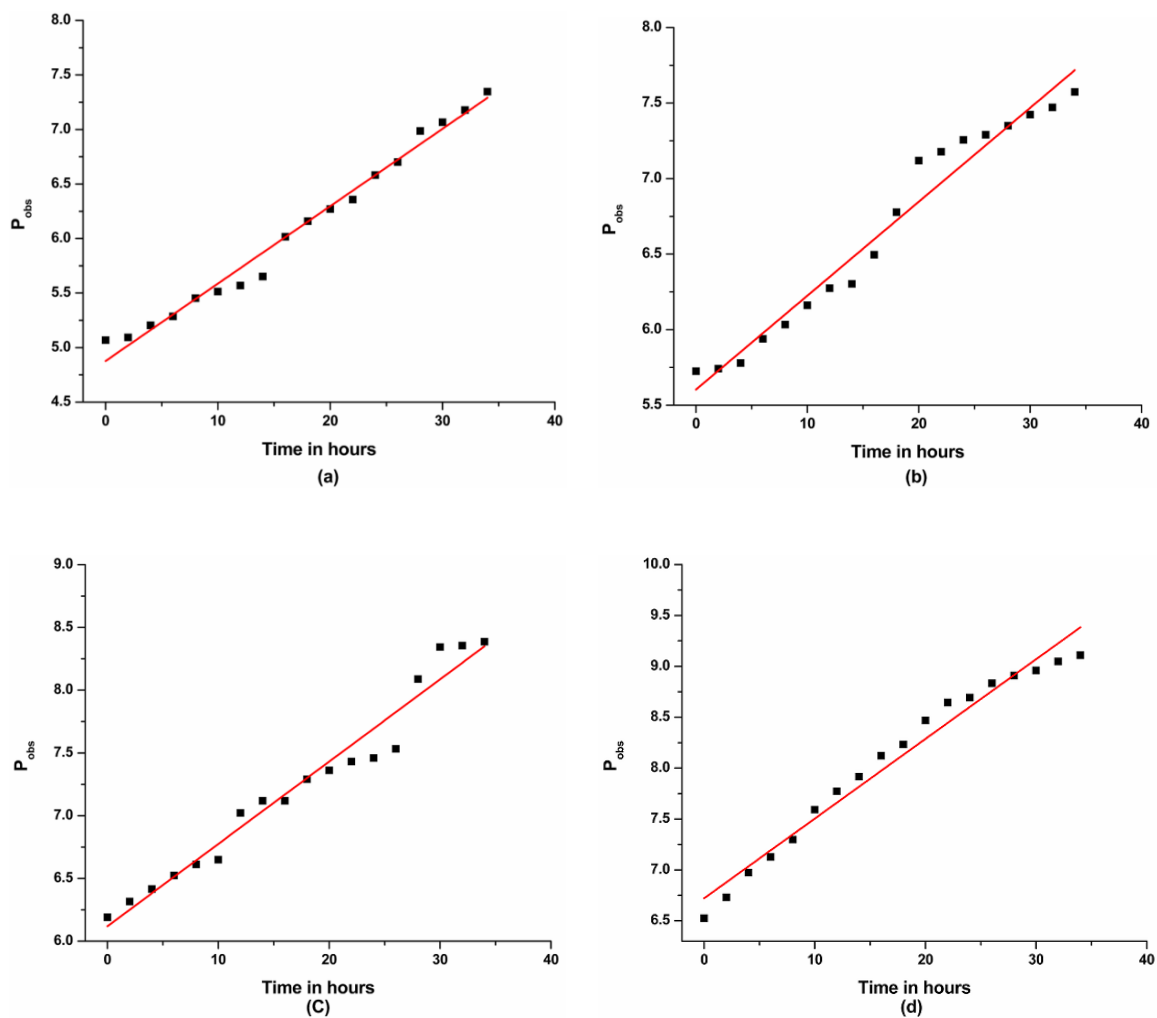


Fig. 5.10: P_{obs} vs Time in hours at different temperatures: (a) 298 K, (b) 303 K, (c) 308 K, (d) 313 K for the $^3\text{H}_4 \rightarrow ^3\text{P}_2$ transition of Pr(III):Leu:Mg(II).

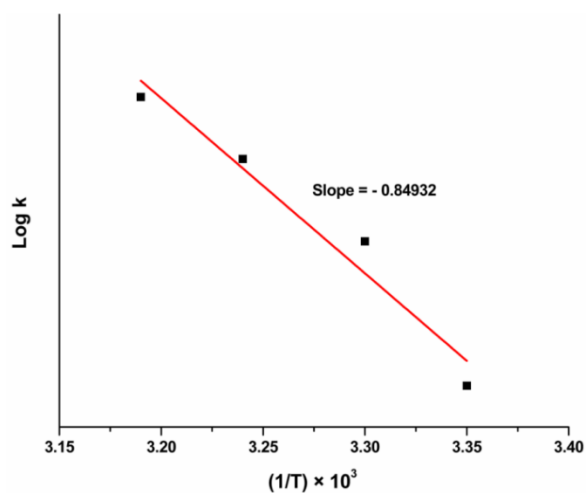


Fig. 5.11: $\log k$ vs $(1/T) \times 10^3$ for Pr(III):Leu:Mg(II) complex.

Table 5.9: Rate Constants and Activation Energy for Pr(III):Leu:Mg(II) complex at various temperatures.

Temperature (K)	$1/T \times 10^3 \text{ K}^{-1}$	Rate Constant (k) $\text{Mol L}^{-1} \text{ h}^{-1}$	Rate Constant (k) $\text{Mol L}^{-1} \text{ S}^{-1} \times 10^{-6}$	log k	Pre-exponential factor (A)	Activation Energy $\Delta E_a (\text{kJ/mol})$
298	3.35	0.00463	16.67	1.22	4.87	0.0162
303	3.30	0.00539	19.40	1.29	5.60	
308	3.24	0.00591	21.27	1.33	6.12	
313	3.19	0.00648	23.33	1.36	6.72	

Table 5.10: Rate constants and thermodynamic parameters for Pr(III):Leu:Mg(II) complex at various temperatures.

Temperature (K)	Rate (k) $\text{Mol L}^{-1} \text{ S}^{-1} \times 10^{-6}$	ΔH^0 (kJmol ⁻¹)	ΔG^0 (JK ⁻¹ mol ⁻¹)	ΔS^0 (kJmol ⁻¹)
298	1.22	0.0162	-6.96	0.039
303	1.29		-7.48	0.040
308	1.33		-7.84	0.041
313	1.36		-8.15	0.042

It has been proven that utilization of absorption spectrophotometry, a newly developed method for researching the chemistry of lanthanides, particularly in solutions can provide insight into complexes with intricate *f*-electron transitions, and the sensitivity of lanthanide to the complex's shape and coordination environment, has made it a viable tool for investigating the chemistry of lanthanides [19–21]. The strength of the metal-ligand bond, coordination geometry, shape of the complex produced, and interaction of chelate-solvent can be determined by the lanthanide ion absorption spectra for 4f-4f transitions [22].

Under various experimental settings, evaluated values of P and T_λ for the pseudohypersensitive transitions of free Pr^{3+} and Pr^{3+} complexed with Leucine and Mg(II) is presented in table 5.1. According to the P levels of various $4f-4f$ transition bands (table 5.1), remarkable variation in the values of P suggests the possibility of Pr^{3+} interacting with L-leucine [23]. Pr^{3+} interaction with the ligand causes the amplitude of T_λ ($\lambda = 2, 4, 6$) increase immensely; this validates L-leucine's ability to bind to Pr^{3+} . Similarly, when Mg^{2+} is incorporated into Pr(III):Leu system, it causes more intensification in the absorption bands of the pseudohypersensitive transitions. This could be because of the ability of praseodymium ion to generate a multimetal complex with Mg^{2+} [12]. T_4 and T_6 values vary greatly and exhibit positive values, allowing them to be employed in the Judd-Ofelt theory of $4f-4f$ transitions. The symmetry characteristics of the complex species are related to changes in both the T_4 and T_6 parameters [24]. As a result, such considerable variations in T_4 and T_6 values could indicate possible changes in the immediate coordination domain of Pr^{3+} in complexation with ligands. In contrast T_2 is ignored even though it is associated with the hypersensitive transition ($^3\text{H}_4 \rightarrow ^3\text{F}_3$), since it is outside of the UV-Visible area and also has negative values. A major change in P and its corresponding T_λ value could represent the possibility of inner-sphere complexation, while a small change in these values could convey the possibility of outer-sphere complexation [25]. The alterations in the values of P and T_λ shown in table 5.1 may bring forth a basis for concluding that L-leucine plays a role in inner-sphere coordination with Pr^{3+} . The computed results show that T_6 is the parameter that could best describe how L-leucine interacts with Pr^{3+} in the presence of Mg^{2+} , and they are listed in the following order: $T_6 > T_4 > T_2$.

The computed values of different energy interaction parameters are shown in table 5.2. The energy of distinct $4f-4f$ bands alter due to the binding of Pr^{3+} with L-leucine. Closed observation of the bonding nature could be taken out in detail from the changes in the energy interaction parameters of Pr^{3+} , Pr(III):Leu and $\text{Pr(III):Leu:Mg(II)}$ in 50%vol/vol water:solvent (ACN, Dioxane, Methanol, and DMF). From the comparison values of the free ionic state of Pr^{3+} with Pr(III):Leu and $\text{Pr(III):Leu:Mg(II)}$, it was found that the obtained values show a steady decrease in Slater-Condon (F_k), Racah parameter E^k and Lande spin-orbit parameter (ζ_{4f}) implying that the inter-electronic repulsion has decreased between the metal and the ligand. Similarly, the consistent drop in β values indicates that the bond length of the metal and ligand has shortened. Table 5.2 shows that the β values are noticeably low in complexes, indicating that the central metal ion orbital expands during complexation. This finding is compatible with the explanation previously put forward for the development and potency of $f-f$ transitions. It was found that the nephelauxetic ratio (β) measured at the site of Pr(III) complexation with L-leucine is in the range below unity, indicating the possibility of a covalent bond formation. The gradual decrease in the ' β ' values explains the reduction of the bond length between the metal ion and the ligand due to the expansion of the central metal ion orbital [26]. As shown in the figures 5.4 and 5.5, the decrease in the β values can also be correlated with the intensification of Pr^{3+} transition bands ($^3\text{H}_4 \rightarrow ^3\text{P}_2$, $^3\text{H}_4 \rightarrow ^3\text{P}_1$, $^3\text{H}_4 \rightarrow ^3\text{P}_0$, and $^3\text{H}_4 \rightarrow ^1\text{D}_2$). The precision of energy interaction parameter values is assessed using root mean square (RMS) values.

Tables 5.1 and 5.2 can be used to explain the preference for complex formation in specific solvents. It appears that the variation in P and T_λ values of various $4f-4f$

transition bands indicate that the interaction of metal's 4f-orbital with the ligand has increased. In the recorded data of DMF solvent, the magnitude and the variation in intensity parameters are higher. This indicates that the solvent has a greater influence on the formation of the complex between Pr^{3+} and the ligand. Therefore, DMF is a better solvent compared to others to form a complex. The greater oscillator strength (P) value was found for DMF solvent as compared to that of the other solvents, clearly showing a preference for this solvent for the formation of the complex. In addition, on a comparison of data obtained by computing $b^{1/2}$ and δ parameters, the values in the case of dimethylformamide system are found to be higher suggesting that it is the ideal solvent for the formation of covalent bonds, and this could be caused by the existence of an N-donor atom [20]. Sensitivity order for various organic solvents is $\text{DMF} > \text{CH}_3\text{CN} > \text{C}_4\text{H}_8\text{O}_2 > \text{CH}_3\text{OH}$.

The four pseudohypersensitive transitions with their comparative absorption spectra of free Pr^{3+} and its complexes in ACN and Dioxane solvent (50% v/v aquated solvent) are shown in figures. 5.4 and 5.5, respectively. As L-leucine interacts with Pr^{3+} and then continues on to interact with Mg^{2+} , the bands could show substantial sensitivity even with minute change around the Pr^{3+} region [23]. When ligand (L-leucine) is added to the pr^{3+} solution, the absorption bands of the complex intensify, and with the addition of Mg^{2+} , the intensity increases even more. This is an indication that Pr^{3+} strongly interacts with L-leucine and Mg^{2+} . The possibility of forming a complex is further substantiated by the redshift shown in figures 5.4 and 5.5.

Table 5.3 shows the obtained values of, $b_{1/2}$, ζ_{4f} , E^k ($k=1,2,3$), and F_k ($k=2,4,6$) for the complexes at varied pH levels. The protonation and deprotonation of L-leucine are

regulated by the pH levels in the ambience which have a substantial influence on the binding sites. According to the observation, the estimated values of electronic repulsive parameters (E^k , ζ_{4f} and F_k) and Nephelauxetic ratio (β) show a steady decrease as the value of pH increases. This explains that the inter-electronic repulsion has decreased and the orbital of metal (Praseodymium) has expanded as the pH increases. The decrease in the values of the β clearly explains the shortening of the bond length of metal-ligand with the rise of pH from 2 to 6. The ligand (L-leucine) has two binding sites - COOH and NH₂, and pH influences which site the metal will coordinate with. Since hard metal (Praseodymium) ions prefer bonding with the hard donor sites, Pr(III):Leu complex will form primarily through the interaction of Praseodymium ion with the carboxylic group of L-leucine. The computed data of the energy interaction parameters explains that the carboxylic group of L-leucine is deprotonated in an acidic media, allowing the metal ion to coordinate via it [11]. An increase in δ and $b^{1/2}$ with an increased in the pH values (2 to 6) implies that there is an increase in the interaction and the potential of covalent bond formation, which may be attributed to an increase in deprotonation capacities as pH increases. Table 5.4 shows the computed data of the intensity parameters and the variations in the values of P and T_λ also demonstrates this effect. The amine group continues deprotonating at increasing pH, as shown by the T_λ , ($\lambda = 2, 4, 6$) values, which are observed to be greater at higher pH. From the comparative absorption spectra in fig 5.6 and 5.7, the intensification of absorption peaks of pseudohypersensitive transitions of Pr(III) is found in tandem with the appearance of a redshift as the pH increases. This further indicates a greater interaction at higher pH.

To explore the kinetics of the complexation, Pr(III):Leu:Mg(II) complex at varying temperatures of 303 K, 308 K, 313 K, and 318 K, the absorption spectra were recorded in aquated organic solvent DMF:H₂O (50%v/v). Figures 5.8 and 5.9 present the comparative absorption spectra of the complex [Pr(III):Leu:Mg(II)] at different time intervals and temperatures (298 K and 303 K). The comparative spectra were used to compute the values of P and T_λ for the pseudohypersensitive transition. Tables 5.5, 5.6, 5.7, and 5.8 illustrates the variations in the computed parameters of P and T_λ for the complex at different temperatures. In comparison to the other $4f-4f$ transitions, pseudohypersensitive transition ($^3H_4 \rightarrow ^3P_2$) was found to be the most sensitive transition. The calculated data shows that T_4 and T_6 have correspondingly higher sensitivity and a rise in value with time and temperature. This pattern denotes an increase in the rate constant for the complex formation of Pr(III):Leu:Mg(II).

The plot of P_{obs} versus time for the transition $^3H_4 \rightarrow ^3P_2$ at different temperatures were shown in figure 5.10. From the graphs (Figure 5.10), the rate constants were calculated using the values of slope and pre-exponential factor, as given in the table 5.9. It is evident from the table that when the temperature increases, the complexation is enhanced as shown by the elevated rate constant values. This is in accordance with the theoretically predicted Arrhenius reaction rate. The rate constant values may be listed in the following order: $313\text{ K} > 308\text{ K} > 303\text{ K} > 298\text{ K}$. Again, the rise in Pre-exponential factor (A) values with temperature growth indicate an increase in the possibility of molecules collision. The probability of a spontaneous reaction is suggested by the activation energy's (E_a) extremely low value. The plot of $\log k$ versus $(1/T) \times 10^3$ has been presented in figure 5.11. The acquired graph's values were utilized for the evaluation of ΔS^0 , ΔH^0 , and ΔG^0 as demonstrated in table 5.10. The

positive value of ΔH^0 reveals an endothermic reaction associated with complexation, whereas the negative value of ΔG^0 represents the spontaneity of the reaction process. While the positive value of ΔS^0 suggests an entropy-driven coordination reaction, and it is a well-formed complex. These kinetic studies based on an investigation of the 4f–4f transition's absorption spectrum, could be used as an alternate method to scrutinize the reaction rates and for predicting potential thermodynamic behavior involved in the complexation of Pr(III):Leu:Mg(II).

5.6 CONCLUSION

The formation of the inner-sphere complexation during the interaction of Pr^{3+} with L-leucine in the presence/absence of Mg^{2+} was indicated by the marked variations in the values of P and T_λ . The significant changes in the values of T_4 and T_6 imply that the structure of the complex formed has changed. The rise in $b^{1/2}$ values and consistent decline in ζ_{4f} , E^k , and F_k values point to a possible interaction between the metal ion and the ligand. Adding the ligand to the pure praseodymium ion intensifies 4f-4f orbitals, thereby revealing the interaction of the metal with the ligand. This is validated by the intensity of absorption bands and the emergence of the redshifts. The drop in values of β indicates that the metal-ligand bond distance has been shortened. The lowering of the coordination number is indicated by the increase in absorption bands of the 4f-4f transition of Pr^{3+} . Out of the four solvents used, DMF has been proven to work best for complexation. For different pH (2, 4, 6), the mode of interaction of Pr(III) with L-leucine was found to increase with the rise in pH.

Analyses based on the intensity parameter values for complexation at different times and temperatures clearly showed that the rates increased proportionately with the rise in temperature and time. The incredibly lower activation energy (E_a) value suggests that Pr(III):Leu:Mg(II) complexation occurs spontaneously. While the +ve values of ΔH^0 suggest an involvement of the endothermic process in the complexation. The -ve value of ΔG^0 reflects the spontaneity of the reaction as well as the favorable nature of the reaction in the solution study. The current investigation of coordination reactions is discovered to be entropy-driven because $T\Delta S^0 > \Delta H^0$. Depending on the possibility of how frequently molecules collide, the frequency/pre-exponential (A) data demonstrates the empirical relations of the reaction rate and the temperature.

REFERENCES

- [1] S. Alghool, M.S. Zoromba, H.F.A. El-Halim, Lanthanide amino acid Schiff base complexes: Synthesis, spectroscopic characterization, physical properties and in vitro antimicrobial studies, *J. Rare Earths*. 31 (2013) 715–721. [https://doi.org/10.1016/S1002-0721\(12\)60347-0](https://doi.org/10.1016/S1002-0721(12)60347-0).
- [2] K. Niu, F. Yang, T. Gaudin, H. Ma, W. Fang, Theoretical Study of Effects of Solvents, Ligands, and Anions on Separation of Trivalent Lanthanides and Actinides, *Inorg. Chem.* 60 (2021) 9552–9562. <https://doi.org/10.1021/acs.inorgchem.1c00657>.
- [3] P. Soni, G. Pagare, S.P. Sanyal, A theoretical study of structural, elastic and thermal properties of heavy lanthanide monoantimonides, *J. Phys. Chem. Solids*. 71 (2010) 1491–1498. <https://doi.org/10.1016/j.jpcs.2010.07.014>.
- [4] C. Chen, H. Li, Synthesis and Crystal Structure of Amino Acid Modified NDI Lanthanide Coordination Complex, *Zeitschrift Fur Anorg. Und Allg. Chemie*. 645 (2019) 888–892. <https://doi.org/10.1002/zaac.201900009>.
- [5] K. Bernot, C. Daiguebonne, G. Calvez, Y. Suffren, O. Guillou, A Journey in Lanthanide Coordination Chemistry: From Evaporable Dimers to Magnetic Materials and Luminescent Devices, *Acc. Chem. Res.* 54 (2021) 427–440. <https://doi.org/10.1021/acs.accounts.0c00684>.
- [6] J.C.G. Bünzli, Review: Lanthanide coordination chemistry: From old concepts to coordination polymers, *J. Coord. Chem.* 67 (2014) 3706–3733. <https://doi.org/10.1080/00958972.2014.957201>.
- [7] S.A. Cotton, J.M. Harrowfield, Lanthanides: Coordination Chemistry, *Encycl. Inorg. Bioinorg. Chem.* (2012). <https://doi.org/10.1002/9781119951438.eibc2062>.
- [8] G. Lanza, Z. Varga, M. Kolonits, M. Hargittai, On the effect of 4f electrons on the structural characteristics of lanthanide trihalides: Computational and electron diffraction study of dysprosium trichloride, *J. Chem. Phys.* 128 (2008). <https://doi.org/10.1063/1.2828537>.
- [9] J.M. Han, S.J. Jeong, M.C. Park, G. Kim, N.H. Kwon, H.K. Kim, S.H. Ha, S.H. Ryu, S. Kim, Leucyl-tRNA synthetase is an intracellular leucine sensor for the mTORC1-signaling pathway, *Cell*. 149 (2012) 410–424. <https://doi.org/10.1016/j.cell.2012.02.044>.

- [10] N. Ranjana Devi, B. Huidrom, N. Rajmuhon Singh, Studies on the complexation of Pr(III) and Nd(III) with glycyl-glycine (gly-gly) using spectral analysis of 4f-4f transitions and potentiometric titrations, *Spectrochim. Acta - Part A Mol. Biomol. Spectrosc.* 96 (2012) 370–379. <https://doi.org/10.1016/j.saa.2012.05.038>.
- [11] Z. Thakro, M.T. Ao, C. Imsong, J. Sanchu, M. Ziekhru, M.I. Devi, Absorption spectral and thermodynamic analysis for the complexation of Pr 3 + with L-phenylalanine in the presence / absence of Mg 2 + using 4f – 4f transitions spectra as probe, *Eur. Phys. J. Plus.* 123 (2022) 1–10. <https://doi.org/10.1140/epjp/s13360-022-02765-w>.
- [12] K.K. Gangu, S. Maddila, S.N. Maddila, S.B. Jonnalagadda, Nanostructured samarium doped fluorapatites and their catalytic activity towards synthesis of 1,2,4-triazoles, *Molecules*. (2016). <https://doi.org/10.3390/molecules21101281>.
- [13] M.F. Bush, J. Oomens, R.J. Saykally, E.R. Williams, Effects of alkaline earth metal ion complexation on amino acid zwitterion stability: Results from infrared action spectroscopy, *J. Am. Chem. Soc.* (2008). <https://doi.org/10.1021/ja711343q>.
- [14] F. Costanzo, R.G. Della Valle, V. Barone, MD simulation of the Na+-phenylalanine complex in water: Competition between cation- π interaction and aqueous solvation, *J. Phys. Chem. B.* (2005). <https://doi.org/10.1021/jp055271g>.
- [15] M. Remko, D. Fitz, R. Broer, B.M. Rode, Effect of metal Ions (Ni 2+, Cu 2+ and Zn 2+) and water coordination on the structure of L-phenylalanine, L-tyrosine, L-tryptophan and their zwitterionic forms, *J. Mol. Model.* (2011). <https://doi.org/10.1007/s00894-011-1000-0>.
- [16] A.L. Sobolewski, D. Shemesh, W. Domcke, Computational studies of the photophysics of neutral and zwitterionic amino acids in an aqueous environment: Tyrosine-(H₂O)₂ and tryptophan-(H₂O)₂ clusters, *J. Phys. Chem. A.* (2009). <https://doi.org/10.1021/jp8091754>.
- [17] J.C.G. Bünzli, C. Piguet, Lanthanide-containing molecular and supramolecular polymetallic functional assemblies, *Chem. Rev.* (2002). <https://doi.org/10.1021/cr010299j>.
- [18] A.M. Măciucă, A.C. Munteanu, V. Uivarosi, Quinolone complexes with lanthanide ions: An insight into their analytical applications and biological activity, *Molecules*. (2020). <https://doi.org/10.3390/molecules25061347>.

- [19] Z. Ahmed, K. Iftikhar, Synthesis and visible light luminescence of mononuclear nine-coordinate lanthanide complexes with 2,4,6-tris(2-pyridyl)-1,3,5-triazine, *Inorg. Chem. Commun.* 13 (2010) 1253–1258. <https://doi.org/10.1016/j.inoche.2010.07.009>.
- [20] Y.F. Zhao, H. Bin Chu, F. Bai, D.Q. Gao, H.X. Zhang, Y.S. Zhou, X.Y. Wei, M.N. Shan, H.Y. Li, Y.L. Zhao, Synthesis, crystal structure, luminescent property and antibacterial activity of lanthanide ternary complexes with 2,4,6-tri(2-pyridyl)-s-triazine, *J. Organomet. Chem.* 716 (2012) 167–174. <https://doi.org/10.1016/j.jorganchem.2012.06.031>.
- [21] L. Sorace, C. Benelli, D. Gatteschi, Lanthanides in molecular magnetism: Old tools in a new field, *Chem. Soc. Rev.* 40 (2011) 3092–3104. <https://doi.org/10.1039/c0cs00185f>.
- [22] C. Sumitra, T.D. Singh, M.I. Devi, N.R. Singh, Absorption spectral studies of 4f-4f transitions for the complexation of Pr(III) and Nd(III) with glutathione reduced (GSH) in presence of Zn(II) in different aquated organic solvents and kinetics for the complexation of Pr(III):GSH with Zn(II), *J. Alloys Compd.* (2008). <https://doi.org/10.1016/j.jallcom.2007.04.153>.
- [23] C. Victory Devi, N. Rajmuhon Singh, Spectrophotometric study of kinetics and associated thermodynamics for the complexation of Pr(III) with L-proline in presence of Zn(II), *Arab. J. Chem.* 10 (2017) S2124–S2131. <https://doi.org/10.1016/j.arabjc.2013.07.044>.
- [24] A.A. Khan, H.A. Hussain, K. Iftikhar, 4f-4f absorption spectra and hypersensitivity in nine-coordinate Ho(III) and Er(III) complexes in different environments, *Spectrochim. Acta - Part A Mol. Biomol. Spectrosc.* (2004). <https://doi.org/10.1016/j.saa.2003.10.042>.
- [25] T. Moaienla, N. Bendangsenla, T. David Singh, C. Sumitra, N. Rajmuhon Singh, M. Indira Devi, Comparative 4f-4f absorption spectral study for the interactions of Nd(III) with some amino acids: Preliminary thermodynamics and kinetic studies of interaction of Nd(III):glycine with Ca(II), *Spectrochim. Acta - Part A Mol. Biomol. Spectrosc.* 87 (2012) 142–150. <https://doi.org/10.1016/j.saa.2011.11.028>.

CHAPTER 6

Absorption spectral study of Nd(III) with L-phenylalanine, L-methionine, L-leucine in presence/absence of Mg(II)

This chapter discusses the mechanism that takes place when the Nd(III) ion interacts with the essential amino acids (L-phenylalanine, L-methionine, and L-leucine) in the presence/absence of Mg^{2+} using the 4f-4f spectra of the lanthanide (Nd^{3+}) as a spectral and structural tool. The experiments were carried out in aquated organic solvents. The nature of the complexation was studied by the changes in the theoretically computed data of the energy interaction parameters [bonding parameters ($b^{1/2}$), percentage covalency (δ), Nephelauxetic ratio (β), Slater-Condon (F_k), Racah energy (E^k), and Spin-orbit interaction (ζ_{4f})].

The text of this chapter has been communicated as:

Absorption spectral study of Nd(III) with selected amino acids in presence/absence of Mg(II): 4f-4f transition as a probe

Zevivonü Thakro^a, M. Indira Devi^{a*}

^aDepartment of Chemistry, Nagaland University, Lumami, Nagaland, India

*E-mail- cam_indira@yahoo.co.in

6.1 INTRODUCTION

The strength of the metal-ligand bond, coordination geometry, shape of the complex produced, and interaction of chelate-solvent can be determined by the lanthanide ion absorption spectra for $4f-4f$ transitions [1]. The chemistry of lanthanides, particularly in solutions can provide insight into complexes with intricate f -electron transitions, and sensitivity of lanthanide to the complex's shape and coordination environment has made it a viable tool for investigating the chemistry of lanthanides [2–4].

The hypersensitive transitions show a high level of sensitivity when their coordination environment is changed. They adhere to the selection rules, $\Delta S = 0$, $\Delta L \leq 2$ and $\Delta J \leq 2$, so that band intensities grow when the metal ion forms complexes with the ligands [5]. The $4f-4f$ transitions are located deep inside the metal's core-shell and are often not affected by the alteration in their coordination region, thereby making them a non-hypersensitive transition [6].

Studies have shown that several Nd^{3+} transition intensities do not adhere to the selection rule, but they can still be very sensitive to even the slightest changes in their coordinating environment. Such transitions are commonly referred to as Ligand Mediated Pseudohypersensitive transitions [7,8]. A large number of absorption studies have employed these pseudohypersensitive transitions for a better understanding of the ligand and Nd^{3+} interactions, as well as their structural conformations in solution [9,10]. The increased intensity of pseudo-hypersensitive transitions vividly could demonstrate Nd^{3+} -ligand interaction and consequently the effect of their sensitivity on complex formation.

There are 13 energy levels involved in the absorption in the UV-vis and near-infrared areas that results from the prohibited transitions inside the $4f$ -orbitals of Nd(III). Out of that 13 energy levels, five bands, with wavelengths spanning from 400 to 900 nm, that are related to $^4I_{9/2} \rightarrow ^4G_{7/2}$, $^4I_{9/2} \rightarrow ^4G_{5/2}$, $^4I_{9/2} \rightarrow ^4F_{7/2}$, $^4I_{9/2} \rightarrow ^4F_{5/2}$, and $^4I_{9/2} \rightarrow ^4F_{3/2}$ transitions have been taken into consideration. Except in a few cases, adding ligand to Nd(III) ion in the absence or presence of Mg(II) has no effect on the structure of the bands. These bands are also sharp and narrow, and they resemble those of free ions greatly due to the weak crystal field splitting. Generally, the coordinating surroundings have little influence on the lanthanide ion's $4f-4f$ transition intensities. Out of the five bands, the $^4I_{9/2} \rightarrow ^4G_{5/2}$ transition of Nd(III) is most susceptible to environmental changes out of the five bands. This transition adhere to the selection requirements and is known as hypersensitive transition [11,12]. However, the nonhypersensitive transitions such as $^4I_{9/2} \rightarrow ^4G_{7/2}$, $^4I_{9/2} \rightarrow ^4F_{7/2}$, $^4I_{9/2} \rightarrow ^4F_{5/2}$, and $^4I_{9/2} \rightarrow ^4F_{3/2}$ that do not follow the selection rules are also known to exhibit significant sensitivity in the presence of ligands and variations in their coordinating environment. Such transitions have been termed Pseudo-hypersensitive transitions [8].

The increase in the use of lanthanide as a probe is due to the similarities and the ability of the lanthanide to replace Ca^{2+} ions in a distinct and isomorphous form [13,14]. Because the ionic radii of calcium and lanthanide ions are comparable, lanthanide ions can be employed as a probe to evaluate the coordination characteristics of calcium ions in biomolecular systems. Additionally, the existence of several spectroscopic indications from $4f$ -electron transitions in lanthanide ions facilitates the electrochemical investigation of these compounds. The spectral analysis of $4f-4f$ transitions can provide insight into the structure of a lanthanide complex.

6.2 METAL COMPLEXES OF LANTHANIDE WITH AMINO ACIDS

The pH levels have an impact on the way the ligand binds to the metal; for instance, in an acidic media, only the oxygen atom bonds to the metal, but in a basic medium, both the nitrogen and oxygen atoms are bonded to the metal [15]. Lanthanides are categorized as class A/hard acceptors, and hence prefer to bind with the hard donor sites of the ligand (in the order $O > N > S$ and $F > Cl$) for complex formation [16].

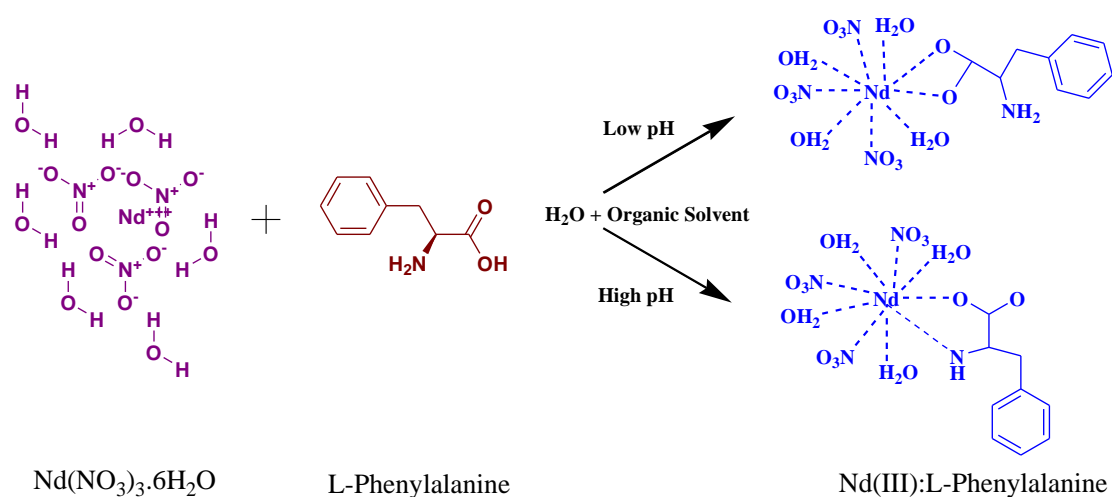


Fig 6.1: Possible interaction between Nd^{3+} and L-phenylalanine in different pH media.

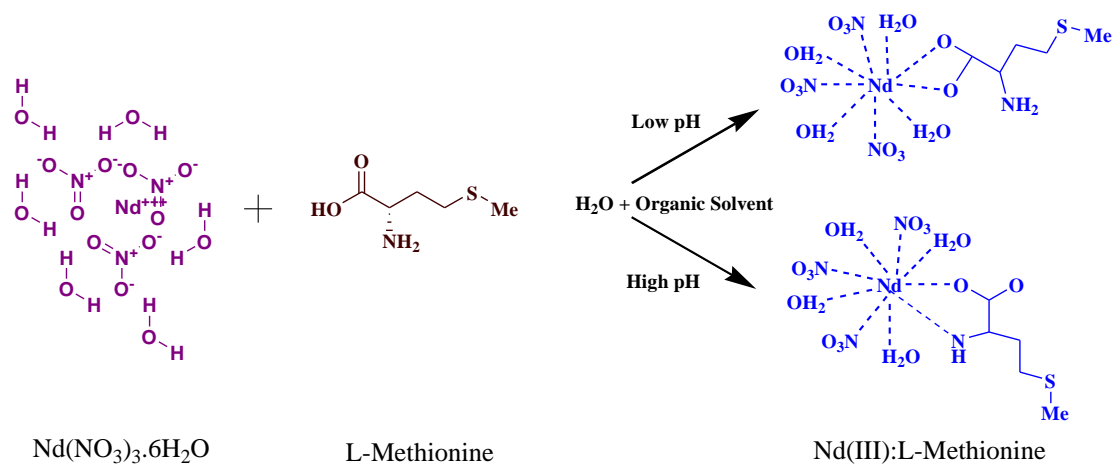


Fig 6.2: Possible interaction between Nd^{3+} and L-methionine in different pH media.

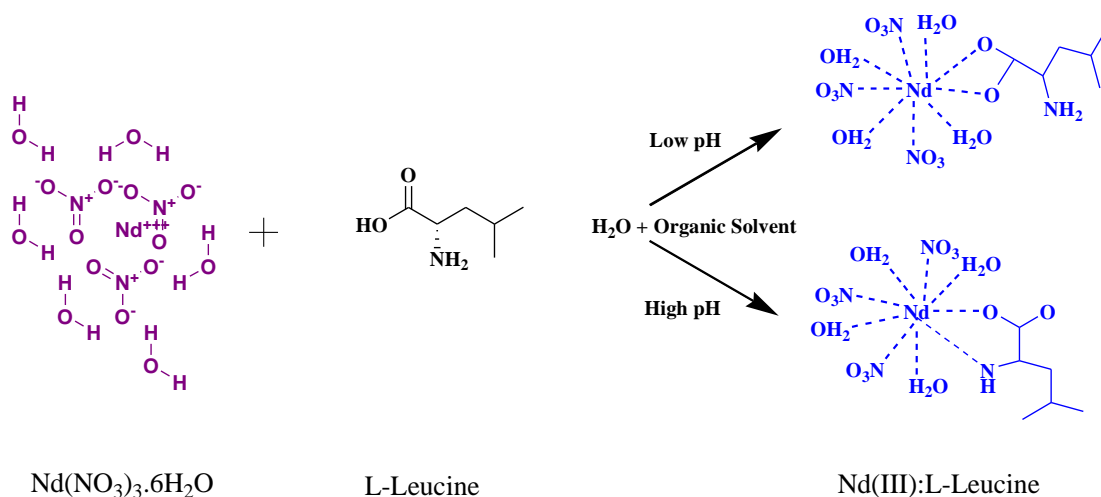


Fig 6.3: Possible interaction between Nd^{3+} and L-leucine in different pH media.

The current study uses the $4f-4f$ transition spectra of Nd^{3+} as a probe to analyze the interaction of Nd(III) ion with three essential amino acids (L-Phenylalanine, L-methionine, and L-Leucine) in the presence/absence of Mg(II) in various aquated solvents: CH_3CN , DMF, $\text{C}_4\text{H}_8\text{O}_2$, and CH_3OH . The nature of the complexation of metal with the ligands was studied by the changes in the theoretically computed data of the energy interaction parameters: percentage covalency (δ), bonding parameter ($b^{1/2}$), Nephelauxetic ratio (β), Spin-orbit interaction (ζ_{4f}), Racah energy (E_k), and Slater-Condon (F_k).

6.3 EXPERIMENTAL SECTION

6.3.1 Materials and Methods

A 99.9% purity of Neodymium(III)nitrate hexahydrate $[\text{Nd}(\text{NO}_3)_3 \cdot 6\text{H}_2\text{O}]$ was purchased from Sigma-Aldrich; the amino acids (L-phenylalanine, L-methionine, and L-leucine) and Magnesium nitrate hexahydrate $[\text{Mg}(\text{NO}_3)_2 \cdot 6\text{H}_2\text{O}]$ of 97.0% purity from HiMedia. The solvents: Dimethylformamide ($\text{C}_3\text{H}_7\text{NO}$), Methanol (CH_3OH),

Dioxane (C₄H₈O₂), and Acetonitrile (CH₃CN) used were purchased from HiMedia with 99.5% purity.

For the absorption analysis, the concentration of the solution used for the Nd³⁺ and its complexes was kept at 5×10⁻³M. The binary mixtures of water with the organic solvents were maintained at 50% v/v. The UV-visible spectra were recorded using Perkin Elmer Lambda 365 UV/Vis spectrometer.

6.4 CALCULATIONS

The energy interaction parameters: Lande spin-orbit interaction (ζ_{4f}), Racah (E^k), Slater-Condon factor (F_k), bonding parameter ($b^{1/2}$), per-cent covalency (δ), and nephelauxetic ratio (β), were used extensively to analyze the nature of complexation of Nd³⁺ with the ligands.

The following equations are used for the calculations of different parameters. The details of the calculations have been discussed in chapter 2.

Nephelauxetic ratio ' β '

$$\beta = \frac{F_K^C}{F_K^f} \text{ or } \frac{E_C^K}{E_f^K} \quad (1)$$

Slater-Condon ' F_k ' and Lande spin-orbit parameters ' ξ_{4f} '

$$F_k = F_k^0 + \Delta F_k \quad (2)$$

$$\xi_{4f} = \xi_{4f}^0 + \Delta \xi_{4f} \quad (3)$$

Racah parameter

$$E^1 = \frac{70F_2 + 231F_4 + 20.02F_6}{9} \quad (4)$$

$$E^2 = \frac{F_2 - 3F_4 + 7F_6}{9} \quad (5)$$

$$E^3 = \frac{5F_2 + 6F_4 - 9F_6}{9} \quad (6)$$

Bonding parameter ($b^{1/2}$) and covalent percentage (δ)

$$b^{1/2} = \left[\frac{1-\beta}{2} \right]^{1/2} \quad (7)$$

$$\delta = \left[\frac{1-\beta}{\beta} \right] \times 100 \quad (8)$$

6.5 RESULTS AND DISCUSSIONS

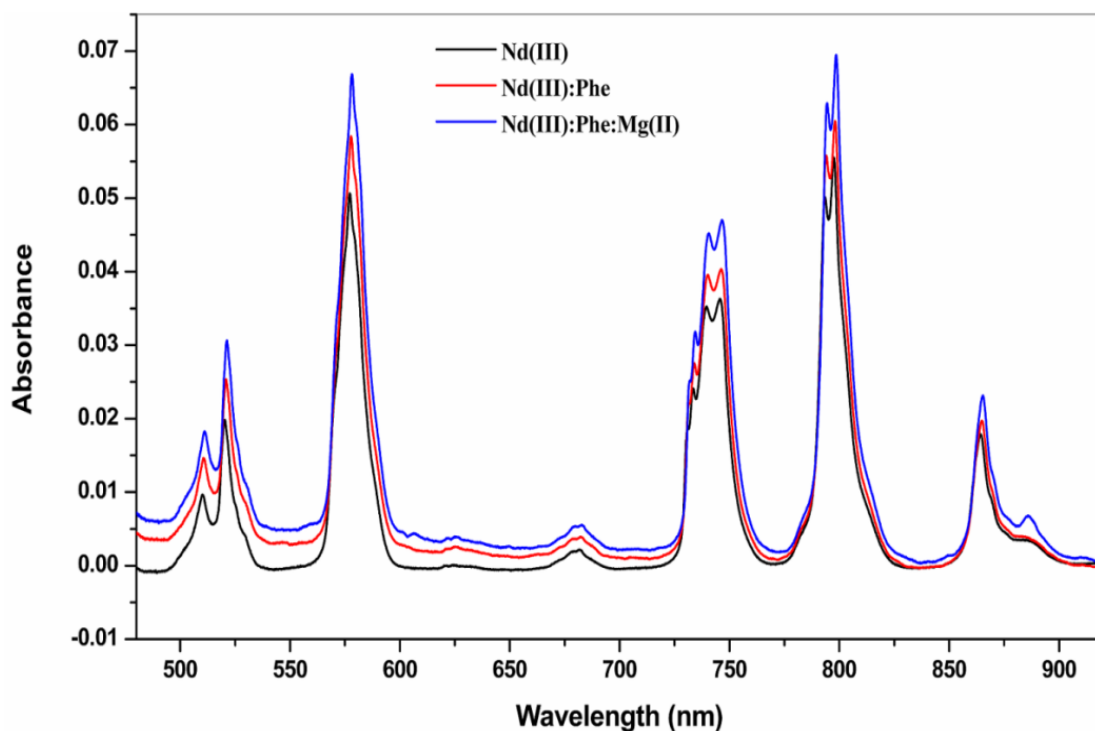


Fig. 6.4: UV-vis absorption spectra of the $4f-4f$ electronic transitions of Nd^{3+} , Nd(III):Phe and $\text{Nd(III):Phe:Mg(II)}$ complexes in DMF:Water (50% v/v) solvent.

Table 6.1: Computed value of energy interaction parameters Slater-Condon F_K (cm^{-1}), Spin-Orbit Interaction ξ_{4f} (cm^{-1}), Nephelauxetic ratio (β), bonding ($b^{1/2}$), and covalency (δ) parameters of Nd(III) free ion, Nd(III) with L-phenylalanine in the presence and absent of Mg^{2+} .

Methanol: Water				Dioxane: Water			ACN: Water			DMF: Water			
Nd(III):Phe:Mg(II)	Nd(III):Phe	Nd(III)	Nd(III):Phe:Mg(II)	Nd(III):Phe	Nd(III)	Nd(III)	Nd(III):Phe:Mg	Nd(III):Phe	Nd(III)	Nd(III):Phe:Mg(II)	Nd(III):Phe	Nd(III)	
331.987	332.274	332.357	331.424	331.643	332.280	330.920	331.021	331.021	332.632	330.998	331.246	332.535	F_2
45.830	45.870	45.882	45.753	45.783	45.871	45.683	45.697	45.697	45.943	45.694	45.728	45.905	F_4
5.013	5.017	5.018	5.004	5.007	5.017	4.996	4.998	4.998	5.092	4.998	5.001	5.021	F_6
901.636	903.252	904.034	901.211	901.608	904.026	894.398	899.647	899.647	910.716	820.262	898.604	908.123	ξ_{4f}
3769.599	3772.865	3773.806	3763.205	3765.700	3772.932	3757.48	3758.63	3758.63	3784.21	3758.368	3761.18	3775.81	E^1
25.509	25.531	25.538	25.466	25.483	25.532	25.427	25.435	25.435	25.565	25.433	25.456	25.556	E^2
660.012	660.584	660.749	658.893	659.330	660.596	657.891	658.093	658.093	660.618	658.0464	658.540	661.101	E^3
0.981	0.983	0.983	0.980	0.981	0.983	0.976	0.979	0.979	0.984	0.935	0.979	0.986	β
0.095	0.091	0.090	0.098	0.096	0.090	0.109	0.101	0.101	0.087	0.179	0.104	0.083	$b^{1/2}$
1.855	1.719	1.662	1.965	1.909	1.674	2.434	2.116	2.116	1.441	2.902	2.142	1.403	δ

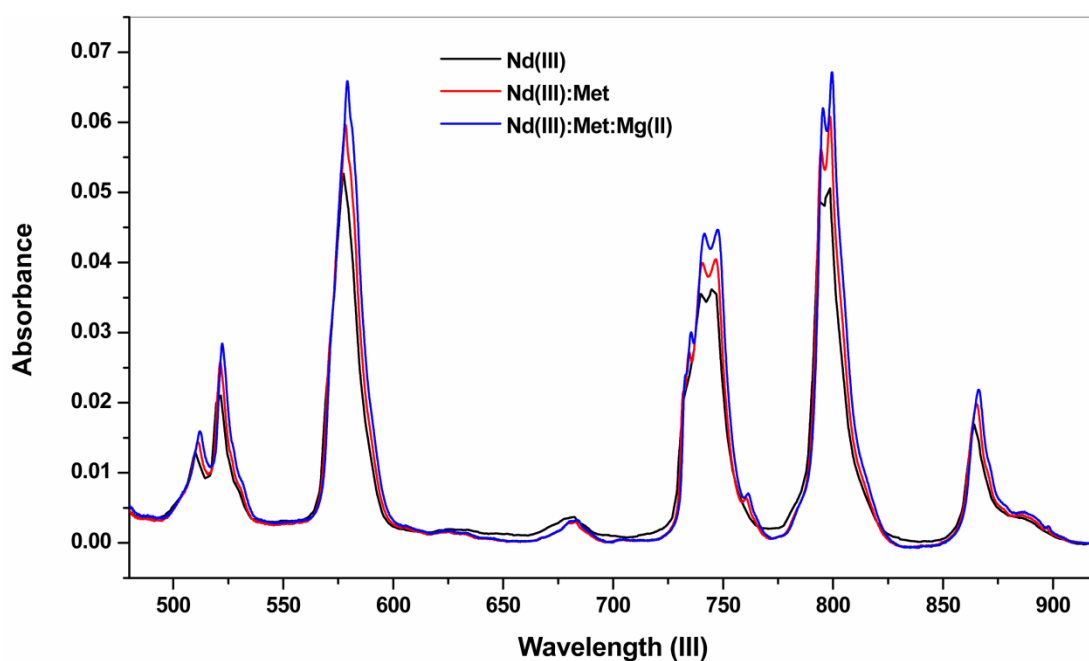


Fig. 6.5: UV-vis absorption spectra of the $4f-4f$ electronic transitions of Nd³⁺, Nd(III):Met and Nd(III):Met:Mg(II) complexes in ACN:Water(50% v/v) solvent.

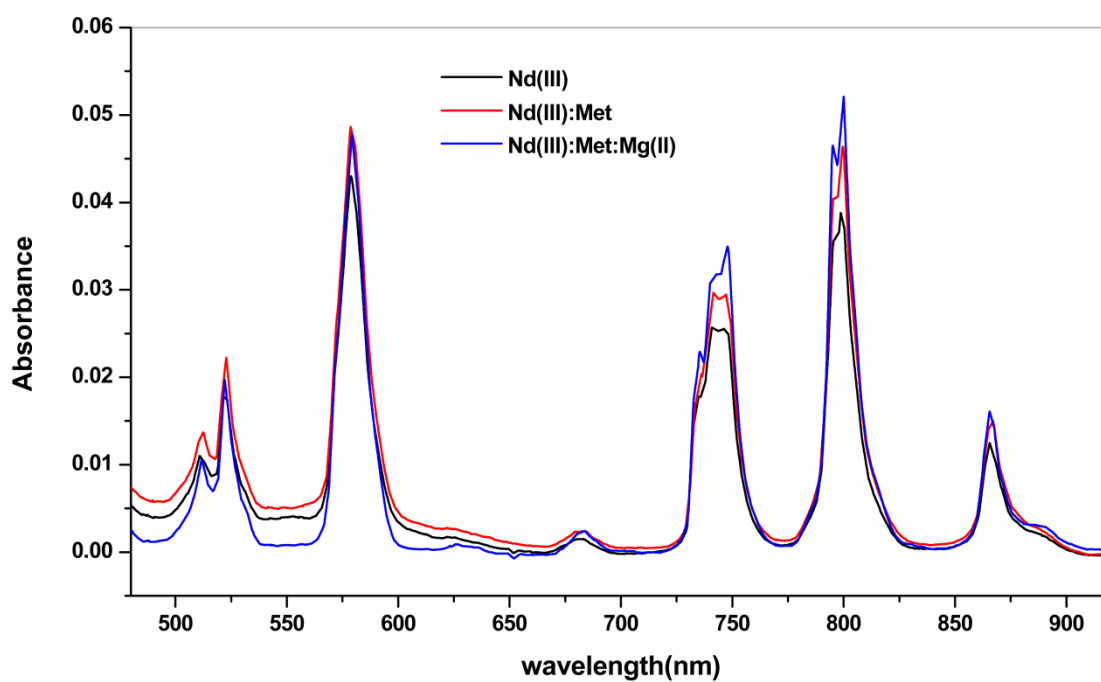


Fig. 6.6: UV-vis absorption spectra of the $4f-4f$ electronic transitions of Nd³⁺, Nd(III):Met and Nd(III):Met:Mg(II) complexes in Dioxane:Water(50% v/v) solvent.

Table 6.2: Computed value of energy interaction parameters Slater-Condon F_K (cm^{-1}), Spin-Orbit Interaction ξ_{4f} (cm^{-1}), Nephelauxetic ratio (β), bonding ($b^{1/2}$), and covalency (δ) parameters of Nd(III) free ion, Nd(III) with L-methionine in the presence and absent of Mg^{2+} .

Methanol:Water			Dioxane:Water			ACN:Water			DMF:Water			
Nd(III):M et:Mg(II)	Nd(III): Met	Nd(III)	Nd(III):M et:Mg(II)	Nd(III): Met	Nd(III)	Nd(III):M et:Mg(II)	Nd(III): Met	Nd(III)	Nd(III):Me t:Mg(II)	Nd(III): Met	Nd(III)	
331.790	331.967	332.357	331.67	331.191	332.280	331.686	331.989	332.632	330.535	331.171	332.535	F_2
45.803	45.828	45.882	45.828	45.721	45.871	45.789	45.831	45.943	45.630	45.718	45.906	F_4
5.010	5.012	5.018	5.012	5.001	5.017	5.008	5.013	5.092	4.991	5.000	5.021	F_6
901.827	900.518	904.034	900.518	902.697	904.026	899.938	901.341	910.716	893.340	898.575	908.12	ξ_{4f}
3767.360	3769.37	3773.80	3769.374	3760.56	3772.932	3766.181	3769.625	3784.21	3753.114	3760.34	3775.81	E^1
25.494	25.508	25.538	25.508	25.448	25.532	25.486	25.509	25.565	25.398	25.446	25.551	E^2
659.620	659.973	660.749	659.973	658.430	660.596	659.414	660.017	660.618	657.1264	658.391	661.101	E^3
0.981	0.981	0.983	0.981	0.981	0.983	0.980	0.981	0.984	0.975	0.978	0.986	β
0.095	0.097	0.090	0.097	0.096	0.090	0.099	0.095	0.087	0.111	0.102	0.083	$b^{1/2}$
1.874	1.922	1.662	1.922	1.915	1.674	1.998	1.872	1.441	2.555	2.155	1.403	δ

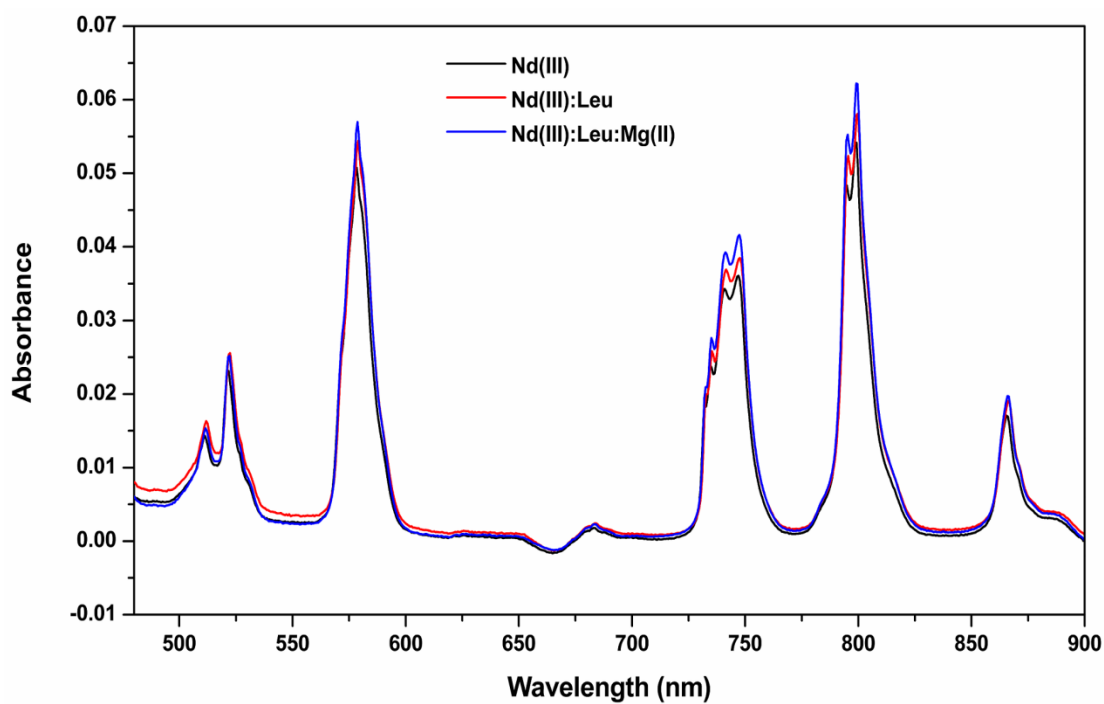


Fig. 6.7: UV-vis absorption spectra of the $4f-4f$ electronic transitions of Nd³⁺, Nd(III):Leu and Nd(III):Leu:Mg(II) complexes in DMF:Water (50% v/v) solvent.

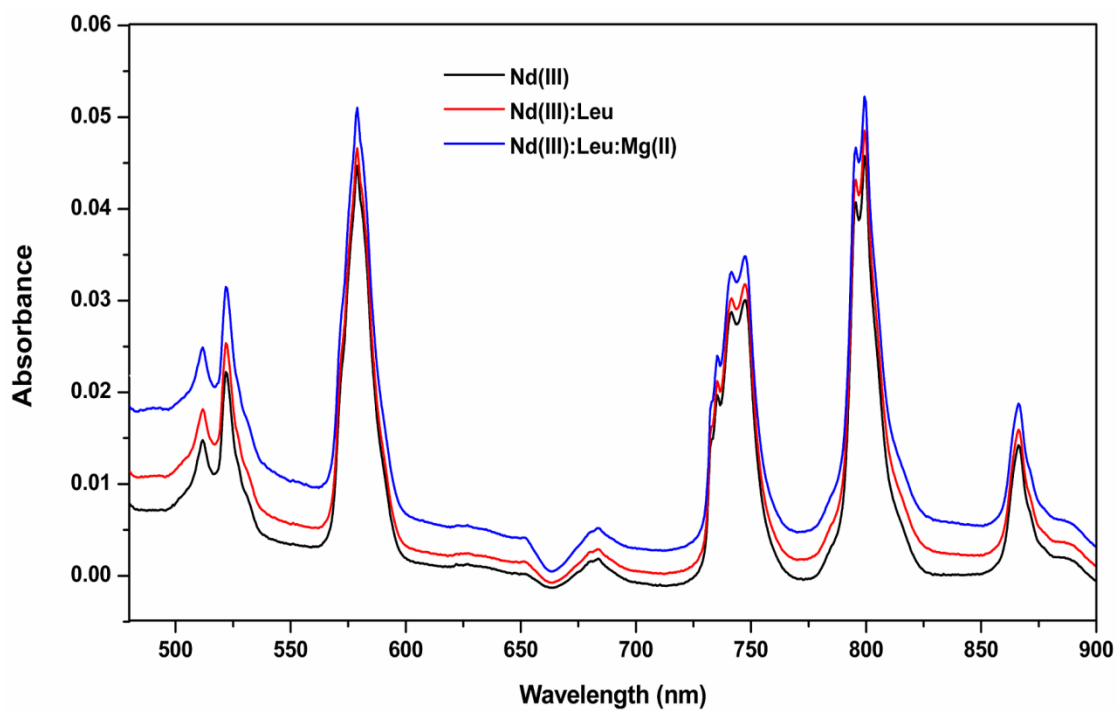


Fig. 6.8: UV-vis absorption spectra of the $4f-4f$ electronic transitions of Nd³⁺, Nd(III):Leu and Nd(III):Leu:Mg(II) complexes in Methanol:Water (50% v/v) solvent.

Table 6.3: Computed value of energy interaction parameters Slater-Condon $F_K(\text{cm}^{-1})$, Spin Orbit Interaction $\xi_{4f}(\text{cm}^{-1})$, Nephelauxetic ratio (β), bonding ($b_{1/2}$), and covalency (δ) parameters of Nd(III) free ion, Nd(III) with L-leucine in presence and absent of Mg^{2+} .

Methanol: Water			Dioxane: Water			ACN: Water			DMF: Water			
Nd(III):M et:Mg(II)	Nd(III): Met	Nd(III)	Nd(III):M et:Mg(II)	Nd(III) :Met	Nd(III)	Nd(III):M et:Mg(II)	Nd(III): Met	Nd(III)	Nd(III):Me t:Mg(II)	Nd(III): Met	Nd(III)	
331.8128	331.989	332.357	331.6725	331.86	332.63	331.3650	331.6051	332.2808	330.5282	330.980	332.53	F_2
45.8068	45.8311	45.8820	45.7874	45.813	45.943	45.7449	45.7781	45.8714	45.6294	45.6919	45.9065	F_4
5.0104	5.0130	5.0186	5.0083	5.0111	5.0925	5.0036	5.0072	5.0174	4.9910	4.9978	5.0213	F_6
902.2215	902.893	904.034	898.5182	901.00	910.71	901.9641	902.3056	904.0265	895.074	899.20	908.12	ξ_{4f}
3767.618	3769.61	3773.80	3766.024	3768.1	3784.2	3762.5339	3765.2599	3772.9322	3753.032	3758.16	3775.82	E^1
25.4961	25.5097	25.5380	25.4853	25.499	25.565	25.4617	25.4802	25.5321	25.3974	25.4322	25.5516	E^2
659.666	660.016	660.749	659.3869	659.76	660.61	658.77574	659.25304	660.596379	657.1121	658.011	661.10	E^3
0.9818	0.9825	0.9836	0.9796	0.9812	0.9848	0.9811	0.9816	0.9835	0.9760	0.9790	0.986	β
0.0953	0.0936	0.0904	0.1010	0.0968	0.0871	0.0973	0.0959	0.0908	0.1095	0.1025	0.083	$b^{1/2}$
1.8486	1.7835	1.6626	2.0823	1.9109	1.4418	1.9311	1.8752	1.6747	2.4557	2.1482	1.4033	δ

Hypersensitive or pseudo-hypersensitive transitions, energy, and intensity are all related to the coordination number and may be used as a diagnostic to determine the lanthanide's coordinating sphere [17]. The variation of the band intensities is interpreted as the increase in the probability of interaction between ligand and the $4f$ -orbital of metal ions [18]. Figures 6.4, 6.5, 6.6, 6.7, and 6.8 shows the comparative UV-vis spectra of Nd(III), Nd(III):AA (AA = Amino acids), and Nd(III):AA:Mg(II) in various aquated organic solvents. From the figures, it is clearly evident that the absorption intensity of the various transition bands increases upon the addition of Amino acids (l-phenylalanine, L-methionine, and L-leucine) to Nd(III) which is further enhanced when Mg(II) is introduced to the complex system. This can be an indication that the ligand and Nd(III) ion are interacting. Additionally, a redshift is seen; this redshift can be attributed to the metal ion orbital expanding during complexation which leads to a reduction in interelectronic repulsion and, as a result, shortens the atomic radii of the core metal ion and the ligand, producing the nephelauxetic effect.

The variations in the transition bands of Nd(III) on complexation have been investigated by evaluating its energy interaction parameters; Slater Condon (F_k), Racah (E^k), Lande (ζ_{4f}), nephelauxetic ratio (β), bonding ($b^{1/2}$) and covalency(δ) parameters. Tables 6.1, 6.2, and 6.3 lists the energy interaction parameters of Nd(III) ion and its complexes with l-phenylalanine, L-methionine, L-leucine, and Mg(II) in a different aquated solvent. The tables show that the nature of the solvent and the complex system has a significant effect on the f - f transitions of Neodymium. When amino acids and Mg(II) are gradually introduced to Nd(III) system, we can see that the values of the Slater Condon (F_k), spin-orbit interaction Racah (E^k), as well as the

Lande (ζ_{4f}) (inter-electronic repulsion parameters) decreases. This occurs as a result of the coordination of amino acids and Mg(II) to Nd(III) during its complexation, which causes the metal orbital to increase. The decreasing values of the inter-electronic interaction parameters imply that the orbital size of Nd(III) is greater after complexation due to significantly less electrostatic repulsion between the two electrons of the doubly occupied metal orbital.

The subsequent increase of bonding ($b^{1/2}$) and covalency(δ) parameter values on going from Nd(III) to Nd(III):AA and Nd(III):AA:Mg(II) indicates shortening of the Ln(III)-ligand bond distance due to stronger binding of Nd(III) with amino acids and Mg(II) as well as the covalent bonding nature of the Nd(III) complexes. The effect of the electron cloud expansion can be explained in one of two ways: either any negative charge on the ligands reduces the effective positive charge on the lanthanide metal, allowing the f -orbitals to slightly expand; or the orbitals' size is increased by the overlap of the metal orbital with the ligand orbital and the formation of covalent bonds. These alterations indicate a binding interaction between the Nd(III) ion and the amino acids and Mg(II) ions in the solution. In all the systems, the values of the bonding parameters are found to be positive and the values for the Nephelauxetic effect (β) were found to be less than unity, this implies the possibility of the formation of covalent bonds in the complexation of Nd(III) with the selected essential Amino acids. The decreased value of β explains the expansion of the orbital of the central metal ion thereby shortening the distance between the metal and the ligand known as the nephelauxetic effect.

From the computed data of energy interaction parameters (F_k , ζ_{4f} , E^k , β , $b^{1/2}$ & δ) shown in tables 6.1, 6.2, & 6.3 respectively, the variations in the energy parameters of the various $4f$ - $4f$ transition bands predict the possibility of the increase in the interaction between $4f$ orbitals of Nd^{3+} with that of the ligand. The significant variations in the interaction energy in the aquated DMF solvent imply that there is a stronger influence of solvent over Nd^{3+} to form a complex with the ligand. This shows that DMF is the better solvent compared to the others in the formation of the complex of Nd^{3+} with the amino acids. On comparing the obtained computed data, it was observed that the maximum values of $b^{1/2}$ and δ parameters are observed in the DMF:H₂O (50% v/v) system, this indicates the preference for covalent bond formation in DMF solvent which may be due to the presence of N-donor. This is probably due to the stronger oxygen-donating capacity of DMF, which allows it to enter the coordination sphere of Nd(III) by replacing one of the water groups. The sensitivity of the organic solvents is in the order of DMF>CH₃CN>C₄H₈O₂>CH₃OH.

6.6 CONCLUSION

From the present work, it can be concluded that the energy interaction parameter values for Nd^{3+} and Nd in its complexes [Nd(III):AA and Nd(III):AA:Mg(II)] vary in different solvents and the heterobimetallic complex Nd(III):AA:Mg(II) is more stable than Nd(III):AA. The nature of binding in the complex is found to be covalent and DMF is found to be the most effective solvent for the interaction. DMF has a greater influence on the energies of the $4f$ - $4f$ transitions out of the four tested solvents

REFERENCES

- [1] C. Sumitra, T.D. Singh, M.I. Devi, N.R. Singh, Absorption spectral studies of 4f-4f transitions for the complexation of Pr(III) and Nd(III) with glutathione reduced (GSH) in presence of Zn(II) in different aquated organic solvents and kinetics for the complexation of Pr(III):GSH with Zn(II), *J. Alloys Compd.* 451 (2008) 365-371. <https://doi.org/10.1016/j.jallcom.2007.04.153>.
- [2] Z. Ahmed, K. Iftikhar, Synthesis and visible light luminescence of mononuclear nine-coordinate lanthanide complexes with 2,4,6-tris(2-pyridyl)-1,3,5-triazine, *Inorg. Chem. Commun.* 13 (2010) 1253–1258. <https://doi.org/10.1016/j.inoche.2010.07.009>.
- [3] Y.F. Zhao, H. Bin Chu, F. Bai, D.Q. Gao, H.X. Zhang, Y.S. Zhou, X.Y. Wei, M.N. Shan, H.Y. Li, Y.L. Zhao, Synthesis, crystal structure, luminescent property and antibacterial activity of lanthanide ternary complexes with 2,4,6-tri(2-pyridyl)-s-triazine, *J. Organomet. Chem.* 716 (2012) 167–174. <https://doi.org/10.1016/j.jorganchem.2012.06.031>.
- [4] L. Sorace, C. Benelli, D. Gatteschi, Lanthanides in molecular magnetism: Old tools in a new field, *Chem. Soc. Rev.* 40 (2011) 3092–3104. <https://doi.org/10.1039/c0cs00185f>.
- [5] T. Moaienla, N. Bendangsenla, T. David Singh, C. Sumitra, N. Rajmuhon Singh, M. Indira Devi, Comparative 4f-4f absorption spectral study for the interactions of Nd(III) with some amino acids: Preliminary thermodynamics and kinetic studies of interaction of Nd(III):glycine with Ca(II), *Spectrochim. Acta - Part A Mol. Biomol. Spectrosc.* 87 (2012) 142–150. <https://doi.org/10.1016/j.saa.2011.11.028>.
- [6] N. Bendangsenla, T. Moaienla, T. David Singh, C. Sumitra, N. Rajmuhon Singh, M. Indira Devi, Evaluation of intensity and energy interaction parameters for the complexation of Pr(III) with selected nucleoside and nucleotide through absorption spectral studies, *Spectrochim. Acta - Part A Mol. Biomol. Spectrosc.* 103 (2013) 160–166. <https://doi.org/10.1016/j.saa.2012.11.011>.
- [7] M.S. N., S.S. O, Absorption Spectra of Lanthanide Complexes in Solution, *Appl. Spectrosc. Rev.* 26 (1991) 151–202. <https://doi.org/10.1080/05704929108050880>.
- [8] S.N. Misra, K. John, Difference and Comparative Absorption Spectra and Ligand Mediated Pseudohypersensitivity for 4f-4f Transitions of Pr (III) and Nd (III) Difference and Comparative Absorption Spectra and Ligand Mediated Pseudo hypersensi tivi ty for 4f-4f Transitions o, 4928 (2016) 285-325. <https://doi.org/10.1080/05704929308018115>.

- [9] N. Bendangsenla, T. Moaienla, T. David Singh, C. Sumitra, N. Rajmuhon Singh, M. Indira Devi, Evaluation of intensity and energy interaction parameters for the complexation of Pr(III) with selected nucleoside and nucleotide through absorption spectral studies, *Spectrochim. Acta - Part A Mol. Biomol. Spectrosc.* 103 (2013) 160–166. <https://doi.org/10.1016/j.saa.2012.11.011>.
- [10] N. Ranjana Devi, B. Huidrom, N. Rajmuhon Singh, Studies on the complexation of Pr(III) and Nd(III) with glycyl-glycine (gly-gly) using spectral analysis of 4f-4f transitions and potentiometric titrations, *Spectrochim. Acta - Part A Mol. Biomol. Spectrosc.* 96 (2012) 370–379. <https://doi.org/10.1016/j.saa.2012.05.038>.
- [11] H. Debecca Devi, C. Sumitra, T. David Singh, N. Yaiphaba, N. Mohondas Singh, N. Rajmuhon Singh, Calculation and Comparison of Energy Interaction and Intensity Parameters for the Interaction of Nd(III) with DL-Valine, DL-Alanine and β -Alanine in Presence and Absence of Ca^{2+} / Zn^{2+} in Aqueous and Different Aquated Organic Solvents, *Int. J. Spectrosc.* 2009 (2009) 1–9. <https://doi.org/10.1155/2009/784305>.
- [12] K.B. C. Gorller-Walrand, Spectral intensities of f-f transitions in Handbook on the Physics and Chemistry of Rare Earths edited by K.A. Gscheneidner Jr. and L. Eyring (North Holland, Amsterdam, 1998), *Handb. Phys. Chem. Rare Earths.* 25 (1998) 101–264.
- [13] T.D. Singh, C. Sumitra, N. Yaiphaba, H.D. Devi, M.I. Devi, N.R. Singh, Comparison of energy interaction parameters for the complexation of Pr(III) with glutathione reduced (GSH) in absence and presence of Zn(II) in aqueous and aquated organic solvents using 4f-4f transition spectra as PROBE, *Spectrochim. Acta - Part A Mol. Biomol. Spectrosc.* 61 (2005) 1219–1225. <https://doi.org/10.1016/j.saa.2004.06.044>.
- [14] S.N. Misra, G. Ramchandriah, M.A. Gagnani, R.S. Shukla, M.I. Devi, Absorption spectral studies involving 4f-4f transitions as structural probe in chemical and biochemical reactions and compositional dependence of intensity parameters, *Appl. Spectrosc. Rev.* (2003). <https://doi.org/10.1081/ASR-120026330>.
- [15] J.C.G. Bünzli, C. Piguet, Lanthanide-containing molecular and supramolecular polymetallic functional assemblies, *Chem. Rev.* (2002). <https://doi.org/10.1021/cr010299j>.
- [16] S.N. Misra, M.I. Devi, The synthesis and determination of the octacoordinated structure of Pr(III) and Nd(III) complexes with β -diketones and diols in non aqueous solutions: Evidence of some participation of π -electron density of diols with Pr(III) and Nd(III) in complexation, *Spectrochim. Acta - Part A Mol.*

- Biomol. Spectrosc. (1997). [https://doi.org/10.1016/S1386-1425\(97\)00064-4](https://doi.org/10.1016/S1386-1425(97)00064-4).
- [17] G.R. Choppin, A. Introduction, C. Theories, Coordinatiqn Chemistzy, 18 (1976).
- [18] C. Victory Devi, N. Rajmuhon Singh, Spectrophotometric study of kinetics and associated thermodynamics for the complexation of Pr(III) with L-proline in presence of Zn(II), Arab. J. Chem. 10 (2017) S2124–S2131. <https://doi.org/10.1016/j.arabjc.2013.07.044>.

APPENDIX-I

PLAGIARISM REPORT



नागालैण्ड विश्वविद्यालय NAGALAND UNIVERSITY

(केंद्रीय विश्वविद्यालय) / (A Central University)

मुख्यालय : लुमामी, जिला : जुन्हेबोटो (नागालैण्ड) – 798 627

Hqrs: Lumami, Dist: Zunheboto, Nagaland – 798 627

Department of Chemistry

Ph.D Thesis Certificate on Plagiarism check

Name of the research scholar	Zevivonü Thakro
Ph.D registration number	787/2017
Title of Ph.D thesis	Spectral analysis of lanthanide complexes with essential amino acids: kinetic and thermodynamic approach
Name & institutional address of the supervisor	Prof. M. Indira Devi Department of Chemistry Nagaland University, Lumami
Name of the department and school	Department of Chemistry, School of Sciences
Date of submission	19/12/2022
Date of plagiarism check	19/12/2022
Percentage of similarity detected by the URKUND software	4%

I hereby declare that/certify that the Ph.D thesis submitted by me is complete in all respect as per the guidelines of Nagaland University (NU) for this purpose. I also certify that the thesis (soft copy) has been checked for plagiarism using URKUND similarity check software. It is also certified that the contents of the electronic version of the thesis are the same as the final hard copy of the thesis. Copy of the report generated by the URKUND software is also enclosed.

Place:

(Name & signature of the Scholar)

Date:

Prof. Mayanglambam Indira Devi
19/12/2022

Name & signature of the Supervisor:

APPENDIX-II

WORKSHOP AND SEMINARS ATTENDED

Workshop and Seminars attended

- Poster presentation at National seminar on Chemistry in interdisciplinary research, organised by Department of Chemistry, Nagaland university, March 16th -17th 2017
- Attended a short term course on “Analytical techniques for physical, Chemical and Bioinspired materials” organised by Department of science and humanities, NIT Nagaland, Chümoukedima, Dimapur, July 23rd-27th 2018
- Oral presentation at National seminar on Bio-resource exploration and utilization: Application in modern biology organised by BIF, Nagaland university, October 9th-10th 2018
- Attended the DBT sponsord national workshop on “Newer frontiers in bioinformatics and research methodology”, organised by BIF centre, Nagaland University, Lumami, October 13thto 19th 2018
- Attended one day workshop on importance of IPR in academic Institutions 29th may 2019
- Paricipated in the International Virtual conference on “Innovations in Chemical Sciences-2020: An international meet for quality and quantity(ICSIMQQ-2020), organised by Division of Chemistry, School of Advanced Sciences, Vellore Institute of Technology, Chennai, August 21st – 22nd 2020
- Oral presentation at National e-Seminar on “Chemistry in emerging trends of interdisciplinary research” (NeSCETIR- 2020), organised by Department of Chemistry, Nagaland university, November 18th-20th 2020
- Participated in the International webinar on “Innovation in science and technology” organised by Department of Chemistry Smt. Narsamma Arts, Commerce and Science college, Mumbai, February 27th 2021

APPENDIX-III

LISTS OF PUBLICATIONS

Lists of Publications

Papers Published:

- **“Absorption spectral and thermodynamic analysis for the complexation of Pr³⁺ with L-Phenylalanine in the presence/absence of Mg²⁺ using 4f-4f transitions spectra as probe”**, Zevivonü Thakro, T. Moaienla Ao, Juliana Sanchu, Chubazenba Imsong, Mhasiriekho Ziekhürü, M. Indira Devi has been published in *The European Physical Journal Plus*, Springer.
- **“Complexation of Pr³⁺ with L-methionine in the presence/absence of Mg²⁺ : their reaction dynamics and thermodynamic properties”**, Zevivonü Thakro, Juliana Sanchu, Chubazenba Imsong, M. Indira Devi was published in the journal of *Chemical Physics Impact*, Elsevier.
- **“Computation of energy interaction and intensity parameters for the complexation of Pr(III) with glutathione at different pH in the presence/absence of Mg²⁺: 4f-4f transition spectra as a probe”**, Mhasiriekho Ziekhürü, Zevivonü Thakro, Chubazenba Imsong, Juliana Sanchu and M. Indira Devi was published in the journal of *Polyhedron*, Elsevier.
- **“Computation of spectral parameters for the complexation of Pr(III) with L-Histidine through 4f-4f transition spectra: Further analysis of its kinetic and thermodynamic parameters”**, Juliana Sanchu, Zevivonü Thakro, Chubazenba Imsong and M. Indira Devi was published in the journal of *Chemical Physics Impact*, Elsevier.
- **“Computational study of multimetal complexation of Nd(III) with GSH and Mg(II) in solution at different pH through 4f-4f transition spectra”**, Mhasiriekho Ziekhürü, Juliana Sanchu, Zevivonü Thakro, Chubazenba Imsong and M. Indira Devi was published in the journal of *Chemical Physics Impact*, Elsevier.
- **“4f-4f Transition Spectra of the Interaction of Pr(III) with L-Valine in Solution: Kinetics and Thermodynamic Studies”** Juliana Sanchu, Mhasiriekho Ziekhürü, Zevivonü Thakro and M. Indira Devi was published in *Asian journal of Chemistry*.
- **“Theoretical study of the heterometal complexation of Pr(III) with L-isoleucine in the presence/absence of Mg(II) in solution: 4f-4f transition spectra as probe”**, Chubazenba Imsong, Mhasiriekho Ziekhürü, Zevivonü Thakro, Juliana Sanchu and M. Indira Devi was published in the journal of *Chemical Physics Impact*, Elsevier.

Papers Communicated:

- **“UV-vis absorption spectral analysis of Pr^{3+} with L-leucine in the presence/absence of Mg^{2+} by employing the 4f-4f transition as a probe”,** has been communicated and is under review.
- **“Absorption spectral study of Nd(III) with selected amino acids in presence/absence of Mg(II): 4f-4f transition as a probe”** has been communicated.